INVERSE SCATTERING INVESTIGATION
QUARTERLY REPORT NO. 4

Vaughan H. Weston
Wolfgang M. Boerner
Dallas R. Hodgins

February 1968

SPACE DEFENSE SPO (496L/474L/N)
DEPUTY FOR SURVEILLANCE AND CONTROL SYSTEMS
ELECTRONIC SYSTEMS DIVISION
AIR FORCE SYSTEMS COMMAND
UNITED STATES AIR FORCE
L. G. Hanscom Field, Bedford, Massachusetts

LEGAL NOTICE

FOREWORD

This report (8579-4-Q) was prepared by the Radiation Laboratory of the Department of Electrical Engineering of the University of Michigan. The work was performed under Contract No. F 19628-67-C-0190, "Inverse Scattering Investigation" and covers the period 3 October 1967 to 3 January 1968. Dr. Vaughan H. Weston is the Principal Investigator and the contract is under the direction of Professor Ralph E. Hiatt, Head of the Radiation Laboratory. The contract is administered under the direction of the Electronic Systems Division, Air Force Systems Command, United States Air Force, Laurence G. Hanscom Field, Bedford, Massachusetts 01730, by Lt. L.E. Nyman, ESSXS. This quarterly report was submitted by the authors 5 March 1968.

This technical report has been reviewed and is approved.

Prior to release of this report to CFSTI (formerly OTS) it must be reviewed by the ESD Office of Public Information, ESTI, Laurence G. Hanscom Field, Bedford, Massachusetts 01730.

Approving Air Force Authority

Bernard J. Filliatreault
Contracting Officer
Space Defense Systems Program Office

ABSTRACT

The plane wave representation is generalized in terms of a three-dimensional Fourier transform, to yield an expression, which when combined with the incident field, gives the total electric field everywhere inside and outside non-magnetic scattering bodies. This representation requires the knowledge of the scattering matrix and its analytic continuation in the frequency domain.

The use of short pulse data to determine the properties of uniformly coated bodies is considered, where the main attention is applied to the illuminated portion of smooth convex bodies at high frequencies.

Computational results are obtained, establishing the conditions that are required to determine the surface of a conducting body from knowledge of the total near field. It is shown for the cases treated (sphere and prolate spheroid), that two separate conditions are required. One of these conditions yields a single surface which is an approximation to the proper surface, whereas, the other condition yields a set of surfaces, among which is the exact surface.

TABLE OF CONTENTS

I

INTRODUCTION

In section II, the plane wave representation is generalized in terms of
a three-dimensional Fourier transform. The resulting expression when combined
with the incident field yields the total field everywhere outside and inside
non-magnetic scattering bodies. This representation requires the knowledge
of the scattering matrix and its analytic continuation in the frequency domain.
The main emphasis is placed upon homogeneous bodies, a special use of which
is the conducting body, and various relations are obtained. The extension to
non-homogeneous bodies is briefly considered. The results presented here are
not complete, since a significant amount of analysis has yet to be performed.
The possibility of correlating monostatic short pulse data and bistatic data
for a fixed frequency and direction of incidence may be achievable.

The use of short pulse data to determine the properties of uniformly coated
conducting bodies is considered in section III. The main attention is focused
upon the illuminated portion of smooth convex bodies in the high frequency case.

Finally in section IV, computational results are presented. It is shown
for the two cases of conducting surfaces, the sphere and prolate spheroid,
that the two conditions $\left| \underline{E}^{s} \right| - \left| \underline{E}^{i} \right| = 0$, and $\underline{E} \times \underline{E}^{*} = 0$ are required to
establish the surface of the body from knowledge of the total near field. The
first condition yields a single surface which is an approximation to the proper
surface. The second condition yields a set of surfaces, among which is the
proper surface.

THE PLANE WAVE EXPANSION AND ITS
APPLICATION TO INVERSE SCATTERING

It has been shown previously, that if the scattered far field (phase, amplitude and polarization) is known over all directions of observation, for a fixed direction of incidence, then a particular class of plane wave representations yielded expressions for the near field which held down to the surface of smooth convex bodies. The plane wave representations involved, contained the far scattered field as an analytic function of the angles of observation. The use of the plane wave representation will be generalized here, to yield expressions that hold everywhere in space including the interior of the scattering body.

To begin, the analysis will be restricted to non-magnetic bodies (although it could be easily generalized to include such cases) and the geometry of the scattering body will be limited by placing certain restrictive analytical properties on the surface S which encloses the volume V of the scattering body. The classes of surfaces chosen, will belong to class C^3 defined by Barrar and Dolph as follows:

A surface S is said to belong to class C^3 if there exists a finite number m of images, $x^\nu = x^\nu(u, v)$, $y^\nu = y^\nu(u, v)$, $z^\nu = z^\nu(u, v)$, $\nu = 1.2.3...$ m of the disk $u^2 + v^2 \leq 1$ that cover the surface S and such that the third derivatives of x^ν, y^ν and z^ν with respect to u and v exist and are continuous.

Harmonic time dependence $\exp(-i\omega t)$ will be taken in which case Maxwell's equations become

$$\underline{\nabla} \wedge \underline{E} = ik \sqrt{\mu_0/\epsilon_0} \ \underline{H} \quad ,$$

$$\sqrt{\mu_0/\epsilon_0} \ \underline{\nabla} \wedge \underline{H} = -i(\underline{E}/k) \begin{Bmatrix} k_1^2 & \text{inside the body} \\ k^2 & \text{outside the body} \end{Bmatrix} \quad ,$$

where k_1^2, the square of the propagation constant in the body, is associated with

the free space propagation constant k, i.e. $k_1^2 = k_1^2(k)$.

The incident electric intensity will be expressed in the form

$$\underline{E}^i = (2\pi)^{-3/2} \underline{a} \; e^{i\underline{k}\cdot\underline{x}} \tag{2.1}$$

where $\underline{k}$ is the direction of the incident wave, and $\underline{a}$, the unit vector denoting polarization, will depend upon both $\underline{k}$ and index j (i.e. $\underline{a} = \underline{a}\,(\hat{\underline{k}}, j)$) where the index j takes on the value 1 if the polarization is in the $\hat{\theta}$ direction of a fixed coordinate system, and takes on the value 2 if the polarization is in the $\hat{\phi}$ direction.

Homogeneous Body

The homogeneous body will be treated first. In this case, it follows from Banar and Dolph, that the total electric intensity $\underline{E}$ induced by the plane wave Eq.(2.1), incident upon the body, satisfies the following integral equation (which has a unique solution)

$$\underline{E}(\underline{x}) = \underline{E}^i(\underline{x}) + \frac{\left(k_1^2 - k^2\right)}{4\pi} \left\{ \int_V \phi \, \underline{E} \, dv - \frac{1}{k^2} \, \underline{\nabla} \cdot \int_S \phi(\underline{E}^-\cdot\underline{n}) \, ds \right\} \tag{2.2}$$

where

$$\phi = \frac{e^{ikR}}{R} \quad , \qquad R = (\underline{x} - \underline{x}')$$

and $\underline{E}^-$ is the value of $\underline{E}$ obtained by approaching the surface from the interior of the body. If $\underline{E}^+$ is the value obtained by approaching the surface from the exterior of the body, it follows that

$$k_1^2 \, \underline{E}^-\cdot\underline{n} = k^2 \, \underline{E}^+\cdot\underline{n} \quad . \tag{2.3}$$

In addition, the magnetic field can be expressed in the form

$$\underline{H}(\underline{x}) = \underline{H}^i(\underline{x}) + \frac{\left(k_1^2 - k^2\right)}{4\pi i \omega \mu_0} \quad \underline{\nabla} \wedge \int_V \underline{E} \, \emptyset \, dv \quad . \tag{2.4}$$

Before deriving a plane wave representation for $\underline{E}(\underline{x})$, the following vector will be introduced

$$\underline{T}(\underline{k}',\underline{k}) = \frac{\left(k_1^2 - k^2\right)}{(2\pi)^{3/2}} \left\{ \int_V e^{-i\underline{k}'\cdot\underline{x}'} \underline{E}(\underline{x}',\underline{k}) \, dv' - \frac{i\underline{k}'}{k^2} \int_S e^{-i\underline{k}'\cdot\underline{x}'} \underline{E}^-\cdot\underline{n} \, ds' \right\} \tag{2.5}$$

From Eq.(2.2), it is seen that when $|x| \longrightarrow \infty$, in the direction given by the unit vector $\underline{k}'$, then the total field becomes

$$\underline{E}(\underline{x}) \underset{|\underline{x}|\to\infty}{\sim} \underline{E}^i(\underline{x}) + \sqrt{\frac{\pi}{2}} \frac{e^{ik|\underline{x}|}}{|\underline{x}|} \quad \underline{T}(\underline{k}',\underline{k}) \tag{2.6}$$

indicating that the vector $\underline{T}(\underline{k}',\underline{k})$ is related to the scattering matrix. When $|k'| = |k|$, $\underline{T}(\underline{k}',\underline{k})$ is a measurable function being proportioned to the far scattered field in direction $\underline{k}'$, produced by a plane wave of frequency ck, incident upon the body with direction of incidence given by $\overset{\wedge}{\underline{k}}$. The following theorem may now be proven.

Theorem:

$$\text{If} \quad \underline{\mathcal{E}}(\underline{k}',\underline{k}) = \frac{1}{(2\pi)^{3/2}} \int e^{-i\underline{k}'\cdot\underline{x}} \underline{E}(\underline{x},\underline{k}) \, d\underline{x} \quad , \tag{2.7}$$

$$\text{then} \quad \underline{\mathcal{E}}(\underline{k}'\cdot\underline{k}) = \delta(\underline{k} - \underline{k}')\underline{a} - \lim_{\epsilon \to 0} \frac{\underline{T}(\underline{k}',\underline{k})}{k^2 - k'^2 + i\epsilon} \tag{2.8}$$

4

Proof:

It follows from Eq.(2.2) that

$$\underline{\zeta}\,(\underline{k}',\,\underline{k}) = \delta\,(\underline{k}-\underline{k}')\,\underline{a}\;+\frac{\left(k_1^2-k^2\right)}{4\pi}\left\{\frac{1}{(2\pi)^{3/2}}\int_V \underline{E}\,(\underline{x}',\underline{k})\int e^{-i\underline{k}'\cdot\,\underline{x}}\;\not\!\phi\;d\underline{x}\;dv\right.$$

$$\left. -\frac{1}{k^2}\int\frac{e^{-i\underline{k}'\cdot\,\underline{x}}}{(2\pi)^{3/2}}\;\underline{\nabla}\cdot\int_S\not\!\phi\,(\underline{E}'\cdot\underline{n})\;ds\right\}\;.$$

On setting

$$\psi = \int_S\not\!\phi\,(\underline{E}^-\cdot\underline{n})\;ds$$

one can show that

$$\int e^{-i\underline{k}'\cdot\,\underline{x}}\;\underline{\nabla}\,\psi\;d\underline{x}\;=\;\lim_{R_\infty\to\infty}\int_{S_\infty} e^{-i\underline{k}'\cdot\,\underline{x}}\;\psi\,ds\;+i\underline{k}'\int e^{-i\underline{k}'\cdot\,\underline{x}}\;\psi\,d\underline{x}$$

when S_∞ is the surface of a sphere of radius R_∞. Letting k have a small imaginary part, it is seen that the surface integral will vanish when $R_\infty\to\infty$. The resulting integrals can be reduced as follows

$$\frac{1}{(2\pi)^{3/2}}\int e^{-i\underline{k}'\cdot\,\underline{x}}\;\not\!\phi\;d\underline{x}\;=\sqrt{\frac{2}{\pi}}\;\frac{1}{(2\pi)^3}\iint dp\,d\underline{x}\;\frac{e^{i\underline{p}\cdot(\underline{x}\cdot\underline{x}')-i\underline{k}'\cdot\,\underline{x}}}{p^2-k^2-i\epsilon}$$

$$=\sqrt{\frac{2}{\pi}}\int d\underline{p}\;\frac{e^{-i\underline{p}\cdot\underline{x}'}}{p^2-k^2-i\epsilon}\;\delta\,(\underline{p}-\underline{k}')$$

5

$$= - \sqrt{\frac{2}{\pi}} \quad \frac{e^{-i\underline{k}' \cdot \underline{x}}}{k^2 - k'^2 + i\epsilon}$$

Combining the above expressions, one obtains the result

$$\underline{\mathcal{L}} \, (\underline{k}' \cdot \underline{k}) = \delta \, (\underline{k} - \underline{k}') \, \underline{a} \, - \, \lim_{\epsilon \to 0} \, \frac{T \, (\underline{k}', \underline{k})}{k^2 - k'^2 + i\epsilon}$$

An immediate consequence of the above theorem, is the following corollary which expresses the total field everywhere in space in terms of the incident field and the quantity $\underline{T} \, (\underline{k}', \underline{k})$,

$$\underline{E} \, (\underline{x} \cdot \underline{k}) = \underline{E}^i \, (\underline{x} \cdot \underline{k}) + \frac{1}{(2\pi)^{3/2}} \int \frac{e^{i\underline{p} \cdot \underline{x}}}{p^2 - k^2} \, \underline{T} \, (\underline{p}, \underline{k}) \, d\underline{p} \quad . \quad (2.9)$$

If the integration space $\underline{p}$ is expressed in spherical polar coordinates (p, θ_p, ϕ_p) where the range of the variables are $-\infty < p < \infty$, $0 \le \theta_p \le \pi/2$, and $0 \le \phi_p \le 2\pi$, then in the above integral, the contour of the variable p bends above the pole at $p = -k$, and below the pole at $p = k$.

It can be shown in a similar manner that the magnetic field can be expressed in a similar form

$$\underline{H} \, (\underline{x}, \underline{k}) = \underline{H}^i \, (\underline{x} \cdot \underline{k}) + \frac{1}{\omega\mu_o (2\pi)^{3/2}} \int \frac{e^{i\underline{p} \cdot \underline{x}}}{p^2 - k^2} \, \underline{p} \wedge \underline{T} \, (\underline{p}, \underline{k}) \, d\underline{p} \quad . \quad (2.10)$$

Integral Equation for $\underline{T} \, (\underline{k}', \underline{k})$

Applying the condition that $\underline{\nabla} \cdot \underline{E} = 0$ in the volume, one can express Eq. (2.5) in the form

6

$$\underline{T}(\underline{k}',\underline{k}) = \frac{\left(k_1^2 - k^2\right)}{(2\pi)^{3/2}} \int_V e^{-i\underline{k}'\cdot\underline{x}} \left\{ \underline{E}(\underline{x}\cdot\underline{k}) - \frac{\underline{k}'(\underline{k}'\cdot\underline{E})}{k^2} \right\} d\underline{x} \qquad (2.11)$$

where the surface integral is replaced by a volume integral. On substitution of Expression (2.9) for $\underline{E}$, Eq. (2.11) reduces to the integral equation

$$\underline{T}(\underline{k}',\underline{k}) = \left(k_1^2 - k^2\right)\left[1 - \frac{\underline{k}'(\underline{k}'\cdot\;)}{k^2}\right] \left\{ \frac{1}{(2\pi)^{3/2}} \int_V e^{-i\underline{k}'\cdot\underline{x}}\; \underline{E}_0(\underline{x},\underline{k})\, d\underline{x} \right.$$

$$\left. + \frac{1}{(2\pi)^3} \int \frac{d\underline{p}}{p^2 - k^2} \int_V e^{i(\underline{p}-\underline{k}')\cdot\underline{x}}\, d\underline{x}\; \underline{T}(\underline{p},\underline{k}) \right\} \qquad .$$

Defining $V(\underline{k}',\underline{k})$ to be the Fourier transform of the body, as follows

$$V(\underline{k}',\underline{k}) = \frac{1}{(2\pi)^3} \int_V e^{i(\underline{k}'-\underline{k})\cdot\underline{x}}\, d\underline{x} \qquad , \qquad (2.12)$$

one obtains the following fundamental integral equation for $\underline{T}$,

$$\left(k_1^2 - k^2\right)\left\{ \underline{a}\, V(\underline{k},\underline{k}') + \int \frac{d\underline{p}\, V(\underline{p},\underline{k}')}{p^2 - k^2}\; \underline{T}(\underline{p},\underline{k}) \right\} = \underline{T}(\underline{k}',\underline{k}) - \frac{\underline{k}'(\underline{k}'\cdot\underline{T})}{k_1^2 - k^2} \qquad .$$

$$(2.13)$$

For the case of almost transparent bodies, i.e. where

$$\left(k_1^2 - k^2\right)\, V(\underline{k},\underline{k}')$$

is small, an approximate solution to the integral equation is obtained through a process of integration, yielding the Born approximation

$$\underline{T}\,(\underline{k}',\underline{k}) \sim \bigwedge\,(k',k) \left\{ \underline{a}\,V(\underline{k},\underline{k}') + \int d\underline{p}\,\,\frac{V(\underline{p},\,\underline{k}')}{p^2 - \kappa^2}\,\bigwedge\,(\underline{p},\,\underline{k})\,V\,(\underline{k},\,\underline{p})\,\underline{a} + \ldots \right\}$$

where $\bigwedge(k',k)$ is the operator

$$\bigwedge = \left(k_1^2 - k^2\right)\left[1 - \frac{k'(k' \cdot \,)}{k^2}\right] \qquad .$$

For the case of a perfect conductor, i.e. $\text{Im}\,k_1^2 \to \infty$, the integral equation (2.13), cannot be used by itself. An additional equation is required. The details on the particular aspect are given later on.

Relationships Among $\underline{T}\,(k',k)$

In order to attempt to reduce the number of measurements needed to determine the scattering body, or in order to correlate different sets of measurements (such as for different directions of incidence), various relationships involving $\underline{T}\,(\underline{k}',\underline{k})$ for different $\underline{k}'$ and $\underline{k}$ are sought.

Denoting the complex conjugate of a quantity be a super bar, it can be shown that

$$\overline{V}(\underline{k},\underline{k}') = V\,(-\underline{k},\,-\,\underline{k}') \qquad .$$

Hence it follows that the complex conjugate of Eq. (2.13) yield for k_1^2 real

$$\left(k_1^2 - k^2\right)\left\{\underline{a}\,\,V(-\underline{k},\,-\underline{k}') + \int d\underline{p}\,\,\frac{V(-\underline{p},\,-\underline{k}')}{p^2 - k^2}\,\,\overline{T}\,(\underline{p},\underline{k})\right\} = \overline{T}\,(\underline{k}',\underline{k}) - \frac{k'(k' \cdot \overline{T})}{k'^2 - k^2} \qquad .$$

$$\tag{2.14}$$

In the above equation, replace $\underline{k}$ by $-\underline{k}$, and $\underline{k}'$ by $-\underline{k}'$. In doing so, the polarization vector $\underline{a}$ must be changed appropriately, i.e.

$$\underline{a}\,(\hat{\underline{k}},\,j) = \epsilon_j\,\,\underline{a}\,(-\hat{\underline{k}},\,j)$$

8

where

$$\epsilon_j = 1 \quad \text{for } j = 1$$

$$= -1 \quad \text{for } j = 2 \quad .$$

This results in the following

$$(k_1^2 - k^2)\left\{ \epsilon_j \, \underline{a} \, (-\hat{\underline{k}}, j) \, V(\underline{k}, \underline{k}') + \int d\underline{p} \, \frac{V(\underline{p}, \underline{k}')}{p^2 - k^2} \, \overline{\underline{T}}(-\underline{p}, -\underline{k}) \right\}$$

$$= \overline{\underline{T}}(-\underline{k}', -\underline{k}) - \frac{\underline{k}'(\underline{k}' \cdot \overline{\underline{T}})}{k'^2 - k^2} \quad . \tag{2.15}$$

It follows that on subtracting Eq. (2.15) from Eq. (2.14) for $j = 1$, and adding them for $j = 2$, that the vector

$$\underline{T}(\underline{k}', \underline{k}, j) - \epsilon_j \, \overline{\underline{T}}(-\underline{k}', -\underline{k}, j)$$

is a solution of the homogeneous equation corresponding to Eq. (2.13).

Since the solution is unique, the following must hold

$$\underline{T}(\underline{k}', \underline{k}, j) = \epsilon_j \, \overline{\underline{T}}(-\underline{k}', -\underline{k}, j) \; ; \; k_1^2 \text{ real} \tag{2.16}$$

This result holds only for k^2, real and finite. However it can be shown that it will also apply to the case of a perfect conductor, where $\text{Im } k_1 \to \infty$.

For general real or complex values of k_1^2, an additional set of relations may be obtained. To proceed, we first note that

$$\int d\underline{k}' \, V(\underline{p}, \underline{k}') \, V(\underline{k}', \underline{k}) = V(\underline{p}, \underline{k}) \, ,$$

hence upon operating on Eq. (2.13) with respect to

$$\int d\underline{k}' \; V(\underline{k}', q) \; . \; . \; .$$

it is seen that the left-hand side is invariant. Defining

$$\widetilde{\underline{T}}(\underline{k}', \underline{k}) = \left[1 - \frac{\underline{k}(\underline{k}' \cdot \;)}{k'^2 - k^2} \right] \underline{T}(\underline{k}', \underline{k}) \tag{2.17}$$

one immediately obtains the result

$$\int d\underline{p} \; V(\underline{p}, \underline{k}') \; \widetilde{\underline{T}}(\underline{p}, \underline{k}) = \widetilde{\underline{T}}(\underline{k}', \underline{k}) \; . \tag{2.18}$$

This equation will be shown to the additional equation required for the case of a perfect conductor. For present purposes, this equation, combined with Eq. (2.14) which can be expressed in the form

$$(k_1^2 - k^2) \left\{ \underline{a} \; V(k, k') + \int d\underline{p} \; \frac{V(\underline{p}, \underline{k}')}{p^2 - k^2} \; \underline{T}(p, k) \right\} = \widetilde{\underline{T}}(\underline{k}', \underline{k}) \tag{2.19}$$

can be used to eliminate the volume factor $V(\underline{k}', \underline{k})$. In Eq. (2.19) replace $\underline{k}'$ by $-\underline{q}$, and operate on the equation with an arbitrary unit vector $\underline{b}$, yielding

$$\underline{b} \cdot \underline{a} \; V(\underline{q}, -\underline{k}) + \int d\underline{p} \; \frac{V(\underline{q}, -\underline{p})}{p^2 - k^2} \; \underline{b} \cdot \underline{T}(\underline{p}, \underline{k}) = \frac{\underline{b} \cdot \widetilde{\underline{T}}(-\underline{q}, \underline{k})}{k_1^2 - k^2} \; .$$

Operate on this equation with the integral operator

$$\int d\underline{q} \; \widetilde{\underline{T}}(\underline{q}, \underline{k}')$$

10

and employ relation (2.18) to yield

$$\underline{b} \cdot \underline{a} \; \widetilde{\underline{T}}(-\underline{k}, \underline{k}') + \int \frac{d\underline{p}}{p^2 - k^2} \left[\underline{b} \cdot \underline{T}(\underline{p}, \underline{k}) \right] \widetilde{\underline{T}}(-\underline{p}, \underline{k}')$$

$$= \frac{1}{\left(k_1^2 - k^2\right)} \int d\underline{p} \left[\underline{b} \cdot \widetilde{\underline{T}}(-\underline{p}, \underline{k}) \right] \widetilde{\underline{T}}(\underline{p}, \underline{k}') \qquad (2.20)$$

Since $\underline{b}$ is an arbitrary unit vector, this equation constitutes three independent equations. For the case of a perfect conductor, the right-hand side of Eq. (2.20) vanishes. It can be shown that for the perfectly conducting case, Eq. (2.20) will yield the law of reciprocity when $|\underline{k}'| = |\underline{k}|$.

Extension of the Integral Equation to the Perfectly Conducting Case.

Before considering the case where $\operatorname{Im} k_1^2 \to \infty$, an analysis upon the decomposition of the field into the interior and exterior components will be treated. The vector $\underline{T}$ will be decomposed into parts $\underline{T}^+$ and $\underline{T}^-$ as follows:

$$\underline{E}^i + \frac{1}{(2\pi)^{3/2}} \int \frac{e^{i\underline{p} \cdot \underline{x}}}{p^2 - k^2} \; \underline{T}^+ \, d\underline{p} = \begin{cases} \underline{E}(\underline{x}, \underline{k}) & \text{for } \underline{x} \text{ outside } V \\ 0 & \text{for } \underline{x} \text{ inside } V , \end{cases} \qquad (2.21)$$

$$\frac{1}{(2\pi)^{3/2}} \int \frac{e^{i\underline{p} \cdot \underline{x}}}{p^2 - k^2} \; \underline{T}^- \, d\underline{p} = \begin{cases} \underline{E}(\underline{x}, \underline{k}) & \text{for } \underline{x} \text{ inside } V \\ 0 & \text{for } \underline{x} \text{ outside } V \end{cases} \qquad (2.22)$$

It then follows from Eq. (2.21) by integrating over V , that

$$\underline{a} \; V(\underline{k}, \underline{k}') + \int d\underline{p} \; \frac{V(\underline{p}, \underline{k}')}{p^2 - k^2} \; \underline{T}^+(\underline{p}, \underline{k}) \, d\underline{p} = 0 \qquad (2.23)$$

11

and from Eq. (2.22)

$$\frac{\underline{T}^-(k',k)}{k'^2 - k^2} = \frac{1}{(2\pi)^{3/2}} \int_V \underline{E}(\underline{x},\underline{k})\, e^{-i\underline{k}'\cdot\underline{x}}\, d\underline{x}$$

$$= \underline{a}\, V(\underline{k},\underline{k}') + \int d\underline{p}\, \frac{V(\underline{p},\underline{k}')}{p^2 - k^2}\, \underline{T}(\underline{p},\underline{k}) = \int d\underline{p}\, \frac{V(\underline{p},\underline{k}')}{p^2 - k^2}\, \underline{T}^-(\underline{p},k) \quad .$$

$$(2.24)$$

Applying these results to Eq. (2.13), one obtains

$$\underline{T}^-(\underline{k}',\underline{k}) = \left(\frac{k'^2 - k^2}{k_1^2 - k^2}\right) \widetilde{\underline{T}}(\underline{k}',\underline{k}) \quad , \qquad (2.25)$$

from which the following relationship between $\underline{T}^+$ and $\underline{T}^-$ may be derived

$$\underline{T}^-(\underline{k}',\underline{k}) = \left(\frac{k'^2 - k^2}{k_1^2 - k'^2}\right)\left\{\underline{T}^+(\underline{k}',\underline{k}) - \frac{\left(k_1^2 - k^2\right)}{k_1^2\left(k'^2 - k^2\right)}\, \underline{k}'(\underline{k}'\cdot\underline{T}^+)\right\} . \quad (2.26)$$

Hence on eliminating $\underline{T}^-$ from Eq. (2.24), one obtains the additional equation for $\underline{T}^+$

$$\underline{T}^+(\underline{k}',\underline{k}) - \frac{\left(k_1^2 - k^2\right)}{k_1^2}\, \frac{\underline{k}'(\underline{k}'\cdot\underline{T}^+)}{k'^2 - k^2}$$

$$= \int d\underline{p}\, V(\underline{p},\underline{k}')\, \frac{\left(k_1^2 - k'^2\right)}{\left(k_1^2 - p^2\right)}\, \left[\underline{T}^+(\underline{p},\underline{k}) - \frac{\left(k_1^2 - k^2\right)}{k_1^2(p^2 - k^2)}\, \underline{p}(\underline{p}\cdot\underline{T}^+)\right] \quad .$$

$$(2.27)$$

12

The case of perfect conductivity may be considered by letting $\text{Im } k_1^2 \to \infty$.

It is seen from Eq. (2.25) that

$$\underline{T}^-(\underline{k}',\underline{k}) \to 0 \left(\frac{1}{k_1^2} \right)$$

i.e.

$$\underline{T} \sim \underline{T}^+ + 0 \left(\frac{1}{k_1^2} \right) ,$$

Eqs. (2.23) and (2.27) reduce to the form

$$\underline{a}\, V(\underline{k},\underline{k}') + \int d\underline{p}\ \frac{V(\underline{p},\underline{k}')}{p^2 - k^2}\ \underline{T}(\underline{p},\underline{k}) = 0 \qquad\qquad (2.28)$$

$$\widetilde{\underline{T}}(\underline{k}',\underline{k}) = \int d\underline{p}\, V(\underline{p},\,\underline{k}')\ \widetilde{T}(\underline{p},\underline{k}) \quad . \qquad\qquad (2.29)$$

These two equations constitute the two integral equations that are required for the case of the perfect conducting body. Eq. (2.28) insures that the total fields vanish inside the body, whereas it can be shown that Eq. (2.29) corresponds to Maue's integral equation. The problem with working with Maue's integral equation by itself, is that it does not always yield a unique solution, since there exists a set of resonant frequencies such that non-vanishing interior fields satisfy the condition $\underline{n} \times \underline{E}$ vanish on the surface of the body. Thus the additional Eq. (2.28), removes this uniqueness problem by requiring that the field vanish inside the body.

Alternative Representation Exterior to the Body

For a fixed direction of incidence, the quantity $\underline{T}(\underline{k}',\underline{k})$ is required for all values of $\underline{k}'$, in order to obtain expressions for the field everywhere in

13

space. However it will be shown that restricting the requirements on the knowledge of $\underline{T}(\underline{k}',\underline{k})$ to the values of $\underline{k}'$ which lie on the sphere $|\underline{k}'| = |\underline{k}|$, the total field can be obtained everywhere outside the minimum convex surface enclosing the body. To show this, let the plane $z = z_o$ be the tangent plane of the body, such that the body lies in the half-space $z \leq z_o$. For points in the half-space $z > z_o$, the following representation of the near scattered field

$$\underline{E}^s(\underline{x}) = \frac{1}{(2\pi)^{3/2}} \int \frac{e^{i\underline{p} \cdot \underline{x}}}{p^2 - k^2} \underline{T}(\underline{p},\underline{k}) \, d\underline{p} \qquad (2.30)$$

can be reduced as follows:

Set $\qquad p_x = k \sin \alpha \cos \beta$

$\qquad\qquad p_y = k \sin \alpha \sin \beta$

$\qquad\qquad p_z = kq$

when the domains of integration are

$$0 \leq \beta \leq 2\pi , \quad 0 \leq \alpha \leq \pi/2 - i\infty , \quad \text{and} \quad -\infty \leq q \leq \infty .$$

Expression (2.30) becomes

$$\underline{E}^s = \frac{k}{(2\pi)^{3/2}} \int_0^{\pi/2 - i\infty} \int_0^{2\pi} \int_{-\infty}^{\infty} \frac{\underline{T}(\underline{p},\underline{k})}{q^2 - \cos^2\alpha - i\epsilon} \, g(\alpha, \beta, q) \cos\alpha \sin\alpha \, d\alpha \, d\beta \, dq$$

$$(2.31)$$

$$g = \exp\left\{ ik\sin\alpha \, (x \cos \beta + y \sin \beta) + iqzk \right\} .$$

From expression (2.5) , it can be seen that for $z > z_o$, the contour in the following integral

14

$$\int_{-\infty}^{\infty} \frac{e^{ikzq} \, \underline{T} \, (p, k) \, dq}{q^2 - \cos^2 \alpha - i\epsilon}$$

may be deformed, to yield the following

$$\pi \, i \, e^{ik\cos\alpha z} \quad \underline{T} \, (k \sin\alpha \cos\beta, \quad k \sin\alpha \sin\beta, \quad k \cos\alpha \, ; \, \underline{k}) \quad .$$

Hence expression (2.31) may be placed in the form

$$\underline{E}^s = \frac{ik}{2\pi} \int_0^{\pi/2-i\infty} \int_0^{2\pi} e^{i\underline{k}',\underline{x}} \quad \underline{E}_0 (\alpha, \beta) \sin\alpha \, d\alpha \, d\beta \qquad (2.32)$$

where

$$\underline{k}' = k \, (\sin\alpha \cos\beta, \, \sin\alpha \sin\beta, \, \cos\alpha)$$

and $\underline{E}^o$ is the amplitude and phase of the far scattered field in direction given by (θ, ϕ), i.e.

$$\underline{E}^s \sim \frac{e^{ikR}}{R} \quad \underline{E}_0 \, (\theta, \phi) \quad .$$

Expression (2.32) was developed by alternative techniques in earlier reports (Weston, Bowman, 1966).

The Inhomogeneous Body

The results may be extended to include inhomogeneous non-conducting bodies, i.e. where $k_1^2 = \omega^2 \epsilon \mu$ (a real function) and k_1^2 varies continuously in the medium. In this case, the appropriate integral equation for the total electric field is (Barrar and Dolph)

$$\underline{E} = \underline{E}^i + \frac{1}{4\pi} \int_V \emptyset \left(k_1^2 - k^2\right) \underline{E}\, dv - \frac{\nabla}{4\pi k^2} \int_S \emptyset \left(k_1^2 - k^2\right)(\underline{E}^- \cdot \underline{n})\, ds$$

$$+ \frac{\nabla}{4\pi} \int_V \left(\underline{\nabla} k_1^2 \cdot \underline{E}\right) \frac{\emptyset}{k_1^2}\, dv \quad,$$

which has been shown to possess a unique solution, although its existance has not yet been proven.

For the homogeneous body, it can be shown that

$$\underline{T}(\underline{k}',\underline{k}) = \frac{1}{(2\pi)^{3/2}} \left\{ \int_V e^{-i\underline{k}'\cdot\underline{x}} \left(k_1^2 - k^2\right) \underline{E}\, dv - i\underline{k}' \int_S e^{-i\underline{k}'\cdot\underline{x}} \frac{\left(k_1^2 - k^2\right)}{k^2}(\underline{E}^- \cdot \underline{n})\, ds \right.$$

$$\left. + i\underline{k}' \int_V \frac{\left(\underline{\nabla} k_1^2 \cdot \underline{E}\right)}{k_1^2} e^{-i\underline{k}'\cdot\underline{x}}\, dv \right\}$$

$$= \frac{1}{(2\pi)^{3/2}} \int_V e^{-i\underline{k}'\cdot\underline{x}} \left(k_1^2 - k^2\right) \left[\underline{E} - \frac{\underline{k}'(\underline{k}'\cdot\underline{E})}{k^2} \right] dv \quad.$$

In this case, the appropriate integral equation becomes

$$\underline{\widetilde{T}}(\underline{k}',\underline{k}) = k^2 \underline{a}\, V^*(\underline{k},\underline{k}') + k^2 \int \frac{V^*(\underline{p},\underline{k}')}{p^2 - k^2}\, \underline{T}(\underline{p},\underline{k})\, d\underline{p}$$

where

$$V^*(\underline{k},\underline{k}') = \frac{1}{(2\pi)^3} \int_V e^{i(\underline{k}-\underline{k}')\cdot\underline{x}} \left[N - 1\right] dv$$

with $k_1^2 = k^2 N(\underline{x})$.

16

III

ASPECTS ON PULSE SCATTERING FOR THE DETERMINATION
OF UNIFORMLY COATED SCATTERING BODIES.

3.1 Introduction.

A convenient method for the identification of uniformly coated scattering
bodies may employ the application of pulse scattering since more information
may be obtained by such a transient analysis than from steady state results.
The distortion of a pulse returned from a scattering obstacle, in fact, does
yield some additional information pertaining to the properties of the scat-
terer, e.g. the behavior of the leading wavefront of a scattered pulse usually
indicates something about the composition of the body, whereas the behavior of
the trailing return of a scattered pulse is related to the shape of the body and
its radii of curvature.

In this preliminary treatment on the identification of coated scatterers,
the merits and the restrictions of such a transient approach will be investigated,
using the solution of pulse scattering by planar layered structures where both
the mono- and bi-static solutions of the scattered field will be considered.

Here the wavefront technique is employed to solve the problem of
scattering of a finite rectangular pulse from a lossy dielectric slab mounted
on a perfectly conducting planar surface. The general case of oblique incidence
is treated, where in particular the behavior at normal and at critical (Brewster's
angle) incidence are demonstrated.

From the presented theoretical results practical methods will be deduced which may be applied to the problem of identification of the properties of uniformly coated scatterers.

3.2 Theory

3.2.1 The Laplace Transform of Maxwell's Equations and the Boundary Conditions.

The solution of a non-steady state problems in electromagnetic theory is facilitated by a transform type approach. Here the Laplace transform will be used since it is defined for a wider class of functions than the Fourier transform, in particular to the extension to more complicated source dependence.

The Laplace transform of a function f(t) is defined by the relation

$$L \left[f(t) \right] = \int_0^\infty f(t) \, e^{-st} \, dt = F(s) \tag{3.2.1}$$

The inverse transform from the s domain to the t domain is accomplished by means of the relation

$$L^{-1} \left[F(s) \right] = \frac{1}{2\pi i} \int_{B-i\infty}^{B+i\infty} F(s) \, e^{st} \, ds \tag{3.2.2}$$

where B, a positive constant, is chosen such that F(s) is analytic for $\mathrm{Re}\left\{s\right\} \geq B$. In particular the relation holds:

$$\frac{\partial^n}{\partial t^n} \left\{ f(t) \right\} \longleftrightarrow s^n F(s) - \sum_{l=0}^{n-1} s^{n-l-1} F^l(0) \tag{3.2.3}$$

The vector wave equation, satisfied by the transformed field vector $\underline{\mathcal{E}}(\underline{r}, s)$ is given by

$$\nabla \times \nabla \times \underline{\mathcal{E}}(\underline{r}, s) + \frac{s^2}{c^2} \left(1 + \frac{\sigma}{\epsilon s}\right) \underline{\mathcal{E}}(\underline{r}, s) \quad \frac{s}{c^2} \left(1 + \frac{\sigma}{\epsilon s}\right) \underline{E}(\underline{r}, 0)$$

$$= + \frac{1}{c^2} \frac{\partial}{\partial t} \underline{E}(\underline{r}, 0) \tag{3.2.4}$$

where $\mu\epsilon = 1/c^2$.

18

The equation of the transformed magnetic field vector $\mathcal{H}(\underline{r}, s)$ is obtained by replacing $\mathcal{E}$ by $\mathcal{H}$ and $\underline{E}$ by $\underline{H}$. Since the quantity of interest here is the scattered field, it is always possible to define the time origin such that the initial values of the scattered field are zero everywhere in space, and thus the transform of the scattered field vector satisfies the homogeneous vector wave equation:

$$\nabla \times \nabla \times \mathcal{E}^s(\underline{r}, s) + \frac{s^2}{c^2} (1 + \frac{\sigma}{\epsilon s}) \mathcal{E}^s(\underline{r}, s) = 0 \qquad (3.2.5)$$

The boundary conditions satisfied by the em field vectors at the interface of two media (the normal to the interface $\underline{n}$, a unit vector, is directed from medium (1) to (2)) are given by the familiar relations:

a) Both media of finite conductivity:

$$\underline{n} \times \left[\underline{E}_2(\underline{r}, t) - \underline{E}_1(\underline{r}, t) \right] = 0 \text{ or } \underline{n} \times \left[\mathcal{E}_2(\underline{r}, s) - \mathcal{E}_1(\underline{r}, s) \right] = 0$$

$$\underline{n} \times \left[\underline{H}_2(\underline{r}, t) - \underline{H}_1(r, t) \right] = 0 \text{ or } \underline{n} \times \left[\mathcal{H}_2(\underline{r}, s) - \mathcal{H}_1(\underline{r}, s) \right] = 0 . \qquad (3.2.6)$$

b) Medium (1) being a perfect conductor:

$$\underline{n} \times \underline{E}_2(\underline{r}, t) = 0 \quad \text{or} \quad \underline{n} \times \mathcal{E}_2(\underline{r}, s) = 0$$

$$\underline{n} \times \underline{H}_2(r, t) = \underline{K}(\underline{r}, t) \quad \text{or} \quad \underline{n} \times \mathcal{H}_2(r, s) = \mathcal{K}(r, s) . \qquad (3.2.7a)$$

In cases where the approximated Leontovich boundary conditions

$$-\underline{n} \times (\underline{n} \times \underline{E}(\underline{r}, t) = Z \underline{n} \times \underline{H}(\underline{r}, t) \qquad (3.2.7b)$$

with Z, the surface impedance, may be implied, the transient problem must be handled with care, since the error introduced in the solution of the diffraction

19

of a harmonic wave $(k = \dfrac{\omega}{c} = i\dfrac{s}{c})$ by a <u>curved</u> obstacle of curvature ρ and refractive index n_{12} is of the order of $(n_{12}\dfrac{s\rho}{c})^{-1}$. Thus only the behavior of the scattered fields in the vicinity of the wavefronts which is related to the asymptotic behavior of the transformed field quantities for large values of the transform variable s, can be properly derived. Consequently the application of the Leontovich type boundary condtions will lead to erroneous results for the field vectors when the time delayed from the arrival of the wavefront is large.

3.2.2 Expansion of the Transformed Field Quantities as a Series of Time-delayed Terms Determined by the Optical Wavefronts.

In Steady state electromagnetic theory it has been shown that the field scattered from an obstacle can be obtained by summing the contribution due to the various optical rays associated with the scatter geometry of the obstacle. In transient analysis such families of rays may in addition be characterized by time delay factors due to the geometry of the obstacle. To verify this aspect two different types of problems will briefly be considered.

3.2.2.1 Pulse Scattering from a Finite Obstacle

Consider the configuration of Fig.3-1 where a plane wave is incident on a finite obstacle of closed surface.
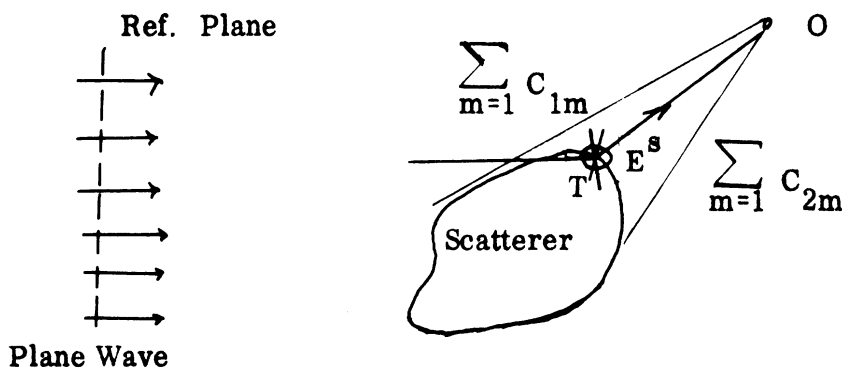

FIG. 3-1: GENERALIZED RAY SYSTEM.

The scattered ray E^s is the conventional geometrical optics result, where the position of the specular point T is determined by the requirement that the optical distance between reference plane-scatterer-observation point is a minimum. In addition two families of rays $\sum_m C_{1m}$ and $\sum_m C_{2m}$, the creeping wave contributions, must be considered, where the mth term in the sum $\sum_m C_{1m}$ is associated with the ray which undergoes m complete circulations around the obstacle and then travels to the observation point. The path on the obstacle taken by each of these rays is determined by the condition that the optical distance be a minimum.

Since wavefronts of non-monochromatic waves satisfy geometrical optics, the above described diffraction process in conjunction leads to the hypothesis that the solution of the pulse diffraction problem will be facilitated if the terms corresponding to the various monochromatic optical rays are identified and treated separately. The result is expressed in the form of an infinite sum of residue and branch cut contributions, where the individual contributions must be summed in a manner such that the rays $\sum_{m=n}^{\infty} S_{1m}$ (i = 1, L) are absent for $t < T_n$.

3.2.2.2 Pulse Scattering from Layered Structures.

Another class of problem is demonstrated in Fig.3-2, the problem of pulse scattering from a nonperfectly conducting slab. The incident pulse will

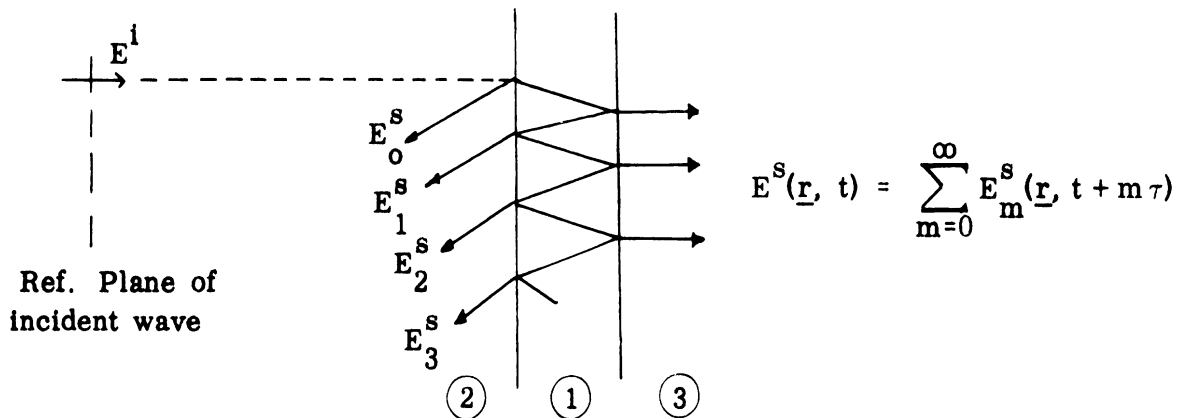$$E^s(\underline{r},\ t)\ =\ \sum_{m=0}^{\infty} E_m^s(\underline{r},\ t + m\tau)$$

FIG. 3-2: PULSE SCATTERING FROM A DIELECTRIC SLAB.

be decomposed into an infinite sum of partial pulse returns, where each of the partial returns are delayed by a time factor T_n, depending upon the material properties and the depth of the layer. The amplitudes of individual partial returns are obtained by selecting the proper coefficient of the expanded CW reflection coefficient.

3.2.2.3 Geometrical Optics Interpretation.

From the two presented examples it consequently seems that the solution of pulse diffraction problems can be handled most efficiently by treating each term in a wavefront expansion separately, where the amplitudes of individual wavefronts are given by the corresponding term of the expanded CW scattering coefficient.

The solution of the vector wave equation (2.5) for the transient case is obtained in the same manner as the solution of the vector wave equation for monochromatic fields. In general, the transform of the field vector $\underline{\mathcal{F}}^s(\underline{r}, s)$ can be expressed as the result of the same vector operations on two scalar functions which are solutions of a scalar wave equation. Consequently, in discussing the decomposition of the field into its optical components, it will suffice to investigate the behavior of a scalar function $F(r, s)$ which satisfies the scalar wave equation:

$$\nabla^2 F(\underline{r}, s) - \frac{s^2}{c^2} (1 + \frac{\sigma}{\epsilon s}) \, F(\underline{r}, s) = 0 \qquad (3.2.8)$$

where $F(\underline{r}, s)$ will be rewritten into the form of a sum of terms which can be identified with the partially delayed optical wavefronts:

$$F(\underline{r}, s) = \sum_{m=0}^{\infty} F_m(\underline{r}, s) = \sum_{m=0}^{\infty} U_m(\underline{r}, s) \, e^{-s(1 + \frac{\sigma}{\epsilon s})^{1/2} T_m^o(\underline{r})} \qquad (3.2.9)$$

Thus the following relation is obtained:

$$\sum_{m=0}^{\infty} \left[\nabla^2 - \frac{s^2}{c^2} (1 + \frac{\sigma}{\epsilon s}) \right] F_m (\underline{r}, s) = 0 \qquad (3.2.10)$$

Operating on $F_m(\underline{r}, s)$ and equating the result to zero, it is found that the functions $U_m(\underline{r}, s)$ and $T_m^o(\underline{r})$ must satisfy the relation:

$$s^2(1 + \frac{\sigma}{\epsilon s}) \left[\left| \nabla T_m^o(\underline{r}) \right|^2 - \frac{1}{c^2} \right] U_m(\underline{r}, s) - s(1 + \frac{\sigma}{\epsilon s})^{1/2} \left[2\nabla U_m(\underline{r}, s) \right.$$

$$\left. \cdot \nabla T_m^o(\underline{r}) + U_m(\underline{r}, s) \nabla^2 T_m^o(\underline{r}) \right] + \nabla^2 U_m(\underline{r}, s) = 0 \qquad (3.2.11)$$

where the spatial time factor $T_m^o(\underline{r})$ must satisfy the Eikonal equation

$$\left| \nabla T_m^o(\underline{r}) \right|^2 = 1/c^2 \qquad (3.2.12)$$

If s is replaced by s = -iω and σ = 0, the remainder of Eq.(3.2.11) is identical with the equation satisfied by amplitudes of the geometrical optics waves in the asymptotic theory of diffraction

3.2.3 Behavior of the Fields in the Vicinity of the Individual Wavefronts.

The field behavior in the vicinity of the individual wavefronts can be obtained by considering the asymptotic behavior of the transform of the field vectors for large values of the complex frequency s. This implies a Tauberian theorem which is obtained from an Abelian theorem given by Bremmer and van der Pol (Brown, 1962) as:

If a one-sided original [here time function f(t)] is represented asymptotically as t →0 + by some power series of not necessarily integral exponents exceeding -1, their the series in s, obtained by transposing the original term by term represents the image [here Laplace transform F(s) = L[f(t)]] asymptotically as s → ∞.

However, here the inverse of the theorem must hold as well which will enable to determine the asymptotic behavior of the original time function as $t \rightarrow O^+$ from the asymptotic representation of the image as $s \rightarrow \infty$. In order to justify the use of the "Tauberian Theorem" which is the inverse to the above Abelian theorem, the nature of the time functions resulting from the inversion of the asymptotic representation of the image must be considered.

A time function of the form:

$$\mathcal{F}(\underline{r}, t) = a \; \delta \left(\frac{t - t_o}{T} \right) + U \, (t - t_o) \sum_{n=0}^{\infty} a_n t^{u - \alpha} \qquad (3.2.13)$$

has a Laplace transform if $\alpha > -1$, where the inverse is given as

$$F(\underline{r}, s) = e^{-s t_o} \left[a + \sum_{n=0}^{\infty} a_n \frac{\Gamma(u - \alpha + 1)}{s^{u - \alpha + 1}} \right] \qquad (3.2.14)$$
$$\alpha > -1$$

consequently, since the transform of the field vectors is obtained as a solution of a vector wave equation and if for such, in general, a Laplace transform exists, it can be said that the transform of a vector field must be representable in the form of Eq.(3.2.13) in the vicinity of a wavefront (for a rectangular pulse similar holds). With the above stated theorem, allowing for an asymptotic expansion for large s, it is reasonable to assert that the asymptotic representation of the inverse of these transforms can be obtained by a term by term inversion of their asymptotic representation for large s.

Using the expansion of Eq.(3.2.9), it can be shown that for large values of s this equation can be rewritten as:

$$\lim_{s \gg 1} F(s) = \sum_{m=0}^{\infty} \lim_{s \gg 1} U_m(\underline{r}, s) \exp\left[-s\left(1 + \frac{1}{2}\frac{\sigma}{\epsilon s} - \frac{1}{8}(\frac{\sigma}{\epsilon s})^2\right) + T_m^o(\underline{r})\right] \qquad (3.2.15)$$

The time function which corresponds to the mth term in (3.2.15) will be zero for $t < T_m^o(\underline{r})$. Since $T_m^o(\underline{r})$ was chosen such that it satisfies the Eikonal equation, the equation $t = T_m^o(\underline{r})$ describes the arrival of the mth wavefront at $\underline{r}$. The amplitude of the disturbance associated with the wavefront is given by $\lim_{s \to \infty} U_m(\underline{r}, s)$. The function $U_m(\underline{r}, s)$ satisfies for $s \to \infty$:

$$2 \nabla U_m(\underline{r}, s) \cdot \nabla T_m^o(\underline{r}) + U_m(\underline{r}, s) \nabla^2 T_m^o(\underline{r}) = 0 \qquad (3.2.16)$$

which is the equation satisfied by the amplitude of waves determined by geometrical optics . Thus it is apparent that in pulse diffraction problems the amplitudes of the waves at the wavefronts are determined by geometrical optics.

3.2.4 Behavior of the Fields when $\left[t - T_m^o(r)\right] \gg 1$.

Neglecting the losses ($\sigma \to 0$), the inverse transform for the mth term in the wavefront expansion (3.2.9) can be formulated as:

$$\mathcal{L}^{-1}\left[F_m(\underline{r}, s)\right] = \frac{1}{2\pi i} \int_{B-i\infty}^{B+i\infty} U_m(\underline{r}, s) e^{s\left[t - T_m^o(\underline{r})\right]} ds \qquad (3.2.17)$$

where a typical amplitude function $U_m(\underline{r}, s)$, in general, will have both poles and branch-points in the region $R(s) < B$. The fact that $\left[t - T_m^o(r)\right] \gg 1$ necessitates the deformation of the contour of integration in (3.2.17) into the left hand plane, where $Re~(s) < 0$. If $\left[t - T_m^o(\underline{r})\right] R \gg 1$, the most significant contribution to (3.2.17) results from the singularity which has the maximum real part. In Fig. 3-3, a distribution of poles and branch cuts is demonstrated for the case of plane wave diffraction by a finite convex body. In this case

$$S = \omega'' + i\omega'$$
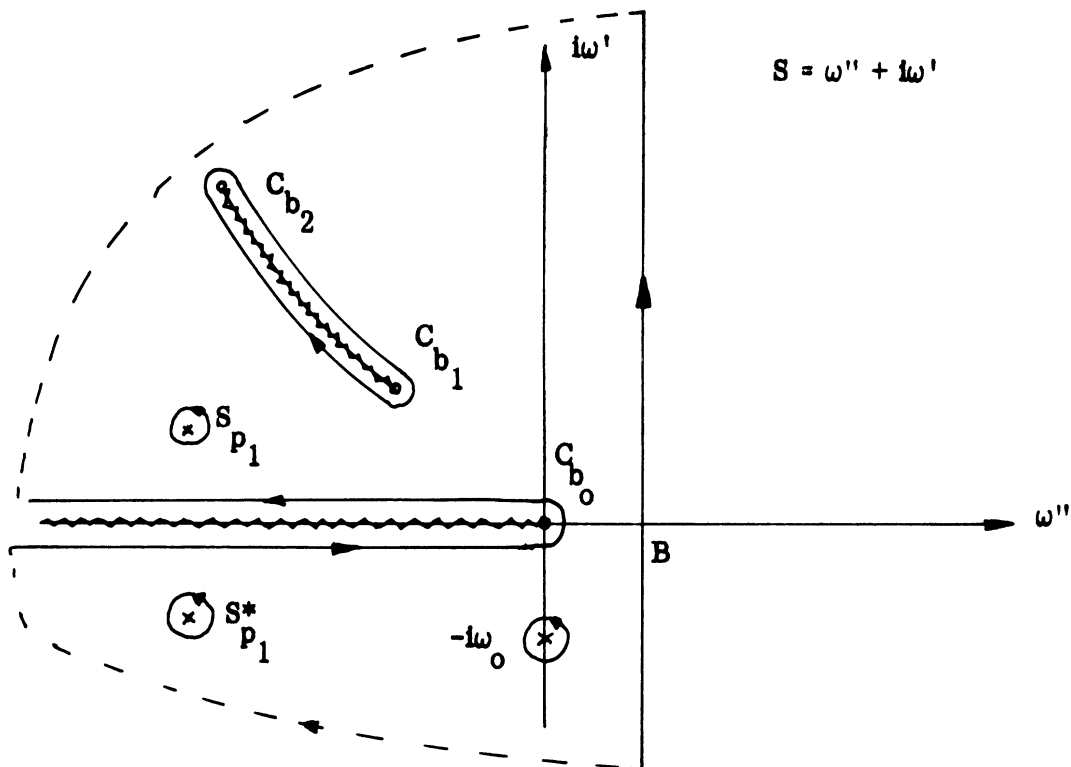
FIG. 3-3:   INTEGRATION IN THE COMPLEX S PLANE.

$$\zeta_1 = \cos\theta_1 \hat{2} + \sin\theta_1 \hat{x}$$

$$\zeta_2 = \cos\theta_2 \hat{2} + \sin\theta_2 \hat{x}$$

$$\zeta_3 = \cos\theta_1 \hat{2} + \sin\theta_1 \hat{x} \qquad (3.3.7)$$
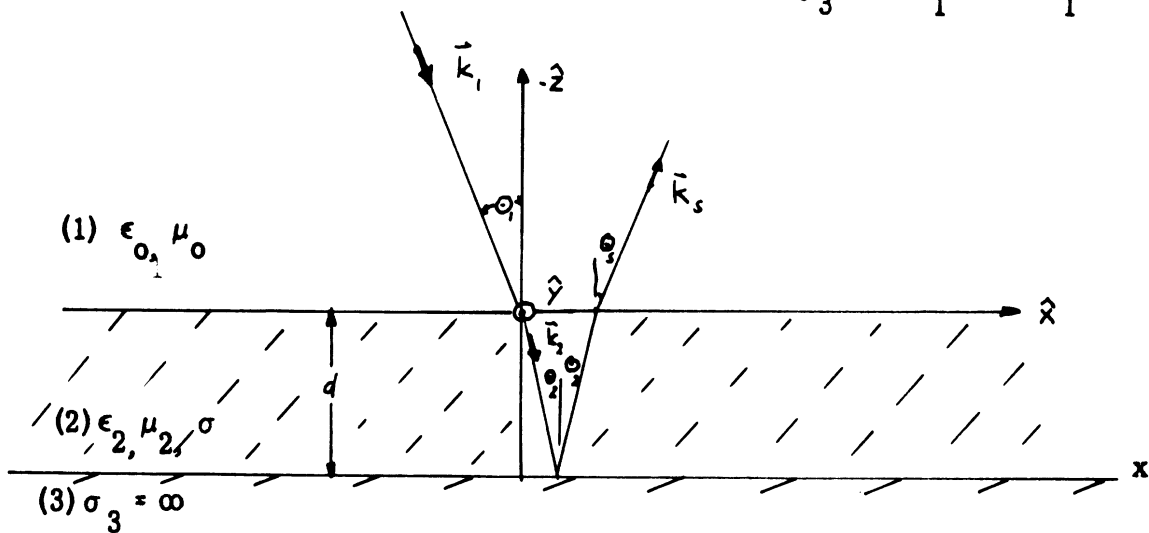

FIG. 3-4:   GEOMETRICAL CONFIGURATION.

26

the pole along the imaginary axis at $s = - i\omega_o$ and the branchpoint $s = c_{b0} = 0$ are the significant singularities, where the contribution from $s = - i\omega_o$ yields the CW behavior and the integration around the branchpoint $c_{b0} = 0$ will describe the deviation of $\mathcal{L}^{-1}\left[\text{Im } (\underline{r}, s)\right]$ from its steady state behavior. Depending upon the relative value of $\left[t - T_m^o (\underline{r})\right] R \sim 1$, the contributions of the other singularities may have to be encountered, not so for $\left[t - T_m^o (\underline{r})\right] R \gg 1$. In fact for $\left[t - T_m^o (\underline{r})\right] R \simeq 1$ the exact solution of $F_m (\underline{r}, s)$ is required, which in most of the cases can only be approximately solved.

3.2.5   The Dispersive Effect Due to the Presence of Finite Con-ductivity or the Properties of Layered Media

3.2.5.1   Finite Conductivity.

Although the constituent parameters μ, ϵ, σ have been assumed to be individually of a nondispersive nature, the fact that $\sigma \neq 0$ introduces a dispersive effect, since

$$\epsilon^1 = \epsilon \left(1 + \frac{\sigma}{\epsilon s} \right) \qquad\qquad (3.2.18)$$

Assuming a non-conducting propagation media, the inherent source of dispersion then may be related to the effects of the conducting obstacle only. Applying the results of section (3.2.3) to equation 3.2.18), the behavior of the reflected wave solution in the vicinity of its wavefront is determined as

$$\lim_{s \to \infty} \epsilon^1 = \lim_{s \to \infty} \epsilon (1 + \frac{\sigma}{\epsilon s}) = \epsilon \qquad\qquad (3.2.19)$$

This indicates that even a good conductor acts like a dielectric in the immediate vicinity of the wavefronts, i.e. the reflection coefficient is determined by the dielectric constant only. This property will be shown in the next section, where the transforms of the individual field vectors are derived explicitely for the scattering from a lossy slab mounted on a perfectly conducting planar surface.

As long as oblique incidence is excluded, in general, it can be said that the dispersive effect of a conducting media is solely caused by the fact that $\sigma \neq 0$. The significant parameter in the assessment of the magnitude of the dispersive effect is the relaxation time $\tau_c = (2\pi)/(\sigma / \epsilon)$, where $\omega_c = (2\pi)/\tau_c = (\sigma / \epsilon)$ may be denoted as the critical radiant frequency of the medium. If $\sigma >> 1$, i.e. $\omega_c >> 1$, then, in general, the dispersive effect can be neglected since signals decay in a time of a few relaxation periods τ. It appears that the dispersive effect cannot be detected if $\omega_c >> \omega_{max}$ where ω_{max} is determined by the high-frequency cut off of the detecting device. Thus only for those materials for which $\omega_c < \omega_0$, the operating frequency, dispersive effects are non-negligible.

3.2.5.2 Layered Structure

Yet there still exists another source of dispersion, although μ, ϵ, σ are of non-dispersive character and σ may even be zero. For instance in the case of oblique incidence on a grounded dielectric slab, dispersion will be encountered due to the superposition of waves which results in a seperation of phase and group velocities, deviating from the intrinsic velocity of the medium.

3.3. Pulse Scattering from a Lossy Dielectric Layer Mounted on a Perfectly Conducting Planar Surface.

To receive more insight into the problem of pulse scattering from finite coated, convex scatterers, the planar case will be treated first for both oblique T E and T M plane wave incidence for the general case of a lossy dielectric layer. For simplicity a rectangular pulse of pulsewidth T, carrier frequency ω_0, and amplitude f o (r = 0, t = 0) = 1 is chosen, propagating at an angle θ, to the normal of the interface as illustrated in FIG. 3-4. The corresponding field quantity, normal to the plane of incidence (in the TE - case the $\underline{E}$ - vector, in the TM - case the $\underline{H}$ - vector) is then

28

described as:

$$\underline{f}^1(\underline{kr}, t) = \hat{x} \begin{cases} 0 & t < \zeta/c \\ \exp i\, (k\zeta_1 - \omega_0 t) & \zeta/c \le t \le \zeta/c + T \\ 0 & \zeta/c + T \le t \end{cases} \tag{3.3.1}$$

where $\quad \zeta_1 = (\cos\theta_1\, z + \sin\theta_1\, y)$ (3.3.2a)

$$f^1(k\,\underline{r}, t) = f_1(k)\,\exp{-i\omega_0 t} \tag{3.3.2b}$$

$$F_1(k, r) = \exp k\,\zeta \tag{3.3.2c}$$

$$\omega = is, \quad s = -i\omega \tag{3.3.2d}$$

This time dependent function $F^1(k\,r, t)$ in turn can be expressed in terms of an inverse Laplace transform:

$$F^1(k\,\underline{r}, t) = \frac{\hat{x}}{2\pi i}\int_{B-i\infty}^{B+i\infty} e^{ts}\, F_1(s, \underline{r})\, ds = \frac{\hat{x}}{2\pi i}\int_{B-i\infty}^{B+i\infty} \frac{e^{ts}(1-e)^{-(s+i\omega_0)}}{(s+i\omega_0)} F_1(s, r)\, ds \tag{3.3.3}$$

Any other shape of finite impulse can be obtained by convolution properties which will not be considered here.

The scattered field in the direction of reflection is given as:

$$f^s(k\,\underline{r}, t) = \frac{\hat{x}}{2\pi i}\int_{B-i\infty}^{B+i\infty} \frac{e^{ts}\left[1-e^{-(s+i\omega_0)T}\right]}{(s+i\omega_0)} F^s\left(\frac{is}{c}, \underline{r}\right)\, ds \tag{3.3.4}$$

Where

$$F^s\left(\frac{is}{c}, \underline{r}\right) = R_{c\omega}^{\nu\,\mu}\left(\frac{is}{c}\right) e^{ik\,\zeta_s} \tag{3.3.5a}$$

$$\zeta_s = (-\cos\theta_1\, z + \sin\theta_1\, y) \tag{3.3.5b}$$

The total reflection coefficient $R_{C\,W}^{\nu,\mu}$ $\left(\dfrac{is}{c}\right)$ is determined from the C W

case, where ν denotes either TE or TM incidence, and μ whether of electric,

magnetic or power type. For proper expansion of the total reflection co-

efficient the derivation of the C W electric, magnetic and power reflection

$V_{C\,W}^{\nu,\mu}$ and transmission $W_{C\,W}^{\nu,\mu}$ coefficients is thus required for the

behavior at one interface where $R_{C\,W}^{\nu,\mu}$ $\left(\dfrac{is}{c}\right)$ describes the case of a

grounded dielectric slab and must be derived as well.

3.3.1 Derivation of C W Reflection and Transmission Coefficients.

The constituent parameters are given as:

a) Medium (1): $\epsilon_1 = \epsilon_o$, $\mu_1 = \mu_o$, $\sigma = 0$, $v_1^2 = \dfrac{1}{\epsilon_1 \mu_1} = c^2$ (3.3.6a)

b) Medium (2): $\epsilon_2 = \epsilon_2 \left(1 + \dfrac{\sigma_2}{\epsilon_2}\,\dfrac{1}{s}\right)$, $\mu_2 = \mu_o$, $\sigma_2 = \sigma$

$$N(s) = N\left(1 + \dfrac{\omega_c}{s}\right)^{1/2} \qquad\qquad N^2 = \dfrac{\epsilon_2}{\epsilon_o},\quad \omega_c = \dfrac{\sigma_2}{\epsilon_2}$$

$$k_2^2 = \dfrac{\omega^2}{v_2^2} = -\dfrac{s^2}{c^2}N^2(s), \qquad\qquad v_2^2 = c^2\,N^{-2}(s) \qquad\qquad (3.3.6b)$$

    d = depth of layer.

c) Medium (3): $\sigma_3 = \infty$

3.3.1.1 TE - Incidence for d = ∞: $f^i(r,\,t) = \stackrel{\wedge}{y}\,E^i(r,\,t)$.

Applying the boundary conditions of equation (2.6) the electric (voltage)

TE reflection coefficitne for the case of d = ∞ is given as:

$$E_V^{TE} = \dfrac{E_y^s}{E_y^i} = E_{V_\perp} = \dfrac{\left(\dfrac{\mu_2}{\mu_o}\right)\cos\theta_1 - \sqrt{N^2 - \sin^2\theta_1}}{\left(\dfrac{\mu_2}{\mu_o}\right)\cos\theta_1 + \sqrt{N^2 - \sin^2\theta_1}} \qquad\qquad (3.3.8a)$$

and the magnetic TE reflection coefficient as.

$$H_V{}^{TE} = - E_V{}^{TE} \tag{3.3.8b}$$

which would be identical with the electric reflection coefficient for the case
of reversed propagation, i.e. if the wave is traveling from the denser into the
less denser medium, which will be denoted as

$$E_{V_-}{}^{TE} = - E_V{}^{TE} = H_V{}^{TE} = - H_{V_-}{}^{TE} \tag{3.3.8c}$$

where the Fresnel's law of reflection is given as $\dfrac{\sin \frac{\theta}{2}}{\sin \theta_1} = N$ $\qquad$ (3.3.9)

The transmission coefficients are given as

$$E_W{}^{TE} = H_{W_-}{}^{TE} = 1 + E_V{}^{TE} = \frac{2 \left(\dfrac{\mu_2}{\mu_0} \right) \cos \theta_1}{\left(\dfrac{\mu_2}{\mu_0} \right) \cos \theta_1 + \sqrt{N^2 - \sin^2 \theta_1}} \tag{3.3.10}$$

$$H_W{}^{TE} = E_{W_-}{}^{TE} = 1 + H_V{}^{TE} = 1 - E_V{}^{TE} = \frac{\sqrt{2 N^2 - \sin^2 \theta_1}}{\left(\dfrac{\mu_2}{\mu_0} \right) \cos \theta_1 + \sqrt{N^2 - \sin^2 \theta_1}} \tag{3.3.11}$$

The power reflection and transmission coefficients are then defined as

$$P_V{}^{TE} + P_W{}^{TE} = 1 \tag{3.3.12a}$$

where

$$P_V{}^{TE} = - E_V{}^{TE} \cdot H_V{}^{TE} \quad \text{and} \quad P_W{}^{TE} = E_W{}^{TE} \cdot H_W{}^{TE} \qquad . \tag{3.3.12b}$$

3.3.1.2 TM - Incidence for $d = \infty$: $\,^i(r, t) = x \, H^i(r, t)$.

Applying the boundary conditions (3.2.6) the magnetic (current) TM
reflection coefficient is given as

$$H_V TM = \frac{H_y^s}{H_y^i} = H_{V_\parallel} = \frac{\left(\frac{\mu_o}{\mu_2}\right) N^2 \cos \theta_1 - \sqrt{N^2 - \sin^2 \theta_1}}{\left(\frac{\mu_o}{\mu_2}\right) N^2 \cos \theta_1 + \sqrt{N^2 - \sin^2 \theta_1}} \qquad (3.3.13a)$$

and the electric TM reflection coefficient as:

$$E_V TM = - H_V TM \qquad (3.3.13b)$$

which again is identical with the magnetic reflection coefficient for the case of reversed propagation, i.e. if the wave is traveling from the denser into the less denser medium, which will be denoted as:

$$H_{V_-} TM = - H_V TM = E_V TM = - E_{V_-} TM \qquad . \qquad (3.3.13c)$$

The magnetic TM transmission coefficient is defined as

$$H_W TM = 1 + H_V TM = E_{W_-} TM = \frac{2\left(\frac{\mu_o}{\mu_2}\right) N^2 \cos \theta_1}{\left(\frac{\mu_o}{\mu_2}\right) N^2 \cos \theta_1 + \sqrt{N^2 - \sin^2 \theta_1}} \qquad (3.3.14a)$$

$$E_W TM = H_{W_-} TM = 1 + E_V TM = \frac{2\sqrt{N^2 - \sin^2 \theta_1}}{\left(\frac{\mu_o}{\mu_2}\right) N^2 \cos \theta_1 + \sqrt{N^2 - \sin^2 \theta_1}} \qquad . \qquad (3.3.14b)$$

The TM power reflection and transmission coefficients are defined as:

$$P_V TM + P_W TM = 1 \qquad (3.3.15a)$$

where

$$P_V TM = - H_V TM \cdot E_V TM \qquad (3.3.15b)$$

32

and

$$P_W{}^{TM} = H_W{}^{TM} \cdot E_W{}^{TM} \qquad (3.3.15c)$$

3.3.1.3 Derivation of the Total Reflection Coefficient $R_{tot}^{\nu,\mu}$ (r, s)

The total reflection coefficient $R_{tot}^{\nu,\mu}$ ($\underline{r}$, s) will be determined by two different methods, namely

a)   The summation of all phase-delayed partial reflection coefficients, and

b)   The application of the equivalent transmission line concept.

3.3.1.3.1 Summation of Phase Delayed Partial Reflection Coefficients.

The reflection coefficients at the perfectly conducting screen are given as

$$V_U{}^{TE} = \lim_{N \to \infty} V_V{}^{TE} = -1; \qquad H_U{}^{TE} = -V_U{}^{TE} \qquad (3.3.16a)$$

$$H_U{}^{TM} = \lim_{N \to \infty} H_V{}^{TM} = +1; \qquad V_U{}^{TM} = -H_U{}^{TM} \qquad (3.3.16b)$$

The delay factor Δ is defined by

$$\Delta = \exp\left(ik_2 \; \zeta_2^* \right) = \exp\left(-\frac{s}{c} \; N(s) \; \zeta_2^* \right) \qquad (3.3.17a)$$

where

$$\zeta_2^* = d \cos\theta_2 + d \sin\theta_2 \; tg\,\theta_2 =$$

$$= d \; \frac{1}{\cos\theta_2} \qquad (3.3.17b)$$

this however is exactly the desired result, namely that the delay factor is related to the group velocity, where

$$\left(V_{pl_2} \right)_2 = C \; \frac{1}{\cos\theta_2 \; N(s)} \qquad (3.3.18a)$$

$$\left(V_{gr_2} \right)_2 = \frac{C \cos\theta_2}{N(s)} \qquad \left(\begin{array}{l} \text{no return in z-direction for} \\ \text{grazing incidence.} \end{array} \right) \qquad (3.3.18b)$$

33

The group delay then can be defined as:

$$T^o(s) = \frac{N(s)}{C}\frac{d}{\cos\theta_2} = \frac{N\,d}{C\cos\theta_2}\sqrt{1+\frac{\omega_c}{s}}$$

$$= T_g\sqrt{1+\frac{\omega_c}{s}} \tag{3.3.19a}$$

$$\Delta = \exp\left\{-s\,T_g\sqrt{1+\frac{\omega_c}{s}}\right\} = \exp\left\{-s\,T^o(s)\right\} \tag{3.3.19b}$$

where

$$T^o_n(s) = 2\,T_g\sqrt{1+\frac{\omega_c}{s}} \tag{3.3.19c}$$

$$n = 0, 1, \ldots\ldots$$

$$\Delta_n = \exp\left\{-s\,T^o_n(s)\right\} \tag{3.3.19d}$$

The algorism for the partial pulse returns can be written down immediately from inspection of figure 2:

$$F^s_0(s) = V \qquad\qquad = V$$

$$F^s_1(s) = W\cdot\Delta\cdot U\cdot\Delta\,W_- \qquad\qquad = W\cdot W_-\cdot\Delta^2\cdot U\ (1)$$

$$F^s_2(s) = W\cdot\Delta\cdot U\cdot\Delta\cdot V_-\cdot\Delta\cdot U\cdot\Delta\cdot W_- \qquad\qquad = W\cdot W_-\cdot\Delta^2\cdot U\ (\Delta^2\,U\,V)$$

$$F^s_3(s) = W\cdot\Delta\cdot U\cdot\Delta\cdot V_-\cdot\Delta\cdot U\cdot\Delta\cdot V_-\cdot\Delta\cdot U\cdot\Delta\cdot W_- \qquad = W\cdot W_-\,\Delta^2\cdot U\ (\Delta^2\,U\,V)^2$$

$$\vdots$$

$$F^s_n(s) = \qquad\qquad = \left[W\cdot W_-\Delta^2 U\right](\Delta^2\,U\,V^-)^{n-1}$$

$$R_{tot}(s) = F^s_0(s) + \sum_{n=1}^{\infty} F^s_n(s) = V + WW_-\Delta^2 U\left[1+(\Delta^2\,U\,V_-)\right.$$

$$\left.+(\Delta^2 U\,V_-)^2 +\ldots\right] = V + \frac{W\,W^-\Delta^2\,U}{1-(\Delta^2 U\,V_-)} = \frac{V+\Delta^2\,U}{1+\Delta^2\,UV} \tag{3.3.20a}$$

Replacing V, Δ and U by the proper expressions associated with the TE or TM cases, will yield the corresponding total reflection coefficient, where the reflection coefficients will be rewritten into:

$$V(s) = \frac{1 - A(s)}{1 + A(s)} \quad \text{then with} \quad U = V_U^{TE} \cdot V_U^{TM} = -1$$

$$R_{tot}(s) = \frac{V + \Delta^2 U}{1 + \Delta^2 UV} = \frac{(1-A(s)) - (1+A(s)) \exp(-2s\, T^0(s))}{(1+A(s)) - (1-A(s)) \exp(-2s\, T^0(s))}$$

$$= \frac{\left[\exp(sT^0(s)) - \exp(-sT^0(s))\right] - A(s)\left[\exp(sT^0(s)) + \exp(-sT^0(s))\right]}{\left[\exp(sT^0(s)) - \exp(-sT^0(s))\right] + A(s)\left[\exp(sT^0(s)) + \exp(-sT^0(s))\right]}$$

thus

$$R_{tot}(s) = \frac{\tan hi\,(s\, T^0(s)) - A(s)}{\tan hi\,(s\, T^0(s)) + A(s)} \qquad (3.3.20b)$$

a) Normal Incidence: $A(s) = N(s)$

$$V_{R_{tot}}(\theta_1 = 0, s) = V_{R_{tot}}^{TE}(\theta_1 = 0, s) = \frac{\tanh\left[s\, T^0(s)\right] - N(s)}{\tanh\left[s\, T^0(s)\right] + N(s)}$$

$$= \frac{i\tan\left[\omega\, T^0(\omega)\right] - N(\omega)}{i\tan\left[\omega\, T^0(\omega)\right] + N(\omega)} \qquad (3.3.21a)$$

b) TE - Incidence $= V_A^{TE}(s) = \dfrac{\cos\theta_2}{\cos\theta_1}\left(\dfrac{\mu_o}{\mu_2}\right) N(s)$

$$V_{R_{tot}}^{TE}(s) = \frac{\left(\dfrac{\mu_r}{\mu_o}\right)\cos\theta_1\,\tanh i\left[s\, T^0(s)\right] - N(s)\cos\theta_2}{\left(\dfrac{\mu_r}{\mu_o}\right)\cos\theta_1\,\tanh i\left[s\, T^0(s)\right] + N(s)\cos\theta_2} \qquad (3.3.21b)$$

c) TM - Incidence $= V_A^{TM}(s) = \left(\dfrac{\mu_o}{\mu_r}\right)\dfrac{\cos\theta_1}{\cos\theta_2} N(s)$

35

$$V_{R_{tot}}^{TM} (s) = \frac{\left(\dfrac{\mu_2}{\mu_o}\right) \cos \theta_2 \ \tanh i \left[s \ T^o(s)\right] - \cos \theta_1 \ N(s)}{\left(\dfrac{\mu_2}{\mu_o}\right) \cos \theta_2 \ \tanh i \left[s \ T^o(s)\right] + \cos \theta_1 \ N(s)} \tag{3.3.21c}$$

3.3.1.3.2 Application of the Equivalent Transmission Line Concept.

The equivalent transmission line concept is derived from proper definition of equivalent impedances which describe the properties of the structure as illustrated in figure 4. The equivalent transmission line input impedance in this case is given as:

$$Z_{in} (s) = \lim_{Z_3 \to 0} Z_2 \ \frac{\dfrac{Z_3}{Z_2} + \tanh i \left[s \ T^o(s)\right]}{1 + \dfrac{Z_3}{Z_2} \ \tanh i \left[s \ T^o(s)\right]}$$

$$= Z_2 \ \tanh i \left[s \ T^o(s)\right] \tag{3.3.22a}$$

where the "voltage" (here electric) reflection-coefficient is defined as:

$$V_{R_{tot}}(s) = \frac{Z_{in} - Z_1}{Z_{in} + Z_1} = \frac{\tanh i \left[s \ T^o(s)\right] - \dfrac{Z_1}{Z_2}}{\tanh i \left[s \ T^o(s)\right] + \dfrac{Z_1}{Z_1}} \tag{3.3.22b}$$

thus to verify the result of the preceding section it is sufficient to show that the $V_A^\nu (s) = \dfrac{Z_1 (s)}{Z_2 (s)}$ and both derivations are identical.

a) TE - case.

$$Z_1 = \frac{Z_{o_1}}{\cos \theta_1}$$
the characteristic impedance of medium (1)

$$Z_{o_1} = \sqrt{\frac{\mu_o}{\epsilon_o}} \tag{3.3.23a}$$

$$Z_2 = \frac{Z_{o_2}}{N(s)\cos\theta_2}$$ the characteristic impedance of medium (2)

$$Z_{o_2} = \sqrt{\frac{\mu_2}{\epsilon_o}}$$ (3.3.23b)

$$V_A{}^{TE}(s) = \left(\frac{Z_1}{Z_2}\right) = \left(\frac{\mu_o}{\mu_2}\right)\left(\frac{\cos\theta_2}{\cos\theta_1}\right) N(s)$$ (3.3.23c)

which is identical with the result obtained before.

b) TM-case

$$Z_1 = Z_{o_1}\cos\theta_1$$ where $$Z_{o_1} = \sqrt{\frac{\mu_o}{\epsilon_o}}$$ (3.3.24a)

$$Z_2 = Z_{o_2}\frac{\cos\theta_2}{N(s)}$$ where $$Z_{o_2} = \sqrt{\frac{\mu_2}{\epsilon_o}}$$ (3.3.24b)

$$V_A{}^{TM}(s) = \left(\frac{Z_1}{Z_2}\right)_{TM} = \left(\frac{\mu_o}{\mu_2}\right)\frac{\cos\theta_1}{\cos\theta_2} N(s)$$ (3.3.24c)

which also checks with the result obtained before. The relationship between the total reflection and total transmission coefficients is identical to that derived for the partial coefficients. Thus the total reflection coefficients always can be expanded as

$$R_{tot}(s) = F_o^s(s) + \sum_n F_n^s(s) = V + (W \cdot W - \Delta^2 U)$$

$$= \left[1 + (\Delta^2 U V_-) + (\Delta^2 U V_-)^2 \ldots\ldots\right]$$ (3.3.24d)

where Δ^2 takes care of the proper time delay of the pulse returns which is strictly related to the group velocity as shown by Eqs.(3.3.18b) and (3.3.19b).

3.3.2 Evaluation of the Inverse Laplace Transform.

Having expanded the C W reflection coefficient $R_{tot}(s)$ into the proper algorism, the backscattered field can be derived by evaluating the Inverse Laplace Transform of equation (3.3.4):

$$\underline{f}^{s}(\underline{r}, t) = \frac{\hat{y}}{2\pi i} \int_{B-i\infty}^{B+i\infty} \frac{e^{+ts}\left[1 - e^{-(s + i\omega_0)T}\right]}{(s + i\omega_0)} R_{tot}\left(\frac{is}{c}\right) e^{ik\zeta}\, ds \; .$$

For proper evaluation, it is convenient to introduce a new special time variable t_o by choosing an observation point at $(0, 0, z, ct_o)$

$$t = \frac{2}{c} + t_o \qquad . \tag{3.3.25}$$

Introducing this variable into (3.3.4) and rewriting the Inverse Transform into two parts, it can be shown that

$$\underline{f}^{s}(\underline{r}, t) = \underline{f}_1^{s}(\underline{r}\,\delta\,t_o) + \underline{f}_2^{s}(r, t_o) \tag{3.3.26a}$$

where

$$\underline{f}_1^{s}(\underline{r}, t_o) = \frac{\hat{y}}{2\pi i} \int_{B-i\infty}^{B+i\infty} \frac{\exp\left[2/c + t_o\right]s}{(s + i\omega_0)} R_{tot}\left(\frac{is}{c}\right)\, ds \tag{3.3.26b}$$

$$\underline{f}_2^{s}(\underline{r}, t_o) = \frac{\hat{y}\, e^{-i\omega_0 T}}{2\pi i} \int_{B-i\infty}^{B+i\infty} \frac{\exp\left[z/c + (t_o - T)\right]s}{s + i\omega_0} R_{tot}\left(\frac{is}{c}\right)\, ds$$

$$= - e^{-i\omega T} \underline{f}_1^{s}(\underline{r}, t_o - T) \tag{3.3.26c}$$

thus for:

$t < 2/c$ or $t_o < 0$: $\qquad\qquad \underline{f}^{s}(\underline{r}, t_o) = 0$

$z/c \leq t \leq z/c + T$ or $0 \leq t_o \leq T$: $\qquad \underline{f}^{s}(\underline{r}, t_o) = \underline{f}_1^{s}(r, t)$

$$t > Z/c + T \text{ or } t_0 > T: \quad \underline{f}^s (\underline{r}, t_0) = f^s (\underline{r}, t_0)$$

$$+ f^s_2 (\underline{r}, t_0) = f^s_1 (\underline{r}, t_0) - e^{-i\omega_0 T} f^s_1 (\underline{r}, t_0 - T) \tag{3.3.27}$$

The last expression rewritten into Fourier Transform terminology becomes:

$$f^s (\underline{r}, t_0) = f^s_1 (\underline{r}, t_0) = f^s_1 (\underline{r}, t_0) \left[1 - U (t_0 - T) \right] \tag{3.3.28}$$

where $U(t)$ is the Heaviside unit step function, and thus for $t_0 > T$ the initial response is cancelled.

3.3.2.1 Normal Incidence

At normal incidence the TE and TM cases cannot be distinguished, and the electric reflectic coefficient is given as:

$$^E V = - ^H V = - ^E V_- = \frac{1 - N(s)}{1 + N(s)} \tag{3.3.29a}$$

and the delay factor as:

$$\Delta^2 = \exp \left[-2 s T^o \sqrt{1 + \frac{\omega_c}{s}} \right] \quad T^o = \frac{Nd}{c} \tag{3.3.29b}$$

Yielding

$$R\left(\frac{is}{c}, \theta_1 = \theta_2 = 0 \right) = \frac{1 - N(s)}{1 + N(s)} - \frac{4 N(s)}{(1+N(s))^2}$$

$$\exp \left[-2 s T^o \sqrt{1 + \frac{\omega_c}{s}} \right] \cdot \sum_{n=1}^{\infty} \left[\left(\frac{1 - N}{1 + N} \right) \exp \left(-2 s T_0 \sqrt{1 + \frac{\omega_c}{s}} \right) \right]^{n-1} \tag{3.3.29c}$$

let

$$T^o_n = n T^o \sqrt{1 + \frac{\omega_c}{s}} \tag{3.3.29d}$$

39

then

$$R\left(\frac{is}{c},\ \theta_1 = 0\right) = \frac{1-N(s)}{1+N(s)} - \frac{4\,N(s)}{1+N(s)} \sum_{n=1}^{\infty} \left(\frac{1-N(s)}{1+N(s)}\right)^{n-1}$$

$$\exp\left[-2\,s\,T_n^o\right] \tag{3.3.30}$$

3.3.2.1.1 Lossless Case: $N(s) = N$, $T^o(s) = T^o$

In this case the Inverse Laplace transform can be evaluated straight forwardly, since only the pole at $s = -i\,\omega_o$ exists, and

$$\mathbf{f}^s(\underline{r},\ t_o,\ T,\ T_n^o) = \hat{y} \sum_{n=0}^{\infty} R_n\ U(t_o - 2n\,T^o)\left[1 - U(t_o - 2n\,T^o - T)\right]\underline{E}_o \tag{3.3.31a}$$

where

$$\underline{E}_o = \hat{x}\ 1\ dxp\left(-\frac{s}{c}\,\zeta^1\right)$$

$$R_o = \frac{1-N}{1+N} \tag{3.3.31b}$$

$$R_n = -\frac{4\,N}{(1+N)^2}\left(\frac{1-N}{1+N}\right)^{n-1} \qquad n = 1, 2, \ldots \tag{3.3.31c}$$

Thus if $2\,T^o > T$, the pulse returns are separated, in Fig. 3-5 the cases $N = 2$, $2\,T^o = 2T$ and $T = 2\,0\,T^o$ are plotted.

A meaningful application of pulse scattering to the problem of inverse scattering requires an operation with pulses of extremely small time-width, or of exceedingly large timewidth where $T < 2\,T^o$. Since it must be assumed that T^o is extremely small and the information from which the electric properties can be determined are the time delay factor T^o of the layer as well as the amplitude ratios of the partial pulse returns, these quantities must be distinctly measureable. The refractive index of the layer in the lossless case can be determined as the average value over the second to the mth time delayed pulse returns, excluding the first return as
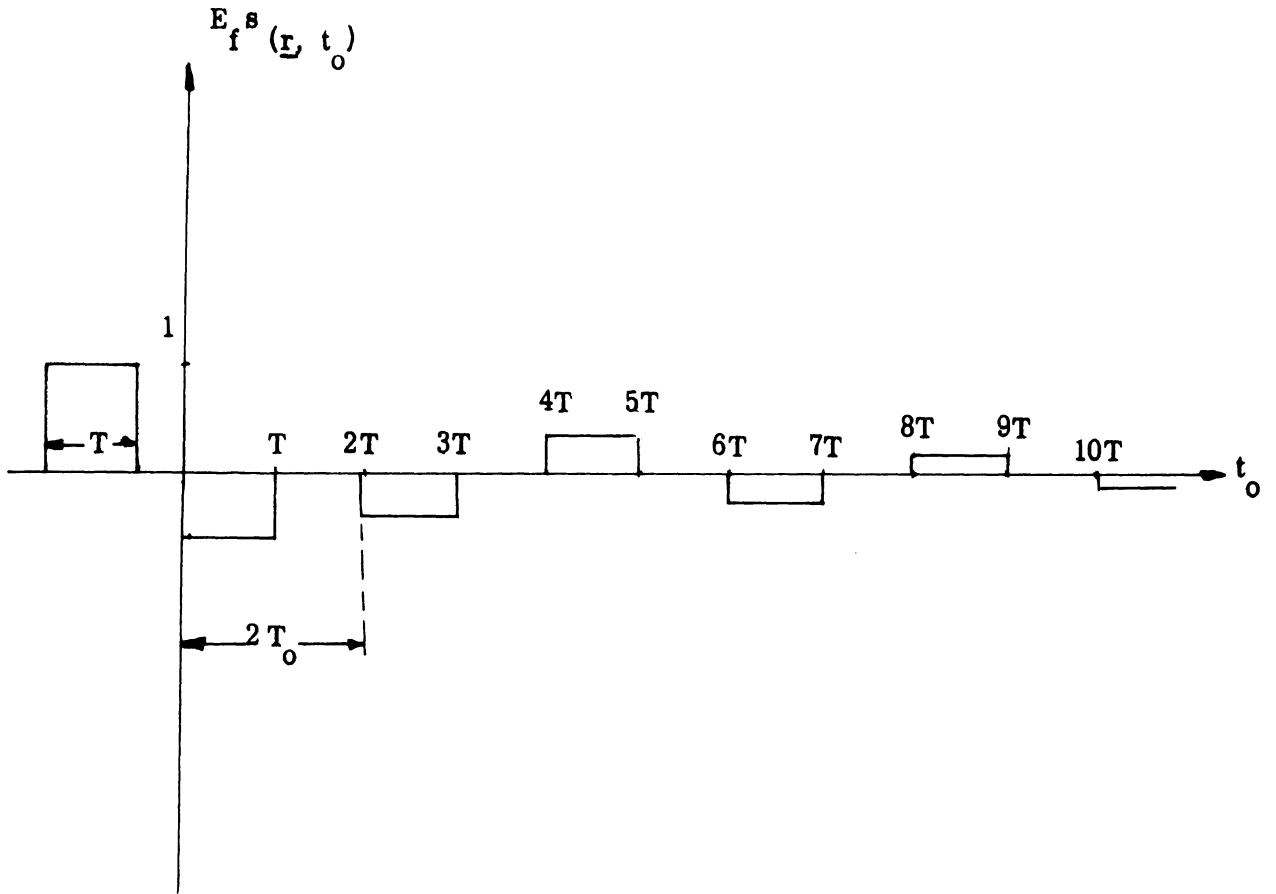
40

FIG. 3-5: PULSE SCATTERING FROM A GROUNDED LOSSLESS
DIELECTRIC SLAB (N = 2, T^o = T).

$$\overline{N} = \sum_{n=1}^{M} J \frac{1-\epsilon_n + 1, n}{\frac{1-1\ \epsilon_n +1,\ n}{in}}$$

(3.3.32a)

$$\epsilon_n + 1,\ n = \frac{R_n + 1}{R_n} = \frac{1-N}{1+N}$$

(3.3.32b)

and the depth of the layer then can be determined from the time delay factor T^o as

$$d = \frac{T^o C}{N}$$

(3.3.32c)

3.3.2.1.2   Lossy Case: $N(s) = N(1 + \frac{\omega_c}{s})^{1/2}$, $T^o(s) = T^o(1+\frac{\omega_c}{s})^{1/2}$

In this case in addition to the pole at $s = i\,\omega_0$ a branch cut will be introduced which degenerates into a pole at $s = -\omega_{c/2}$ for the slightly lossy case, where the following approximation may be implied:

$$N(s) = N\left(1 + \frac{\omega_c}{s}\right)^{1/2} = N\left(1 + \frac{1}{2}\ \frac{\omega_c}{s} - \frac{1}{8}\left(\frac{\omega_c}{s}\right)^2 \pm \right)$$

$$N\left(1 + \frac{\omega_c}{2s}\right) = \frac{N}{s}\left(s + \frac{\omega_c}{2}\right)$$

(3.3.33)

In general, the partial reflection coefficients for the lossy case at normal incidence are given as

$$E_V = \frac{1 - N(s)}{1 + N(s)} = \frac{\left[1 - N\left(1 + \frac{\omega_c}{s}\right)^{1/2}\right]}{\left[1 + N\left(1 + \frac{\omega_c}{s}\right)^{1/2}\right]} = \frac{1-N}{1+N}$$

$$+ \frac{2N}{1+N}\ \frac{\left[1 - \left(1 + \frac{\omega_c}{s}\right)^{1/2}\right]}{\left[1 + N\left(1 + \frac{\omega_c}{s}\right)^{1/2}\right]}$$

(3.3.34a)

42

$$E_W = 1 + E_V = \frac{2}{1+N} + \frac{2\,N}{1+N} \; \frac{\left[1 - \left(1 + \frac{\omega_c}{s}\right)^{1/2}\right]}{\left[1 + N\left(1 + \frac{\omega_c}{s}\right)^{1/2}\right]} \qquad (3.3.34\text{b})$$

$$H_W = 1 + H_V = 1 - E_V = \frac{2\,N}{1+N} - \frac{2N}{1+N} \cdot \frac{\left[1 - \left(1 + \frac{\omega_c}{s}\right)^{1/2}\right]}{\left[1 + N\left(1 + \frac{\omega_c}{s}\right)^{1/2}\right]} \qquad (3.3.34\text{c})$$

$$R_o = \frac{1-N}{1+N} + \frac{2\,N}{1+N} \; \frac{\left[1 - \left(1 + \frac{\omega_c}{s}\right)^{1/2}\right]}{\left[1 + N\left(1 + \frac{\omega_c}{s}\right)^{1/2}\right]} \qquad (3.3.35\text{a})$$

$$R_1 = - \frac{4\,N\left(1 + \frac{\omega_c}{s}\right)^{1/2} \Delta^2}{\left[1 + N\left(1 + \frac{\omega_c}{s}\right)^{1/2}\right]^2} = - \frac{4\,N}{(1+N)^2}$$

$$\cdot \frac{\left[1 - \frac{\left[1 - \left(1 + \frac{\omega_c}{s}\right)^{1/2}\right]\left[1 - N^2\left(1 + \frac{\omega_c}{s}\right)^{1/2}\right]}{\left[1 + N\left(1 + \frac{\omega_c}{s}\right)^{1/2}\right]^2}\right]}{}$$

$$\cdot \exp\left[-2\,s\,T^o\left(1 + \frac{\omega_c}{s}\right)^{1/2}\right] \qquad (3.3.35\text{b})$$

$$R_2 = - \frac{4\,N\left(1 + \frac{\omega_c}{s}\right)^{1/2}\left[1 - N\left(1 + \frac{\omega_c}{s}\right)^{1/2}\right]}{\left[1 + N\left(1 + \frac{\omega_c}{s}\right)^{1/2}\right]^3} = - \left\{ \frac{4N\,(1-N)}{(1+N)^3} \right.$$

$$\cdot \frac{\left[1 - \frac{\left[1 - \left(1 + \frac{\omega_c}{s}\right)^{1/2}\right]\left[1 - N^2\left(1 + \frac{\omega_c}{s}\right)^{1/2}\right]}{\left[1 + N\left(1 + \frac{\omega_c}{s}\right)^{1/2}\right]^2}\right]}{} \left. \right]$$

$$-\ \frac{8\,N^{2}\left(1+\dfrac{\omega_{c}}{s}\right)^{1/2}\left[1-\left(1+\dfrac{\omega_{c}}{s}\right)^{1/2}\right]^{3}}{+\,N\left(1+\dfrac{\omega_{c}}{s}\right)^{1/2}}\ \exp\left\{\left[-4s\,T^{o}\left(1+\dfrac{\omega_{c}}{s}\right)^{1/2}\right]\right. \qquad (3.3.35c)$$

$$R_{n}\ =\ \frac{4N\left(1+\dfrac{\omega_{c}}{s}\right)^{1/2}\left[1-N\left(1+\dfrac{\omega_{c}}{s}\right)^{1/2}\right]^{n-1}}{\left[1+N\left(1+\dfrac{\omega_{c}}{s}\right)^{1/2}\right]^{n+1}}\ \exp\left[-2n\,s\,T^{o}\left(1+\dfrac{\omega_{c}}{s}\right)^{1/2}\right] \quad (3.3.35d)$$

By inspection of (3.35) it follows that in the vicinity of the wavefronts of the partial pulse returns, i.e. for $(t_o - 2\pi\,T_o)\sim 0$, the behaviour is identical to that of the lossless case according to the Tauberian theorem of section 2.3. In general, the exact evaluation is tedious, since two branch points are introduced at $s_{b_1} = 0$ and $s_{b_2} = -\omega_c$, which for a small loss approximation degenerate into a pole at $S_p = -\dfrac{\omega_{c}/2}{N+1}$ since $N(s) \simeq N\left(1 + \dfrac{\omega_c}{2}\dfrac{1}{s}\right)$.

In this case the integrals can be evaluated straight forwardly and will be treated next:

Small Losses: $\quad N(s) \quad N\left(1 + \dfrac{\omega_c}{2}\dfrac{1}{s}\right)$

Applying the approximation of eq. (3.33), the partial reflection coefficients can be rewritten into:

$$R_o = \frac{1 - N(s)}{1 + N(s)} = \frac{1-N}{1+N}\cdot\frac{s+a}{s+b} \qquad\qquad a = \frac{\omega_c/2\ N}{N-1} \qquad (3.3.36a)$$

$$b = \frac{\omega_c/2\ N}{N+1}$$

$$R_1 = -\frac{4\,N(s)}{(1+N(s))^{2}}\ \exp\left(-2\,s\,T^{o}(s)\right) = \qquad\qquad c = \omega_c/2$$

$$= -\frac{4\,N}{(1+N)^{2}}\ \frac{s\,(s+c)}{(s+b)^{2}}\ \exp\left[-2\,T^{o}\,(s+\omega_c/2)\right] \qquad (3.3.36b)$$

44

$$R_n = \frac{4\,N}{(1+N)^2} \; \frac{s\,(s+c)}{(s+b)^2} \; \left(\frac{1-N}{1+N}\right)^{n-1} \left(\frac{s+a}{s+b}\right)^{n-1} \exp - n\,\omega_c\,T^o$$

$$\exp - 2n\;T^o\,s \qquad (3.3.36c)$$

The total reflection coefficient is thus given as

$$R_{tot}\,(s,\;\omega_c,\;T_o,\;N) = \frac{1-N}{1+N}\,\frac{s+a}{s+b} \; - \frac{4\,N}{(1+N)^2}\,\frac{s(s+c)}{(s+b)^2}$$

$$\chi \; \sum_{n=1}^{\infty} \left(\frac{1-N}{1+N}\right)^{n-1} \left(\frac{s+a}{s+b}\right)^{n-1} \cdot \exp\,(\,-n\,\omega_c\,T^o)\;\;dxp\,(-2n\,s\,T^o) \qquad (3.3.37)$$

The integration in the complex s-plane thus results simply in the evaluation of the pole at $s = -i\,\omega_0$ and about the nth order pole at

$s_p = -\dfrac{\omega_c}{2}\,\dfrac{N}{N+1}$, as illustrated in Fig. 3-6, there the inverse transform is
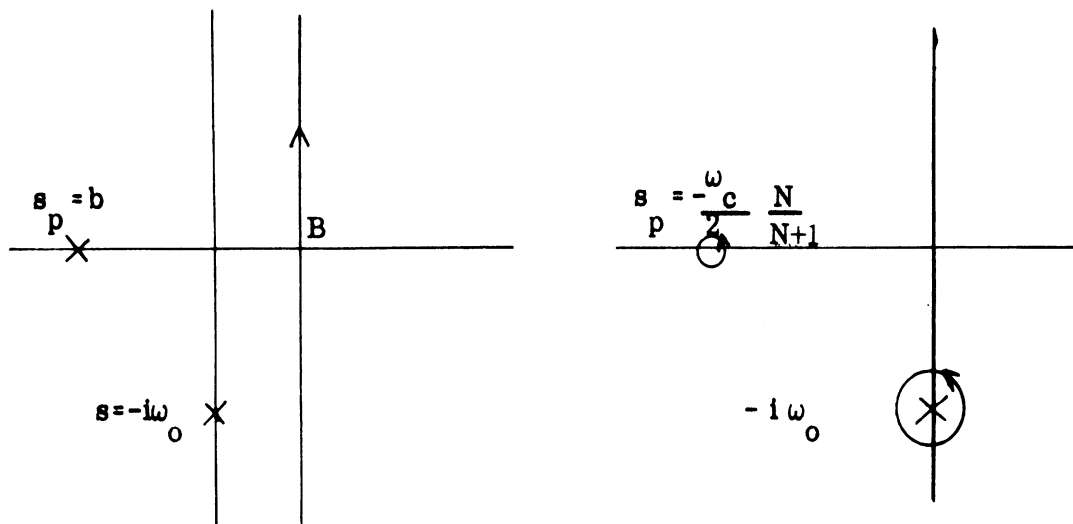
is given by:

FIG. 3-6: DEFORMATION OF CONTOUR FOR THE SLIGHTLY
LOSSY CASE $N(s) \simeq N\,(1 + \dfrac{\omega_c}{2}\,\dfrac{1}{s})$.

is given by:

$t_o = (t - Z/c)$	$\neq (s)$	$\overline{I}^- \left\{ \neq (s) \right\}$
$0 \leq t_o \leq T$ (3.3.39a)	$\left(\dfrac{1-N}{1+N}\right) \dfrac{(s+a)}{(s+i\omega_o)(s+b)}$	$\left(\dfrac{1-N}{1+N}\right)\left\{\dfrac{a-i\omega_o}{b-i\omega_o}\, e^{-i\omega_o t_o} - \dfrac{(a-b)}{b-i\omega_o}\, e^{-b t_o}\right\}$
$2T^o \leq t_o \leq T+2T^o$ (3.3.39b)	$\dfrac{-4N\exp(-\omega_c T^o)\, s(s+c)}{(1+N)^2\,(s+i\omega_o)(s+b)^2}$	$\dfrac{-4N\exp(-\omega_c T^o)}{(1+N)^2}\left\{\dfrac{-(\omega_o^2 - ic\omega)}{(b-i\omega)^2}\, e^{-i\omega t_o} - \left[\dfrac{b^2-bc}{i\omega_o-b}\, t_o - \dfrac{b(2i\omega-b)-ic\omega}{(i\omega-b)^2}\right]e^{-}\right\}$
$2nT^o \leq t_o \leq T+2nT^o$ $n = 1,2,\ldots$ (3.3.39c)	$\dfrac{-4N\exp(-n\omega_c T^o)\, s(s+c)(s+a)^{n-1}}{\left\lvert\dfrac{(1+N)}{(1-N)}\right\rvert^{n+1}(s+i\omega_o)(s+b)^{n+1}}$	$\dfrac{-4N(1-N)^{n-1}\exp(-n\omega_c T^o)}{(1+N)^{n+1}}\left\{-k_n e^{-i\omega t_o} + \left[k_o^1 + k_1 t + k_n t^n\right]e^{-bt}\right\}$

$$\underline{f}_1 (\underline{r}, t_0) = \frac{\hat{y}}{2\pi i} \int_{B-i\infty}^{B+i\infty} \frac{e^{s(t_0 +2/c)} R_{tot} (s, \omega_c, T_0, N)}{(s + i\omega_0)} \qquad (3.3.38)$$

The spatial time variable t_0 then is given by $t_0 = t - 2/c + 2 n T^0$ for the nth partial pulse return. The inverse transforms in this case yield:

(See Table)

Immediately it is recognized that at the trailing end of the pulse $(T \gg 2T^0)$, the transient contributions only will be present if b is small. The complete solution can be given as:

$$f^s (t_0, 2 n T^0) = R_0 (A_0 e^{-i\omega t_0} + B_0 e^{-b t_0}) \; U(t_0) \left[1 - U(t_0 - T) \right]$$

$$+ \sum_{n=1}^{\infty} R_n \left[A_n e^{-i\omega t_0} + (B_{n_0} + B_{n_1} t + B_{n_2} t^2 + \dots B_{nn} t^n) e^{-bt_0} \right]$$

$$\cdot U(t_0 - 2n T^0) \left[1 - U(t_0 - T - 2n T^0) \right] \qquad (3.3.39d)$$

where

$$R_0 = \frac{1-N}{1+N} \qquad (3.3.39e)$$

$$R_n = - \frac{4 N (1 - N)^{n-1}}{(1 + N)^{n+1}} \; \exp(-n \omega_c T^0) \qquad (3.3.39f)$$

and the A_n, B_{nn} may be determined by Heaviside's expansion theorem.

For $N \gg 1$, $a = b = c = \frac{\omega_c}{2}$, it can be seen that 3.3.37 simplifies to

$$R_{tot} (s, \omega_c, N \gg 1) = \frac{1-N}{1+N} - \frac{4 N}{(1+N)^2} \frac{s}{s+\omega_{c/2}} \sum_{n=1}^{\infty} \frac{1-N}{1+N}^{n-1}$$

$$\exp \left[-2n T^0 \left(\frac{\omega_c}{2} + s \right) \right] \qquad (3.3.40)$$

47

in which case the inverse transform of (3.3.39a) can be applied, yielding with
(3.3.39e, f):

$$f^s(t_0, 2n\,T^o, N \gg 1) = R_0\, e^{-i\omega t_0}\, U(t_0)\, \left[1 - U(t_0 - T)\right]$$

$$+ \left[A_0\, e^{-i\omega t_0} + B_0\, e^{\frac{-\omega_c}{2}\, t_0}\right] \sum_{n=1}^{\infty} R_n\, U(t_0 - 2n\,T^o)\, \left[1 - U(t_0 - T - 2n\,T^o)\right] \qquad (3.3.41)$$

Before the question will be answered, whether the parameters N, ρ, d of the layer can be uniquely determined from pulse scattering methods, the case of large losses will be treated briefly.

Large Losses: $N(s) = N\, \sqrt{1 + \frac{\omega_c/2}{}}^{1/3}$

The partial reflection coefficients for large losses are defined by Eq.(3.3.35) where it was shown that the behaviour in the vicinity is aside from the material attenuation factor $\exp(-n\,T^o \omega_c)$ identical to that of the lossless case. An exact evaluation of the I. L. T. in general will imply convolution methods, where the pole at $s = i\omega_c$ will be extracted and the I. L. T. then must be solved for the case of delta pulse incidence and the following types of integrals must be evaluated in the complex s-plane:

$$f^s_{0_1}(\underline{r}, t_0) = \frac{\hat{y}}{2\pi i} \int_{B-i\infty}^{B+i\infty} \frac{e^{st}\left[1 - N\,(1 + \frac{\omega_c}{s})^{1/2}\right]}{\left[1 + N\,(1 + \frac{\omega_c}{s})^{1/2}\right]^{n+1}}\, ds \qquad (3.3.42a)$$

and

$$f^s_{n_1}(\underline{r}, t_0) = \frac{\hat{y}\, 4N}{2\pi i} \int_{B-i\infty}^{B+i\infty} \frac{e^{st}\left[1 - N\,(1 + \frac{\omega_c}{s})^{1/2}\right]^{n-1}}{\left[1 + N\,(1 + \frac{\omega_c}{s})^{1/2}\right]^{n+1}}$$

$$\cdot (1 + \frac{\omega_c}{s})^{1/2}\, \exp\left[-2n\,T_0\,(1 + \frac{\omega_c}{s})^{1/2}\right]\, ds \qquad (3.3.42b)$$

48

Introducing the following transformation $U = \frac{s}{\omega_c}$ it can be seen that both types of integrals have branch points at $U = 0$ and $U = -1$, where 3.3.47a, b become:

$$f_{o_1}^s (\underline{r}, p = \omega_c t) = \frac{\hat{y}\,\omega_c}{2\pi i} \int_{B^1-i\infty}^{B^1+i\infty} \frac{e^{up} \left[\lceil u \rceil - N(u+1)^{1/2} \right]}{\lceil u \rceil + N(u+1)^{1/2}} du \qquad (3.3.43a)$$

$$f_{n_1}^s (\underline{r}, p = \omega_c t_o) = - \frac{2 N \omega_c \hat{y}}{\pi i} \int_{1-i\infty}^{B^1+i\infty} \frac{e^{up}(u+1)^{1/2} u^{1/2} \left[u^{1/2} - N(u+1)^{1/2} \right]^{n-1}}{\left[U^{1/2} + N(u+1)^{1/2} \right]^{n+1}}$$

$$\cdot\, e^{-2n T_o \omega_c u^{1/2}(u+1)^{1/2}} du \qquad (3.3.43b)$$

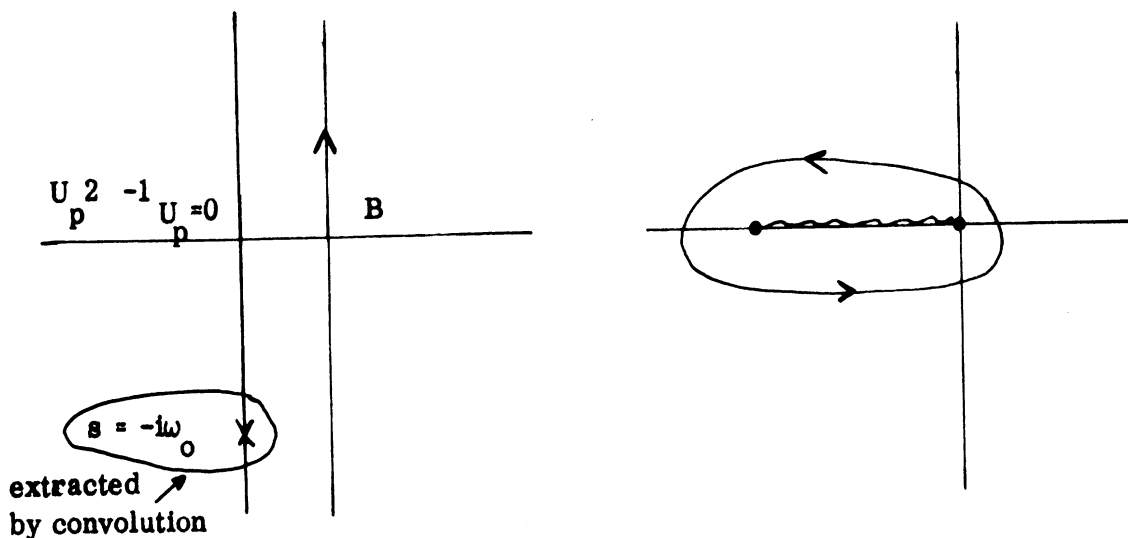The behaviour in the complex u - plane is illustrated in Fig. 3-7:

FIG. 3-7: DEFORMATION OF CONTOUR.

Introducing the new variable $U = V_e \pm i \pi$, where the positive sign corresponds to the top sheet, it can be shown that by adding the contributions of both sides around the branchcut, 3.3.43a becomes:

$$\hat{y} \cdot \underline{f}^s_{o_1}(\underline{r},\ p=\omega_c t) = \frac{\omega_c N}{2\pi i} \int_0^1 \frac{-4\,i\,v^{1/2}(1-v)^{1/2}\,e^{-vp}}{\left[v + (1-v)\,N\right]}\,dv$$

$$= -\frac{2\omega_c}{\pi} \int_0^1 \frac{v^{1/2}(1-v)^{1/2}\,e^{-vp}}{\left[1 - (1-\frac{1}{N})\,v\right]}\,dv \qquad (3.3.44a)$$

which for N = 1 only is tabulated, then

$$\hat{x} \cdot f^s_{o_1}(\underline{r},\ p=\omega_c t) = -\frac{8}{\pi}\,\frac{1}{t}\,e^{-\frac{\omega_c}{2}t}\ I_1\left(\frac{\omega_c}{2}t\right) \cdot U(t) \qquad (3.3.44b)$$

Also the contribution to the second pulse return can be evaluated for N=1 , using the transform pair 5.6.45 of $\left[\text{Bateman}\ \right]$ by proper repeated differentiation with respect to b = 2 $T^o \omega_c$:

$$\hat{y} \cdot \underline{f}^s_{11}(\underline{r},\ p=\omega_c t) = -\frac{16\,(t-2\,T^o)}{\omega_c\,(t+2\,T^o)^3}\,e^{-1/2\,\omega_c t}\ I_2\left(\frac{\omega_c}{2}\right)t \cdot U(t-2\,T^o) \qquad (3.3.45a)$$

Similarly the consequent pulse returns can be evaluated using convolution properties and the transform pair (5.6.22) of $\left[\text{Bateman}\ \right]$ The exact results will not be given here, but it can be concluded that for $t > 2n\ T^o$:

$$\hat{x} \cdot f^s_{n_1}(\underline{r},\ p=\omega_c t) \sim \frac{1}{t^{n+1}}\,e^{-1/2\,\omega_c t}\ I_{n+1}\left(\frac{\omega_c}{2}\ t\right)\ U(t-2n\ T^o) \qquad (3.3.45b)$$

In Fig. 3-8 the results of x $f^s_{n_1}(\underline{r},\ p=\omega_c t)$ are plotted for N=1 It can be immediately recognized that the higher order pulse returns decay exceedingly fast.
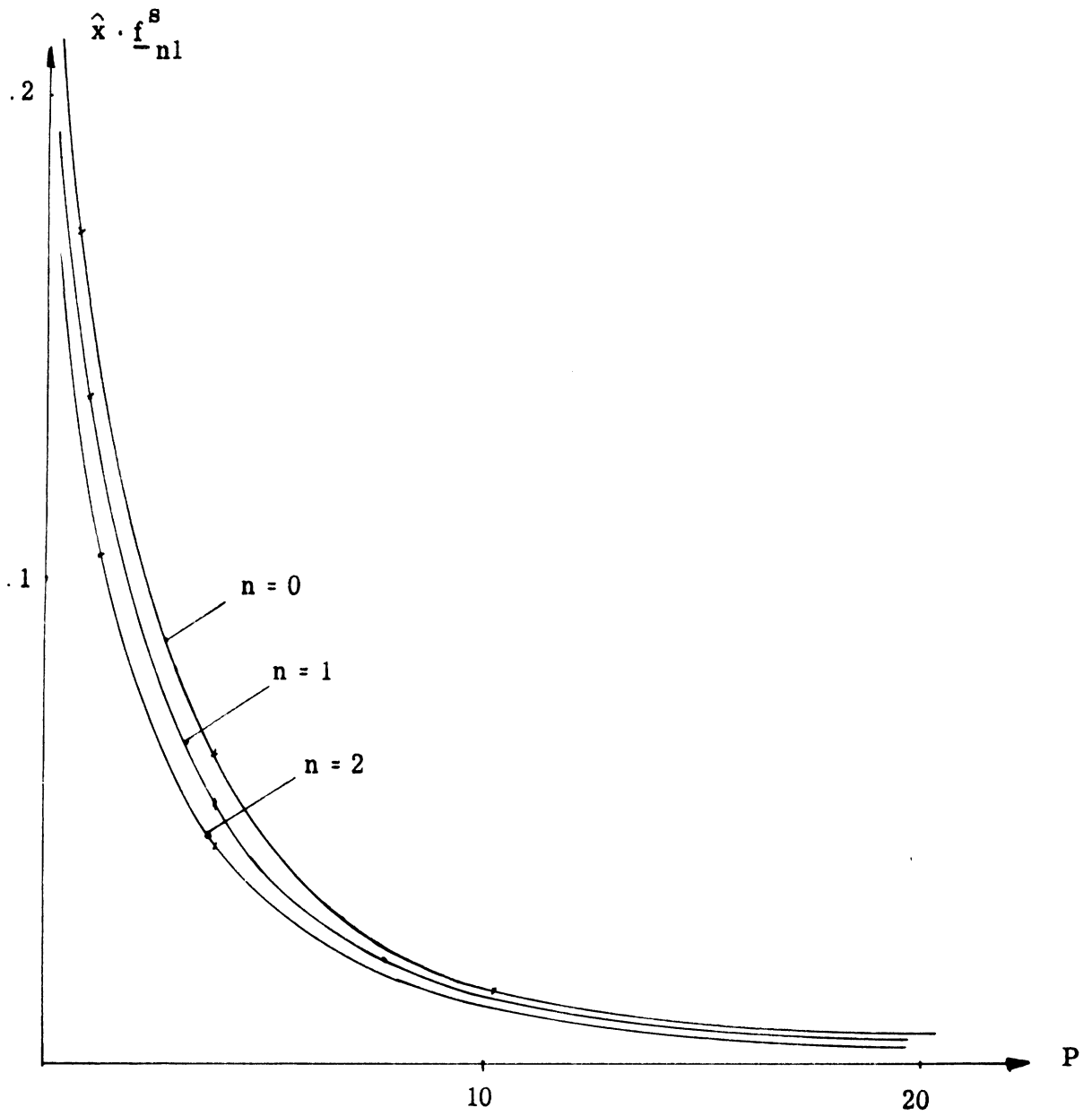
50

FIG. 3-8: $\hat{x} \cdot \underline{f}^{s}_{n1}$ $(\underline{r}_1 p = \omega_c t)$ $= \dfrac{\exp\left(-\dfrac{1}{2}\,\omega_c t\right)}{t^{\,n+1}}\; I_{n+1}\left(\dfrac{\omega_c}{2}\,t\right)$

For $N \neq 1$ no closed form solutions exist for any of 3.3.43. Yet enough information has been obtained to derive conclusions about the possibility of identifying the parameters N, ω_c, T, from which ϵ_2, σ_2 and d may be determined.

If the wavefront amplitudes are distinctly determinable and the pulse returns seperated, i.e. $T < 2 T^o$, then the ratio

$$\bar{\epsilon} = \frac{1}{m} \sum_{n=1}^{m} \frac{R_{n+1}}{R_n} \approx \left(\frac{1-N}{1+N} \right) e^{-\omega_c T^o} \qquad (3.3.46)$$

can be determined and T^o from the seperation of the individual pulse returns. The attenuation factor exp $(-\omega_c T^o)$ must be determined from the oscillogram of the individual partial pulse returns. Thus for lossy coating the pulse scattering method seems not to be the best approach. In figure the pulse returns for $N =$ const., d $=$ const. are plotted for various values of σ to illustrate this point.

3.3.2.2 Oblique Incidence.

At oblique incidence the TE and the TM-cases must be treated se-perately, however as long as $\sigma_2 = 0$ and $N(s) = N$, the evaluation of the inverse transforms is identical to that of normal incidence on a lossless structure For the TE-case the reflection coefficient are given by Eqs.(3.3.8) to (3.3.11) and (3.3.21b) and the delay time of the partial pulse returns by (3.3.19a) which is the same for the TM-case. For the TM-case the reflection and trans-mission coefficients are given by Eqs.(3.3.13) to (3.3.15) and (3.3.21c).

Since the plane wave concept was applied, it is arbitrary where the observation point is located, thus let R $(0, 0, Z_o)$ and r $= Z_o \cos \theta$, see Fig.3-4. The solution then is given as:

$$\underline{f}^s (r, t_o, \theta_1) \Big|_{TE, TM} = \hat{y} \sum_{n=0}^{\infty} R_{n_{TE, TM}} U(t_o - 2n T^o)$$

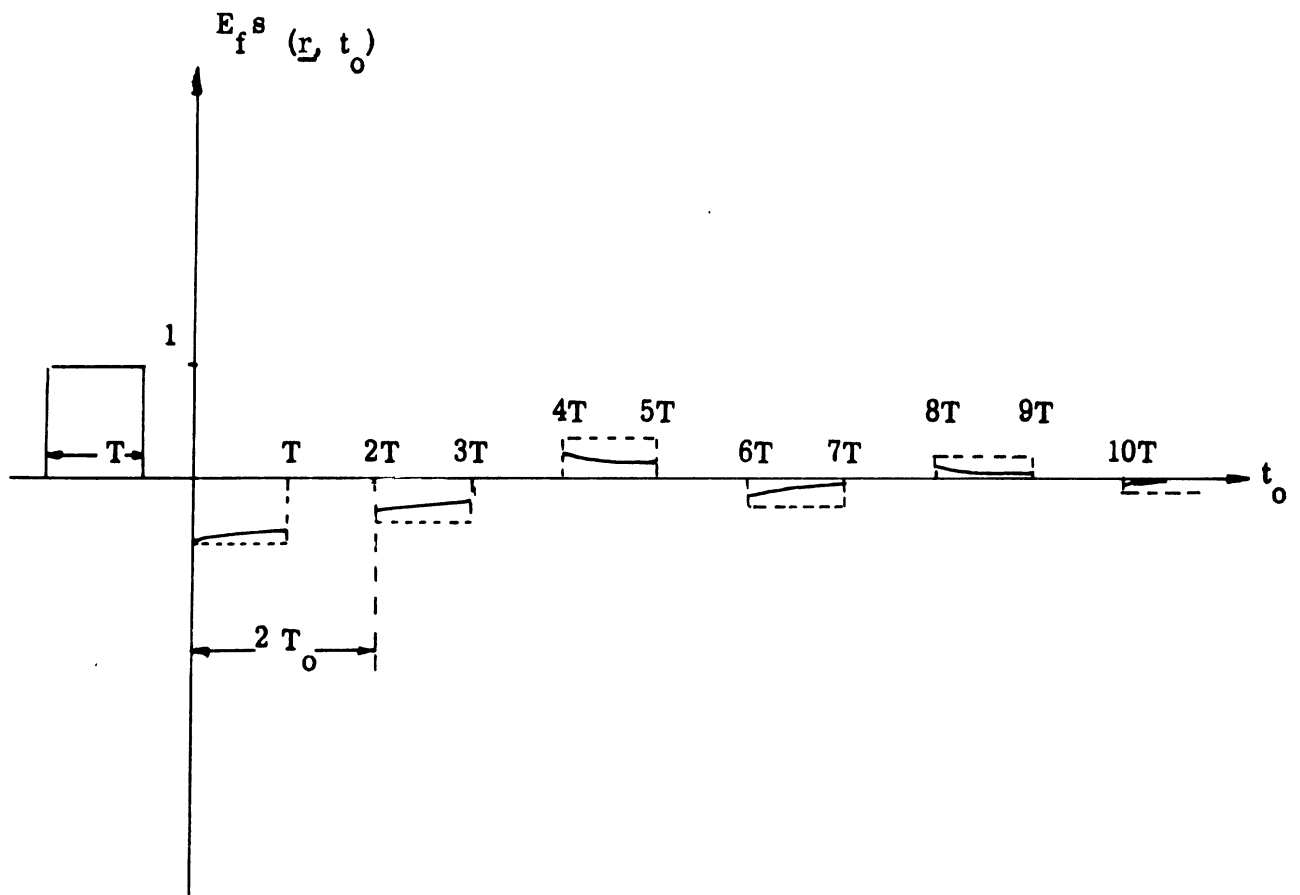$$\left[1 - U (t_o - 2n T^o \underline{\ }T \right]$$

52

FIG. 3-9: PULSE SCATTERING FROM A LOSSY GROUNDED DIELECTRIC SLAB (N = 2, T^o = T, $\omega_c \neq 0$).

One special case is of interest, namely the TM-case at critical incidence,

i. e. if $\tan \theta_{1_{Br}} = N$, $(\theta_{1_{Br}} \triangleq$ Brewster angle) which will be discussed in more detail.

3.3.2.3. Behaviour at the Brewster Angle for TM-Incidence.

In this case ${}^{H}V^{TM} = -{}^{E}V^{TM} = 0$, and ${}^{E}W^{TM} = 1$ ${}^{H}W^{TM}$, thus it follows from (3.20) that there only will exist one partial pulse return, namely the second pulse return or the first internally reflected one, where

$$R_o = {}^{H}V^{TM} = 0$$

$$R_1 = {}^{H}W^{TM} \; U \; {}^{H}W^{TM} \cdot \Delta^2 = - \exp (-i2 \; T^o \omega)$$

$$R_n \; (n>1) = 0 \tag{3.3.48}$$

and

$$R_{tot}^{TM} \; (\theta_1 = \theta_{1_{Br}}) = \frac{i \tan (T^o \omega) - 1}{i \tan (T^o \omega) - 1} = - \exp (- i \, 2 \; T^o \, \omega) \tag{3.3.49}$$

This particular behaviour that at Brewster angle incidence only one pulse return will be observed, may be used to determine the refractive index if the angle of incidence is known precisely. However from this measurement alone the depth of the layer cannot be determined. To find some information about the depth of the layer, the angle of incidence has to be changed such that the delay time T^o (θ_1) can be determined.

In this case $\sigma \neq 0$, the behaviour becomes too complex and pulse scattering at oblique incidence is not useful. Only in the case of small losses and at Brewster angle incidence satisfactory results for the determination of the refractive index may be obtained.

ANALYSIS OF THE COMPUTATIONAL RESULTS FOR
THE APPLICATION OF THE BOUNDARY CONDITIONS
$$\underline{E}_T \times \underline{E}_T^* = 0, \text{ AND } \left|\underline{E}_i\right| - \left|\underline{E}_s\right| = 0.$$

4.1 Introduction.

In the following outlines, further computational results will be presented

in addition to those given in Quarterly Report No. 8579-3-Q (Weston et al, 1967)

where the application of these two boundary conditions to the test case of a

perfectly conducting sphere of electric measure $ka = 2$ was discussed. There

the expressions for $\underline{E}_i$ (incident field), $\underline{E}_s$ (scattered field), and $\underline{E}_T = \underline{E}_i + \underline{E}_s$

are defined as well as the properties of the two boundary conditions.

In particular, it was shown that $\left\{\left|\underline{E}_i\right| - \left|\underline{E}_s\right|\right\}$ possesses only one minimum

apart from a limited conical section about the focal point in the shadow region.

Because of the vector nature, this condition proves to be rather dependent

upon local polarization properties and in general will not yield the proper

surface locus, apart from a limited conical section about the specular point.

The boundary condition $\underline{E}_T \times \underline{E}_T^*$; in contrast, is applicable far into the

shadow region with a very pronounced minimum at the proper point which lies

on the surface of the scatterer. The application of this condition is however

limited due to the fact that in addition to the proper surface locus, a family of

concentric surface loci (hyperboloids of revolution) will be obtained, though of

less pronounced minima (see Figs. 3-3a to 3-3d of 8579-3-Q) which were found

to lie exterior to the proper surface locus. The resulting minima in specular

direction ($\theta = 180^{\circ}$) are spaced at equidistant intervals of $k \triangle R = \pi/2$. Finally

it was pointed out that both boundary conditions have to be employed simulta-

neously to precisely determine the point which may lie on the surface of the

scatterer.

These properties of how to employ the boundary conditions properly,

required the computation of further test cases, including spherical test cases

of larger electric measure as well as prolate spheroids. The results obtained

are presented in the following.

4.2 Spherical Test Cases.

Employing the notation of Stratton (1941), the expansion coefficients for spheres of electric measure $ka = 5$ and $ka = 10$ were computed as

$$f^s_{o1n} = (i)^n \frac{n(n+1)}{2} \quad a_n = -(i)^n \frac{n(n+1)}{2} \left[\frac{j_n(\rho)}{h^{(1)}_n(\rho)} \right] \quad \rho = ka \qquad (4.1)$$

$$g^s_{e1n} = -(i)^{n+1} \frac{n(n+1)}{2} \quad b_n = (i)^{n+1} \frac{n(n+1)}{2} \left[\frac{(\rho j_n(\rho))^1}{(\rho h^{(1)}_n(\rho))^1} \right] \quad \rho = ka . \qquad (4.2)$$

In Tables 1 and 2, the coefficients for the particular test samples are given.

Applying the two boundary conditions $\underline{E}_T \times \underline{E}^*_T = 0$, and $\left\{ \left| \underline{E}_i \right| - \left| \underline{E}_s \right| \right\} = 0$ to the near field expansions, computational results are obtained (see Figs. 4-1a to 4-1g) which are very similar to those of the spherical test case $ka = 2$ as presented in Figs. 3-3a to 3-3d of 8579-3-Q.

Because of the symmetry properties, the obtained results for azimuthal dependence ϕ, $\phi + \pi$ are identical and it is sufficient to plot the resulting curves for one ϕ quadrant over $\theta = 180^\circ (-n\, 7.5^\circ)\, 0^\circ$, where in Figs. 4-1a to 4-1g the results for both $ka = 5$ and $ka = 10$ are plotted. It can be seen that except for additional pseudo surface loci within the proper surface locus of the associated sphere, the distribution of the surface loci of either condition is identical in character for all three cases $ka = 2, 5, 10$. The presence of the additional pseudo loci within the proper surface locus of the particular sphere in question required further investigation. It was then found that the appearance of these additional surface loci depends upon the number of expansion terms which are used in the near field expansion. This is illustrated in Figs. 4-2a to 4-2f, where the values of $\left\{ \underline{E}_T \times \underline{E}^*_T \right\}$ and $\left\{ \left| \underline{E}_i \right| - \left| \underline{E}_s \right| \right\}$ are

TABLE 4-1: EXPANSION COEFFICIENTS FOR THE SPHERICAL TEST CASE ka = 5.

n	$\mathrm{Re}\{f_{oln}\}$	$\mathrm{Im}\{f_{oln}\}$	$\mathrm{Re}\{g_{eln}\}$	$\mathrm{Im}\{g_{eln}\}$
1	0.4124466	-0.2173557	-0.7760094	0.4169158
2	1.200139	-1.469722	1.449289	-1.886731
3	-0.4013607	5.973030	0.1973786E-02	0.1088063
4	-5.010763	-4.999988	4.409093	2.642056
5	4.499645	-1.499734	-3.963083	6.613639
6	0.1782615	1.926581	-3.339949	-0.5453657
7	-0.4877635	0.8499482E-02	0.1734405E-01	-0.6966581
8	-0.1805431E-03	-0.8061960E-01	0.1020575	0.2893283E-03
9	0.9469407E-02	-0.1992659E-05	-0.2831584E-05	0.1128810E-01
10	0.1284376E-07	0.8404801E-03	-0.9685428E-03	-0.1705591E-07

TABLE 4-2: EXPANSION COEFFICIENTS FOR THE SPHERICAL TEST CASE ka = 10.

n	$\mathrm{Re}\{f_{oln}\}$	$\mathrm{Im}\{f_{oln}\}$	$\mathrm{Re}\{g_{eln}\}$	$\mathrm{Im}\{g_{eln}\}$
1	-0.4878377	-0.6096100	-0.3913659	-0.4880560
2	1.767869	1.475888	-1.474155	-1.222750
3	2.121697	0.8790562	5.150302	2.091937
4	-9.997529	0.1571675	-0.2891902	0.8370103E-02
5	6.574667	-3.891155	-10.79425	6.737797
6	3.204104	-7.551152	6.915772	-18.40077
7	9.203276	24.54987	4.963214	10.69282
8	-32.51425	-10.64596	5.994395	1.027457
9	22.34951	-19.90205	-11.65034	19.71129
10	6.768880	18.06850	-24.09158	-14.23931
11	-9.214209	1.312489	3.855611	-15.47917
12	-0.1428198	-3.334598	4.980965	0.3193848
13	0.8995424	-0.8892920E-02	-0.1527055E-01	1.178722
14	0.3389343E-03	0.1886478	-0.2287811	-0.4984860E-03
15	-0.3196965E-01	0.8517152E-05	0.1147929E-04	-0.3711489E-01
16	-0.1493902E-06	-0.4507445E-02	0.5094764E-02	0.1908575E-06
17	0.5398010E-03	-0.1904478E-08	-0.2346889E-08	0.5992278E-03
18	0.1818520E-10	0.5576441E-04	-0.6109958E-04	-0.2183134E-10
19	-0.5030335E-05	0.1331804E-12	0.1567326E-12	-0.5457031E-05
20	-0.7627612E-15	-0.4002248E-06	0.4307819E-06	0.8836814E-15

$\phi = 0^o$

$\theta = 0^o$

ka = 5
N = 10

ka = 10
N = 20

$\theta = 45^o$

$\theta = 45^o$

$C_{ext.}$

$\theta = 90^o$

$\theta = 90^o$

$C_{int.}$

$\theta = 135^o$

$\theta = 135^o$

$\theta = 180^o$

$\left\{ |\underline{E}_i| - |\underline{E}_s| \right\}$

$\left\{ -|\underline{E}_T \times \underline{E}_T^*|^2 \right\}$
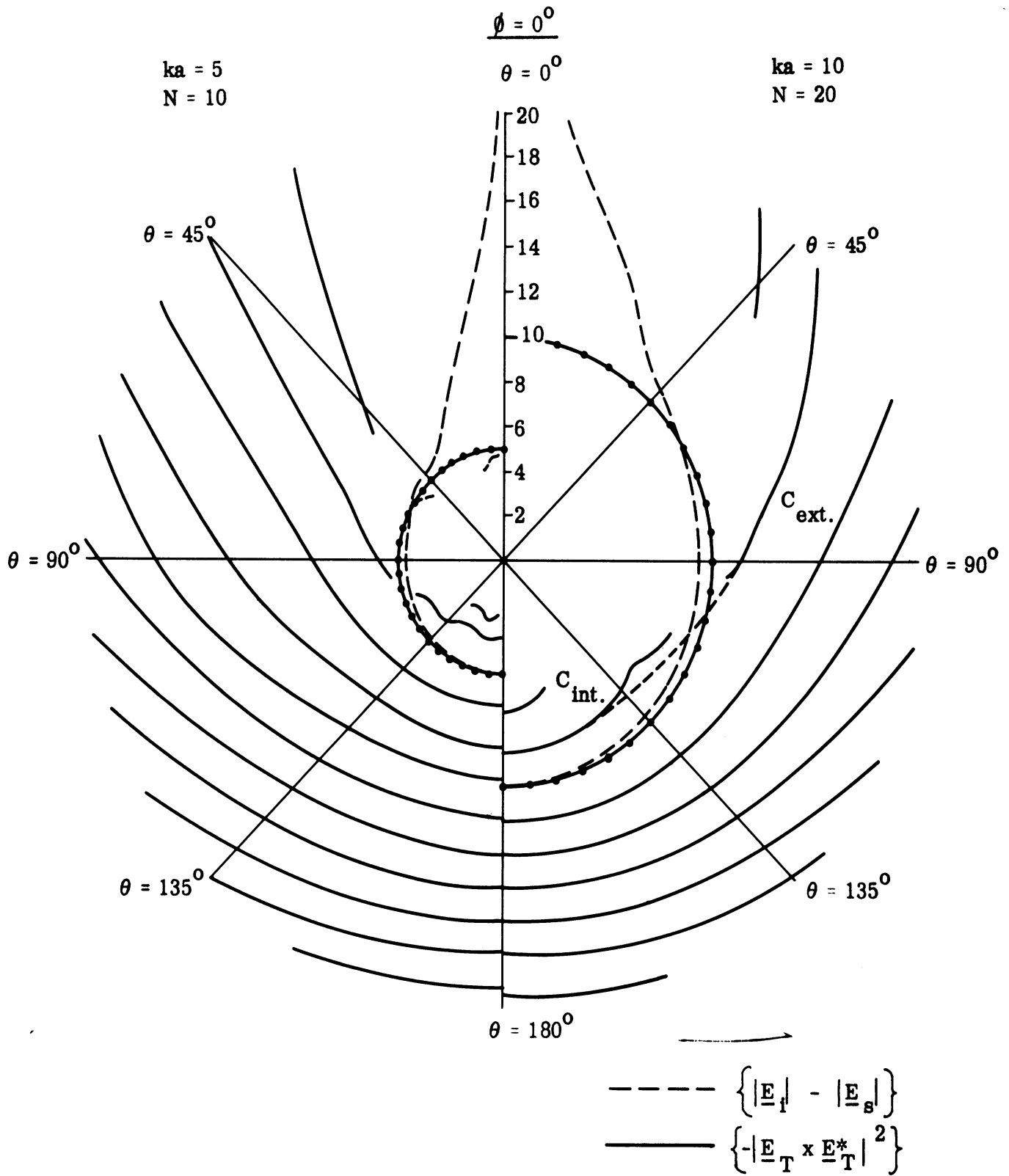
FIG. 4-1a: RESULTING SURFACE LOCI FOR THE SPHERICAL
TEST CASES ka = 5, 10. $\phi = 0^o$.

58

$$\phi = 15^O$$

ka = 5
N = 10

$$\theta = 0^O$$

ka = 10
N = 20

$$\theta = 45^O \qquad \theta = 45^O$$

$$\theta = 90^O \qquad \theta = 90^O$$

$$\theta = 135^O \qquad \theta = 135^O$$

$$\theta = 180^O$$

$$----\left\{ |\underline{E}_i| - |\underline{E}_s| \right\}$$

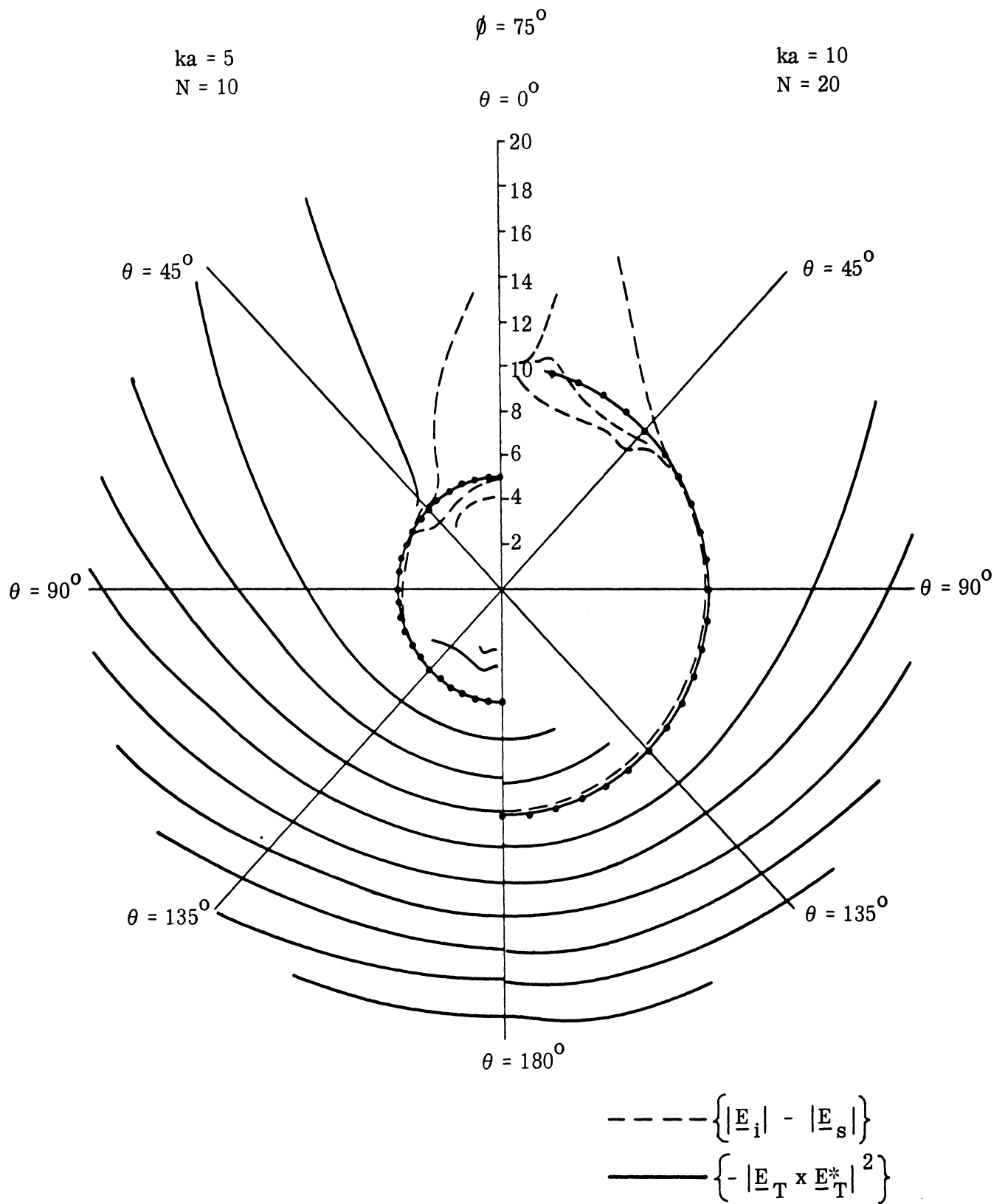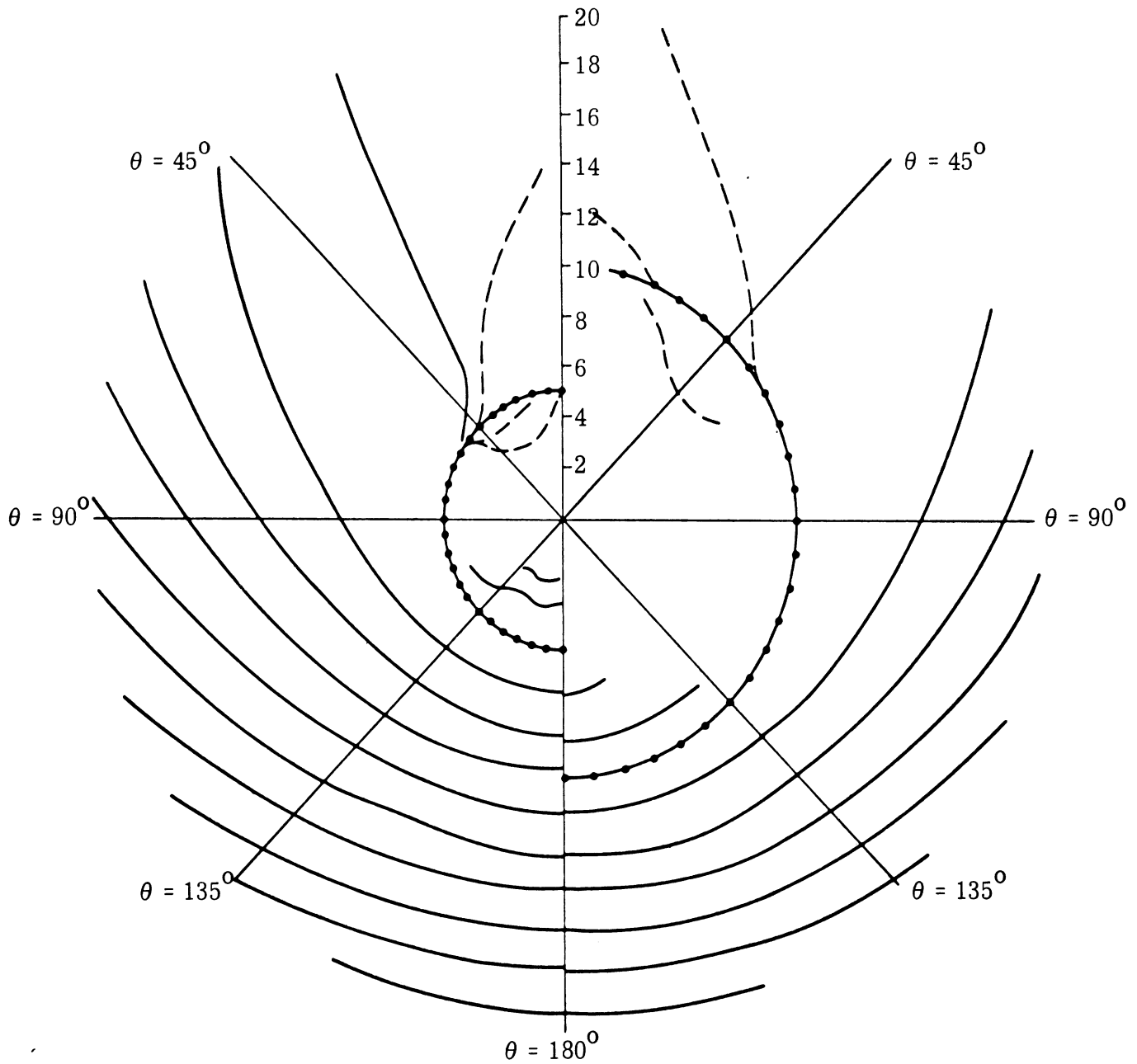$$\rule{1cm}{0.4pt}\left\{ -|\underline{E}_T \times \underline{E}_T^*|^2 \right\}$$
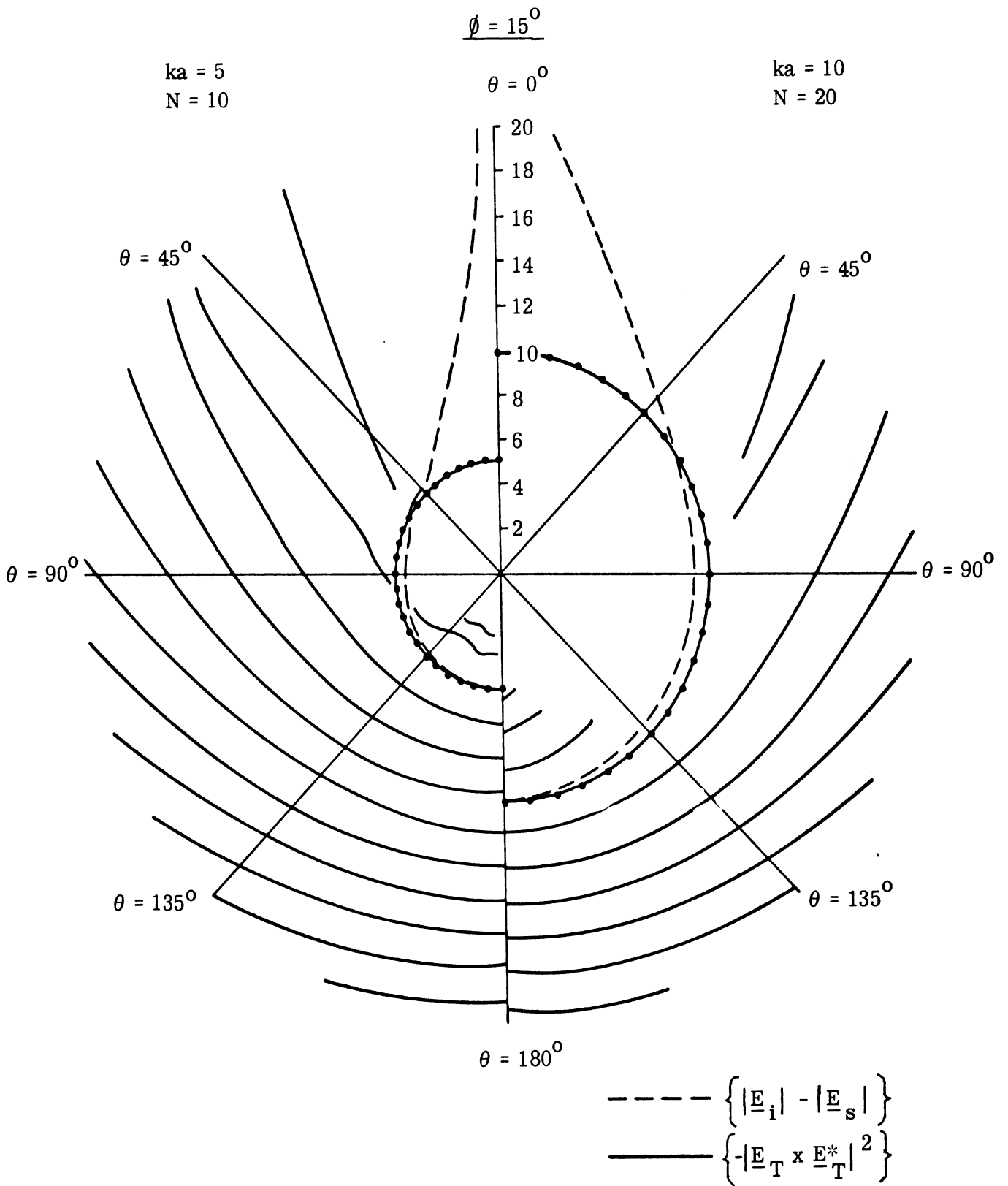
FIG. 4-1b: RESULTING SURFACE LOCI FOR THE SPHERICAL
TEST CASES ka = 5, 10. $\phi = 15^O$.

59

$\phi = 30^{\rm o}$

ka = 5
N = 10

ka = 10
N = 20

$\theta = 0^{\rm o}$

$\theta = 45^{\rm o}$

$\theta = 45^{\rm o}$

$\theta = 90^{\rm o}$

$\theta = 90^{\rm o}$

$\theta = 135^{\rm o}$

$\theta = 135^{\rm o}$

$\theta = 180^{\rm o}$

$- - - - \left\{ \left| \underline{E}_i \right| - \left| \underline{E}_s \right| \right\}$

$------ \left\{ - \left| \underline{E}_T \times \underline{E}_T^* \right|^2 \right\}$
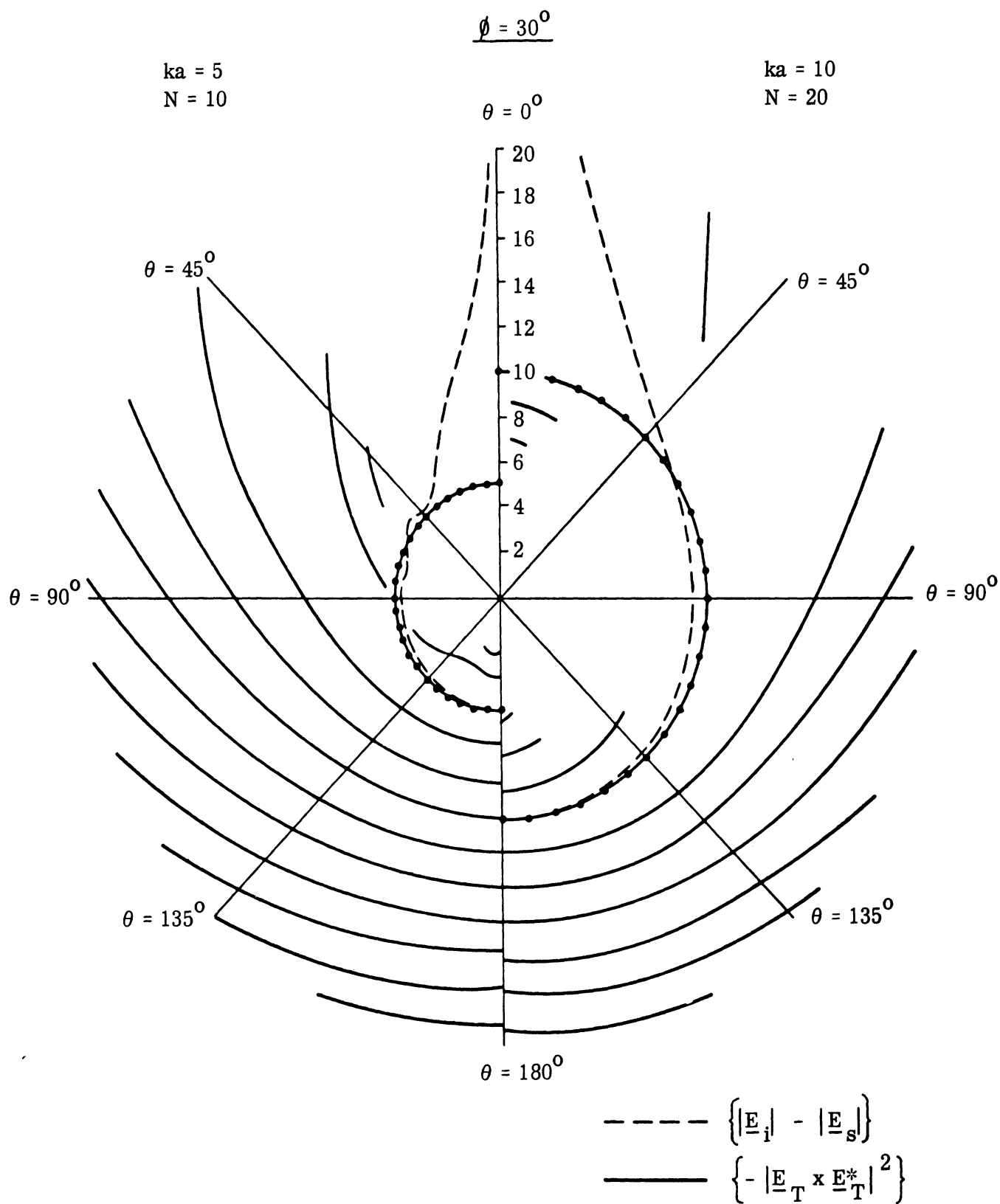
FIG. 4-1c: RESULTING SURFACE LOCI FOR THE SPHERICAL
TEST CASES ka = 5, 10. $\phi = 30^{\rm o}$.

60

$\phi = 45^\circ$

ka = 5
N = 10

$\theta = 0^\circ$

ka = 10
N = 20

$\theta = 45^\circ$

$\theta = 45^\circ$

$\theta = 90^\circ$

$\theta = 90^\circ$

$\theta = 135^\circ$

$\theta = 135^\circ$

$\theta = 180^\circ$
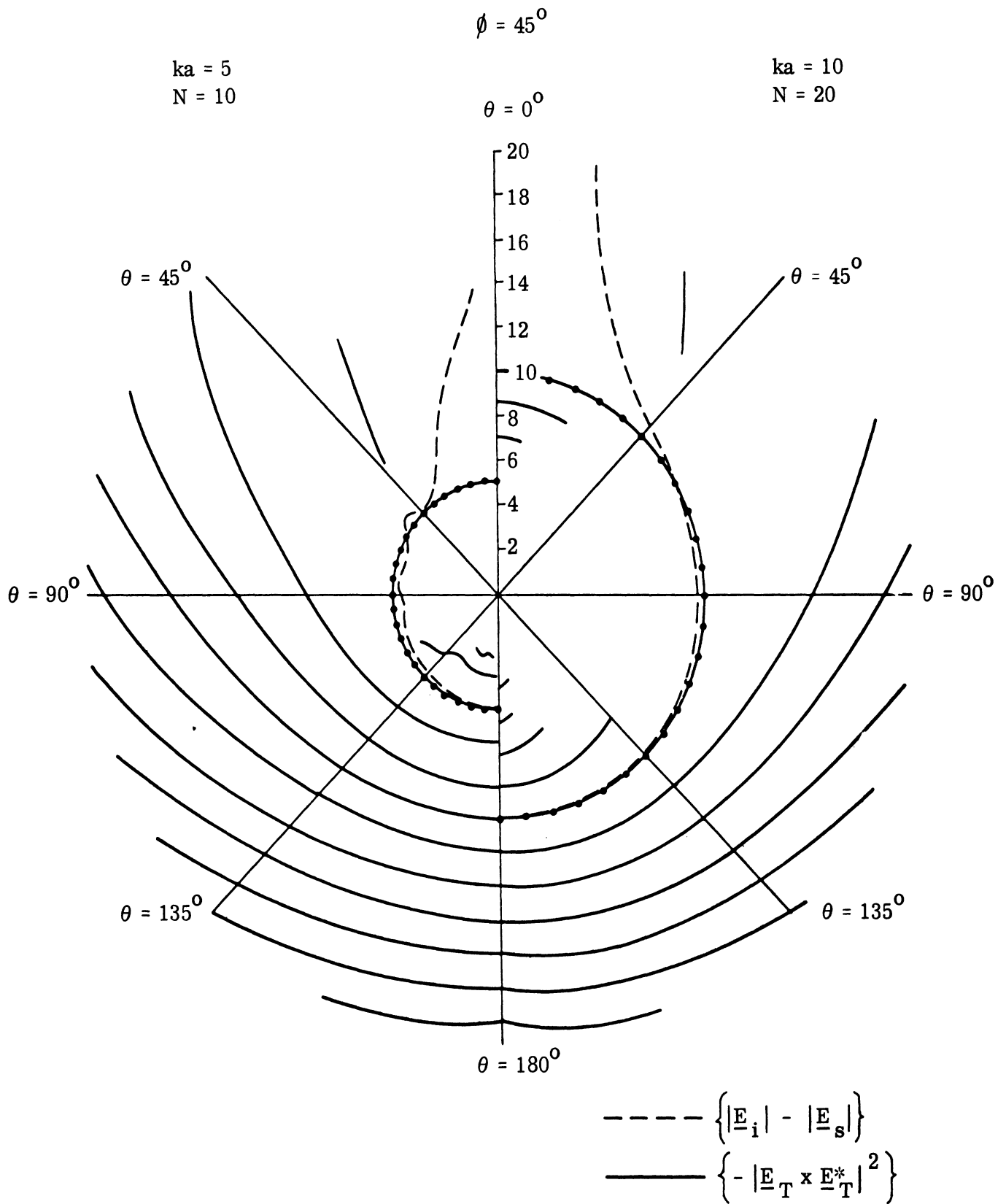
$- - - -\ \left\{ |\underline{E}_i| - |\underline{E}_s| \right\}$

$-\!\!-\!\!-\ \left\{ - |\underline{E}_T \times \underline{E}_T^*|^2 \right\}$

FIG. 4-1d: RESULTING SURFACE LOCI FOR THE SPHERICAL
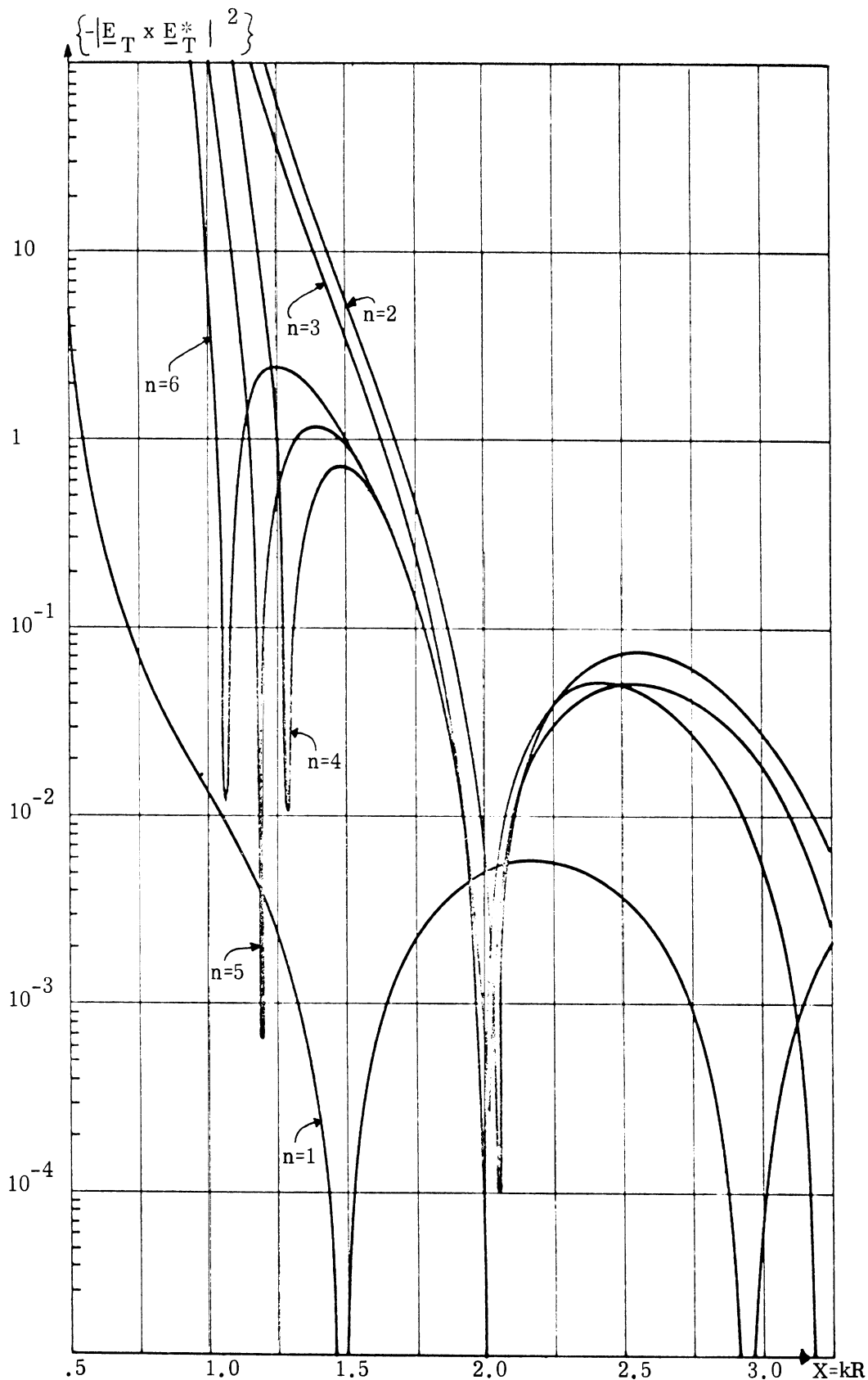TEST CASES ka = 5, 10. $\phi = 45^\circ$.

61
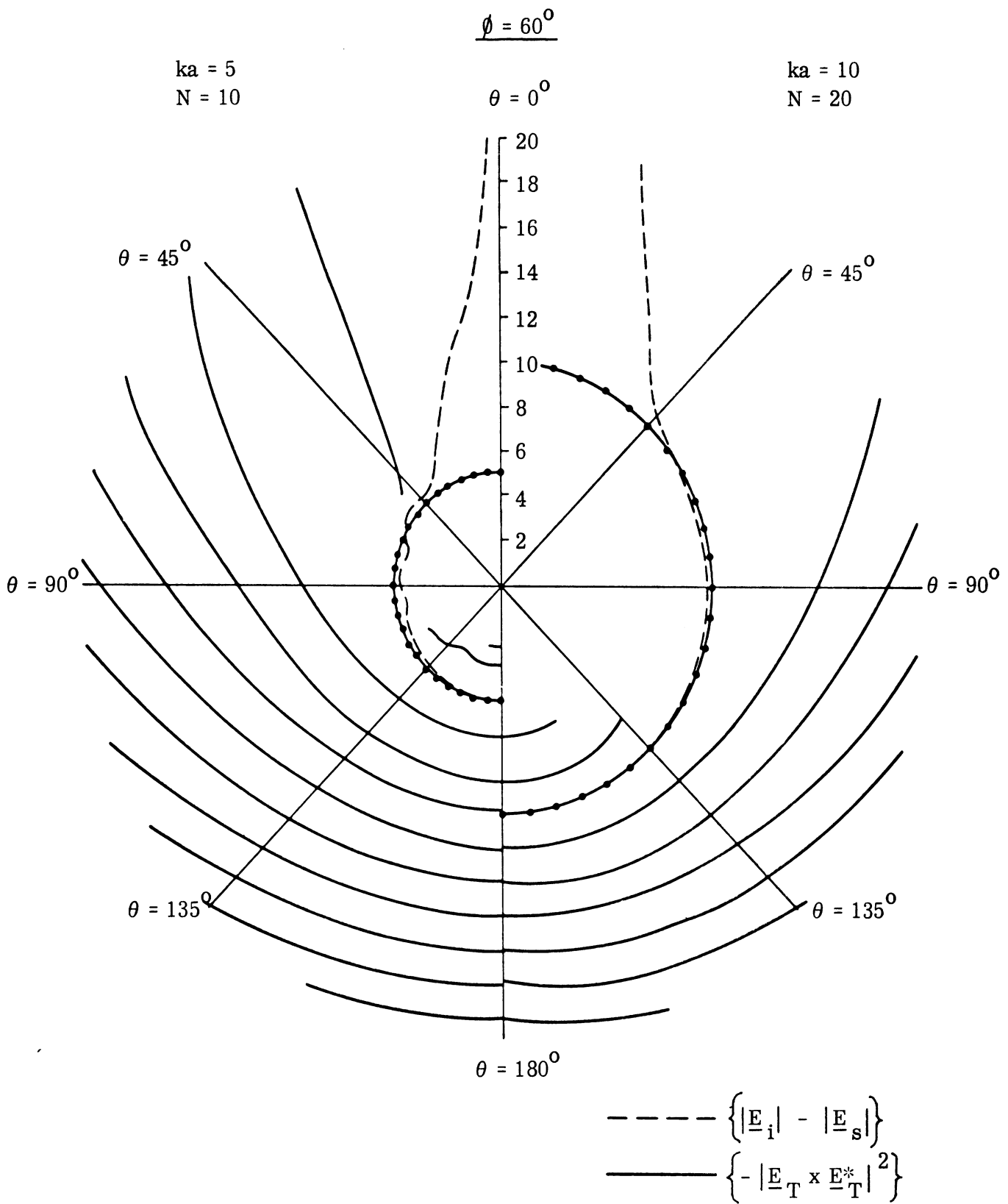
FIG. 4-1e: RESULTING SURFACE LOCI FOR THE SPHERICAL
TEST CASES ka = 5, 10. $\phi = 60^{\circ}$.

FIG. 4-1f: RESULTING SURFACE LOCI FOR THE SPHERICAL
TEST CASES ka = 5, 10. $\phi = 75^{\circ}$.

63

$\phi = 90^{\circ}$

ka = 5
N = 10

$\theta = 0^{\circ}$

ka = 10
N = 20

$\theta = 45^{\circ}$

$\theta = 45^{\circ}$

20
18
16
14
12
10
8
6
4
2

$\theta = 90^{\circ}$

$\theta = 90^{\circ}$

$\theta = 135^{\circ}$

$\theta = 135^{\circ}$

$\theta = 180^{\circ}$

$- - - - \left\{ |\underline{E}_i| - |\underline{E}_s| \right\}$

$\underline{\hspace{1cm}} \left\{ - |\underline{E}_T \times \underline{E}_T^{*}|^{2} \right\}$

FIG. 4-1g: RESULTING SURFACE LOCI FOR THE SPHERICAL
TEST CASES ka = 5, 10. $\phi = 90^{\circ}$.

64

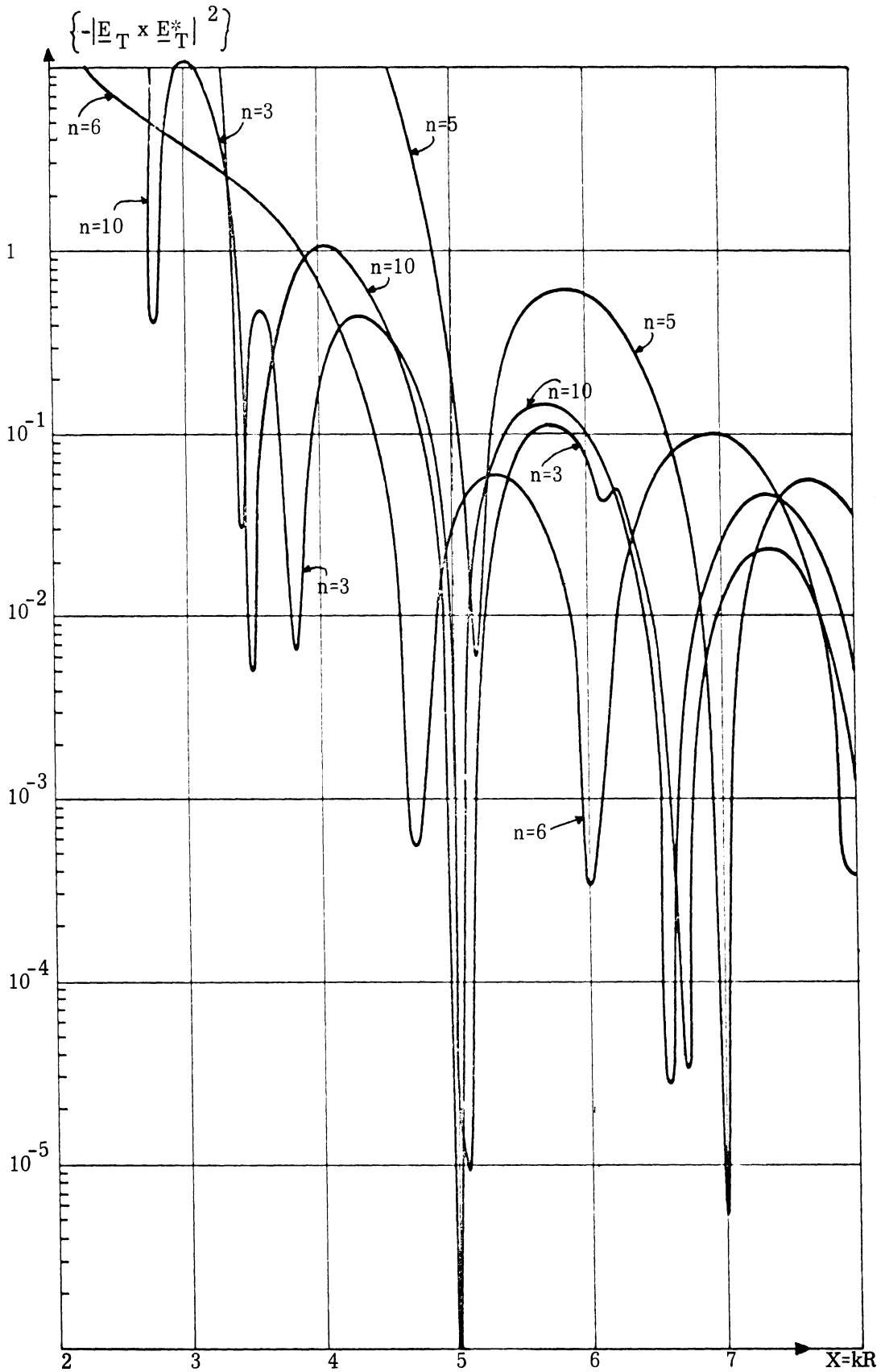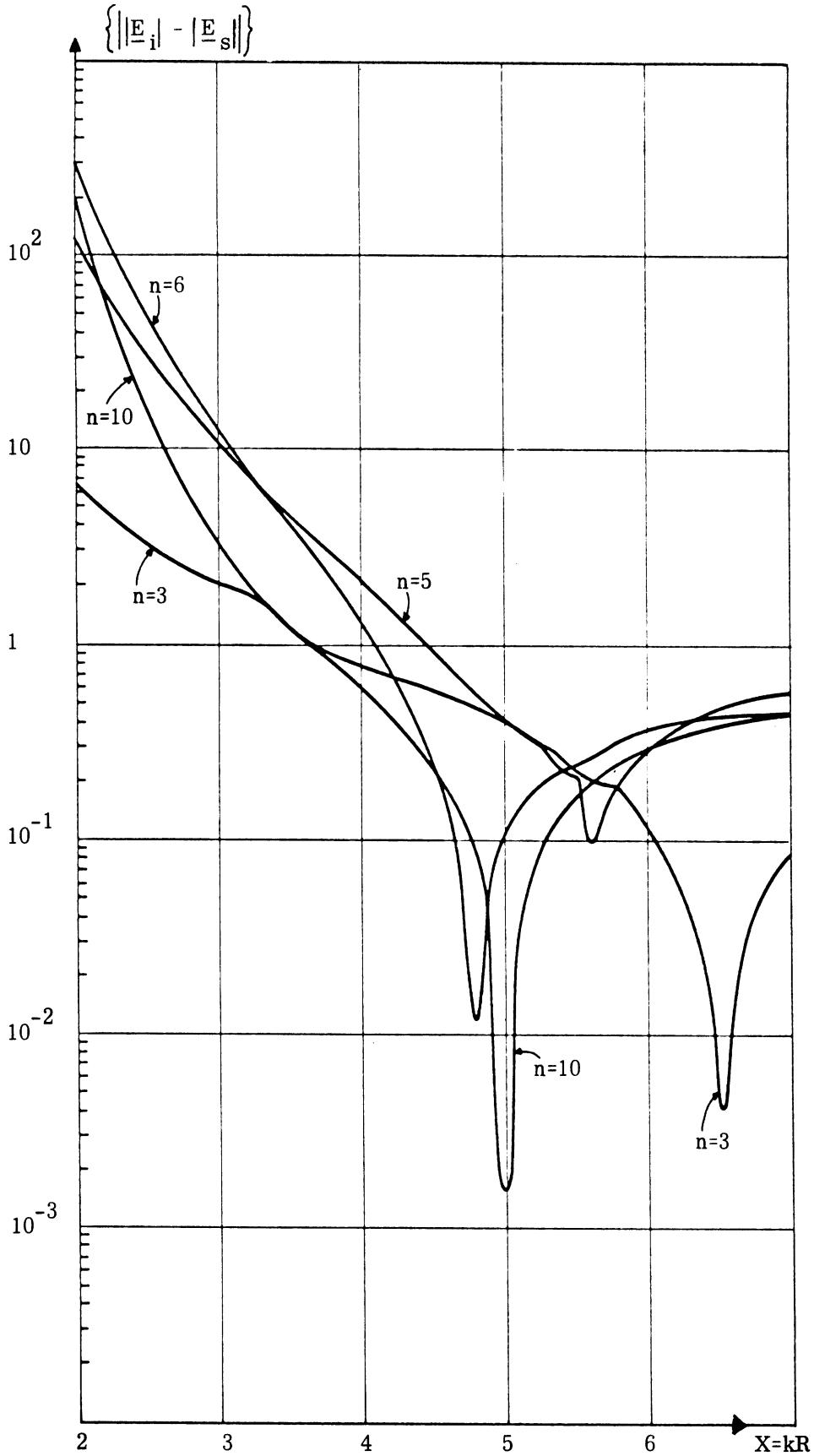FIG. 4-2a: PLOT OF $\{-|\underline{E}_T \times \underline{E}_T^*|^2\}$ VERSUS THE RADIANT VECTOR X=kR FOR THE SPHERICAL TEST CASE ka=2, FOR A VARYING NUMBER OF EXPANSION TERMS n=1,2,3,4,5,6. $\phi = 0^o$, $\theta = 135^o$.

65
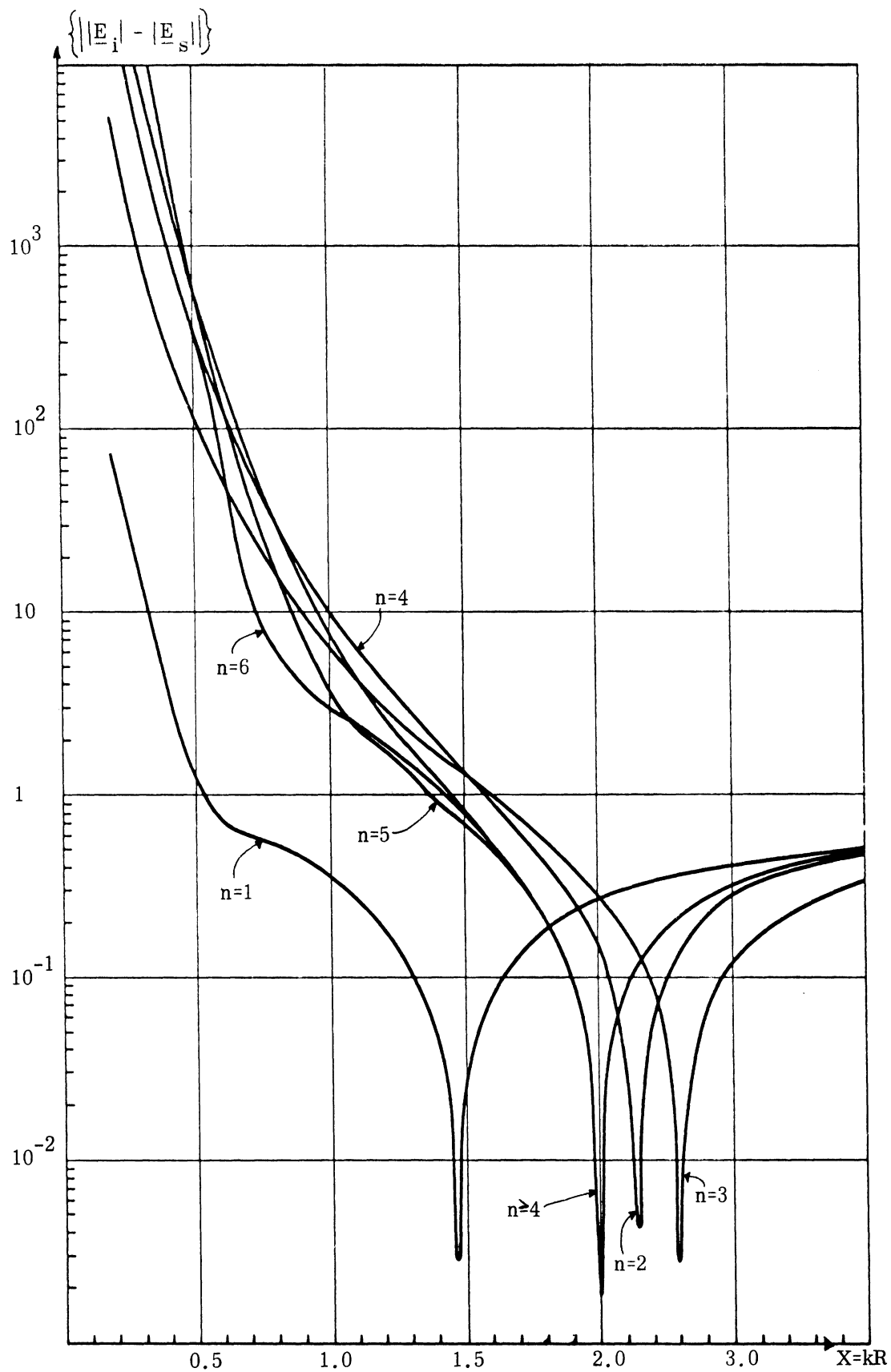
FIG. 4-2b: PLOT OF $\left\{ \left| \left| \underline{E}_i \right| - \left| \underline{E}_s \right| \right| \right\}$ VERSUS THE RADIANT VECTOR FOR THE SPHERICAL TEST CASE ka=2, FOR A VARYING NUMBER OF EXPANSION TERMS n=1, 2, 3, 4, 5, 6. $\phi = 0^o$, $\theta = 135^o$.

FIG. 4-2c: PLOT OF $\left\{-|\underline{E}_T \times \underline{E}_T^*|^2\right\}$ VERSUS THE RADIANT VECTOR X = kR FOR THE SPHERICAL TEST CASE ka=5, FOR A VARYING NUMBER OF EXPANSION TERMS n=3, 5, 6, 10. $\phi = 0^o$, $\theta = 135^o$.
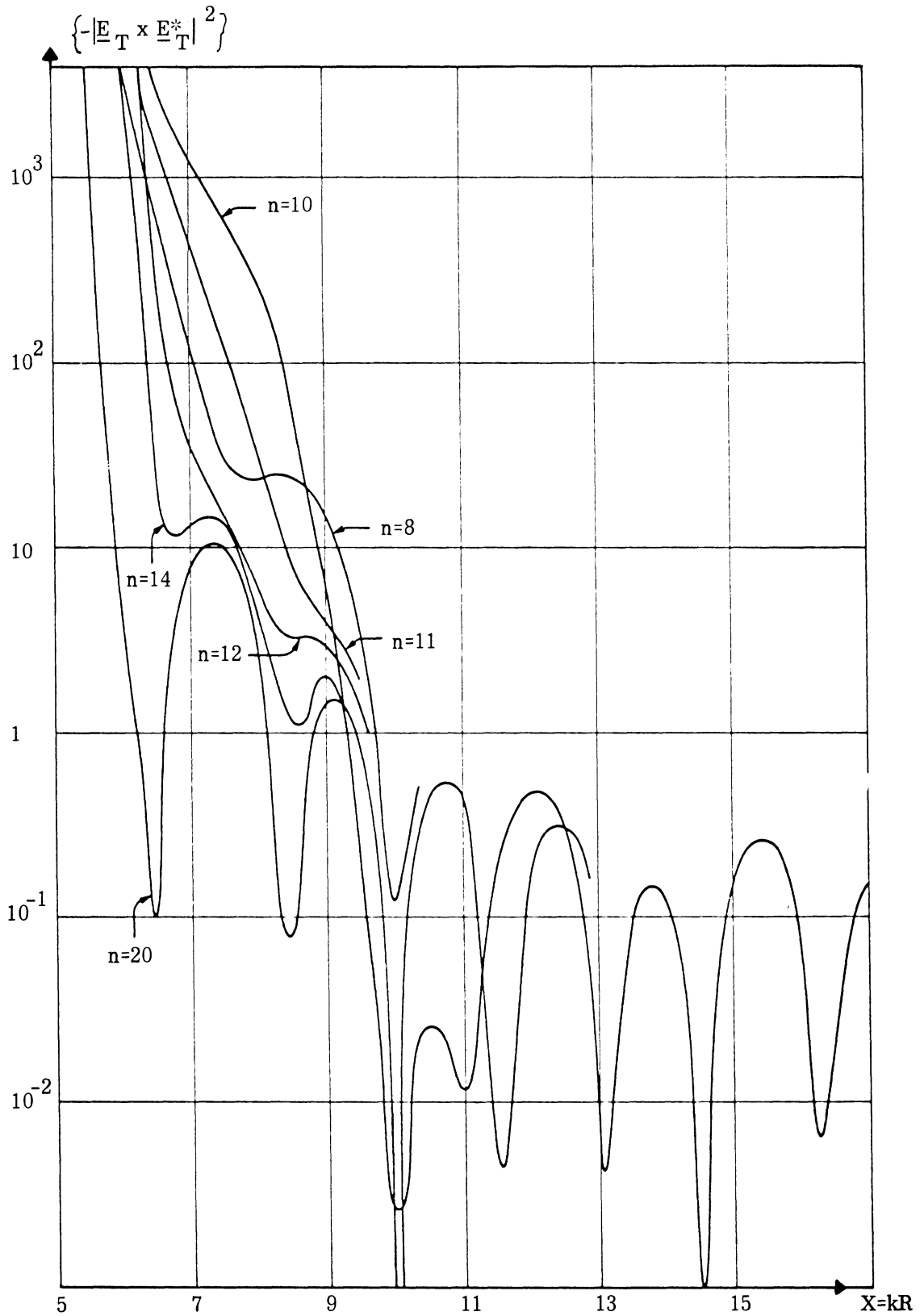
67

FIG. 4-2d: PLOT OF $\left\{\left|\,|\underline{E}_i|\, - \,|\underline{E}_s|\,\right|\right\}$ VERSUS THE RADIANT VECTOR X=kR
FOR THE SPHERICAL TEST CASE ka=5, FOR A VARYING NUMBER
OF EXPANSION TERMS n= 3, 5, 6, 10. ϕ = 0°, θ = 135°.

FIG. 4-2e: PLOT OF $\left\{-\left|\underline{E}_T \times \underline{E}_T^*\right|^2\right\}$ VERSUS THE RADIANT VECTOR X=kR
FOR THE SPHERICAL TEST CASE ka = 10, FOR A VARYING NUMBER
OF EXPANSION TERMS n = 8, 10, 11, 12, 14, 20. $\phi = 0^o$, $\theta = 135^o$.

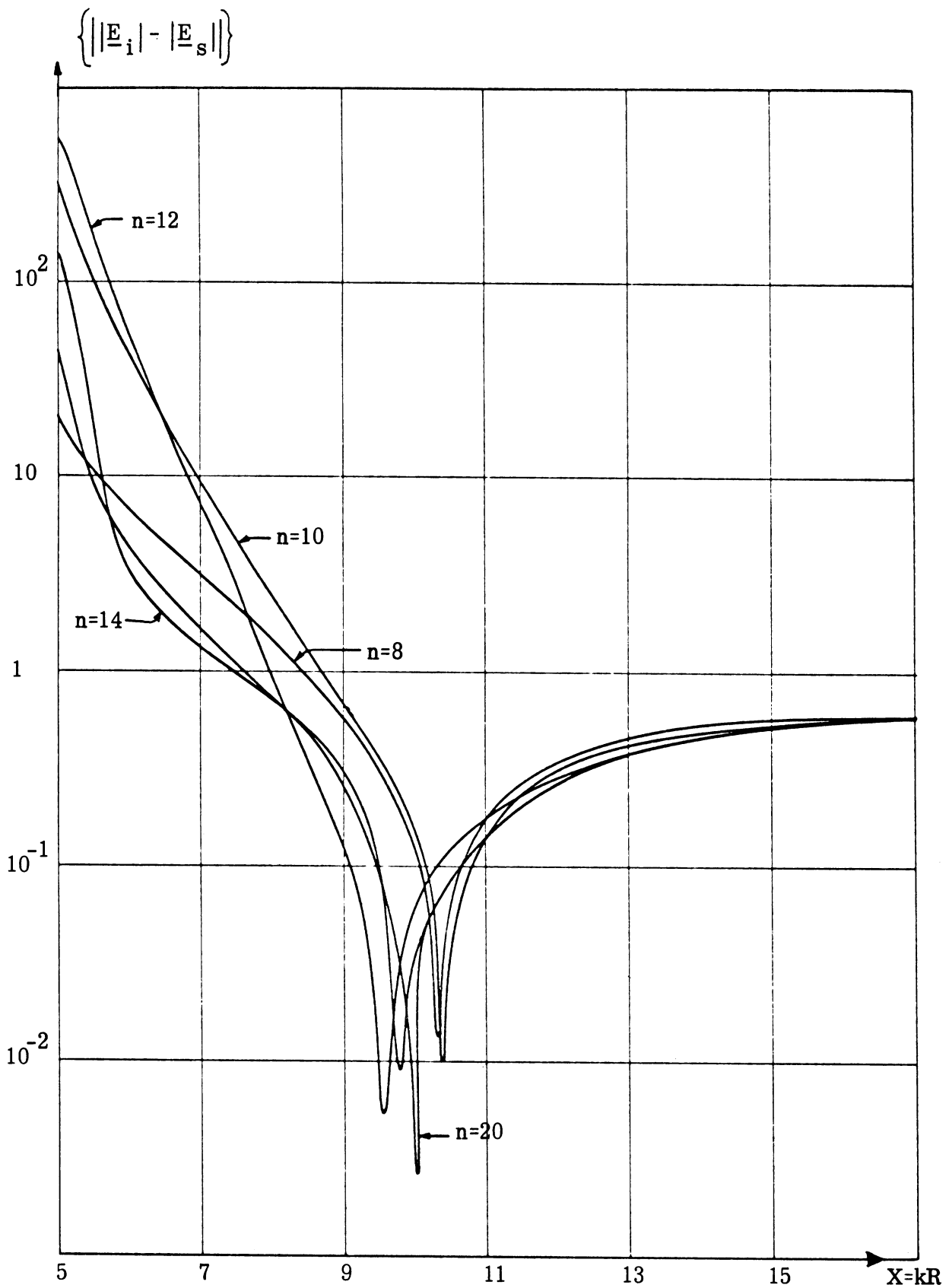FIG. 4-2f: PLOT OF $\left\{\left|\,|\underline{E}_i| - |\underline{E}_s|\,\right|\right\}$ VERSUS THE RADIANT VECTOR X=kR
FOR THE SPHERICAL TEST CASE ka = 10, FOR A VARYING NUMBER
OF EXPANSION TERMS n = 8, 10, 12, 14, 20. $\phi = 0^{\circ}$, $\theta = 135^{\circ}$.

plotted respectively versus the radial dependence for $\phi = 0$, $\theta = 172.5^o$.

Inspecting the curves closely, it can be seen that these undesired pseudo surface loci of the condition $\left\{\underline{E}_T \times \underline{E}_T^*\right\}$ will not appear if the number of expansion terms n is equal to the electric measure ka or if

$$\widehat{n} \leq \left[ka + (ka)^{1/3}\right] \tag{4.3}$$

whereas with increasing deviation of n from this value such additional minima will be present and for large n, i.e. $n > \left[ka + (ka)^{1/3}\right]$ these minima again show equidistant spacing of $k \triangle R \cong \pi/2$. For constant dimensions of the scatterer, the number of such minima will increase with decreasing operational frequency, where the innermost is exterior to the spherical caustic. Furthermore, it can be seen that these additional hyperbolic pseudo loci show minima which are relatively small compared to the pronounced dip of the proper surface locus and disappear in the vicinity of the latter, then appearing again exterior to the pronounced dip of the proper surface locus as indicated in Fig. 4-1a by the curves $C_{p_{in}}$ and $C_{p_{ext}}$. This phenomenon of additional surface loci for the case where the employed number of expansion terms is much larger than the electric measure (4.3), may be explained by the fact that in the geometrical optics limit these interior surface loci are caused by rays emanating from the caustic of the sphere. This explanation, however, does not hold for the case where n is smaller than ka, these minima are due to zeroes of lower order Bessel functions of the vector spherical harmonics.

Inspecting the behaviour of $\left\{\left|\underline{E}_i\right| - \left|\underline{E}_s\right|\right\}$ for varying number of expansion terms, it can be seen that for $n \leq \left[ka + (ka)^{1/3}\right]$ the obtained minima will oscillate about the proper locus and only for $n > \left[ka + (ka)^{1/3}\right]$ the minima will occur at the proper surface locus, however, depending upon local polarization properties, only within a limited cone about specular direction of apex angle

71

$\theta \simeq 30^{\circ}$. Except for the conical region about the focal point in the shadow region of apex angle $\theta_o \simeq 60^{\circ}$ this condition will only show one minimum in any other radial direction.

Summarizing the results, the following can be concluded for the simultaneous application of both boundary conditions for the precise determination of the proper surface locus:

1) First apply the boundary condition $\left\{ \left| \underline{E}_i \right| - \left| \underline{E}_s \right| \right\}$, starting at the lower bound $k\,R_o \simeq .5$, and search for the first point Y_{10} where $\left\{ \left| \underline{E}_i \right| - \left| \underline{E}_s \right| \right\}$ reverses signs or $\left| \left\{ \left| \underline{E}_i \right| - \left| \underline{E}_s \right| \right\} \right| < 1$ with a searching increment of approximately $k\,\Delta R \simeq .25$.

2) Apply the boundary condition $\left\{ \underline{E}_T \times \underline{E}_T^* \right\}$ about this point Y_{10} within the range

$$Y_{10} - \pi/2 \leq X_2 \leq Y_{10} + \pi/2$$

employing a rather small searching increment of $.01 \leq k\,\Delta R_2 \leq .1$ to eliminate additional minima and search for the proper point which shows the most pronounced minimum.

3) In addition, it is advisable to employ the procedure at two or more different operational frequencies and plot the points of successive minima along one ray versus R , since then the loci of additional minima will be shifting whereas the proper one will be independent of the origin. In Fig. 4-3 these properties are illustrated.

4.3 Prolate Spheroidal Test Cases.

The computation of the near field was again based upon an expansion into vector spherical wave functions (Stratton,1941), where the approximate expansion coefficients were provided by P.C. Waterman (1965). The following three test cases are chosen

a) $ka = 1$, $a/b = 2$, $n = 6$
b) $ka = 10$, $a/b = 5$, $n = 16$.
c) $ka = 20$, $a/b = 2$, $n = 28$.

$k_1 a = 5$
$k_1 = .5$

$\theta = 0^{\circ}$

$k_2 a = 10$
$k_2 = 1$

$\theta = 45^{\circ}$

$\theta = 45^{\circ}$

20
18
16
14
12
10
8
6
4
2

$\theta = 90^{\circ}$

$\theta = 90^{\circ}$

C_{i_1}
C_{i_2}
C_o
C_1
C_2

C_{i_2}
C_{i_1}
C_o
C_1
C_2
C_3

$\theta = 135^{\circ}$

$\theta = 135^{\circ}$

C_4
C_5

C_3

C_6

$\theta = 180^{\circ}$
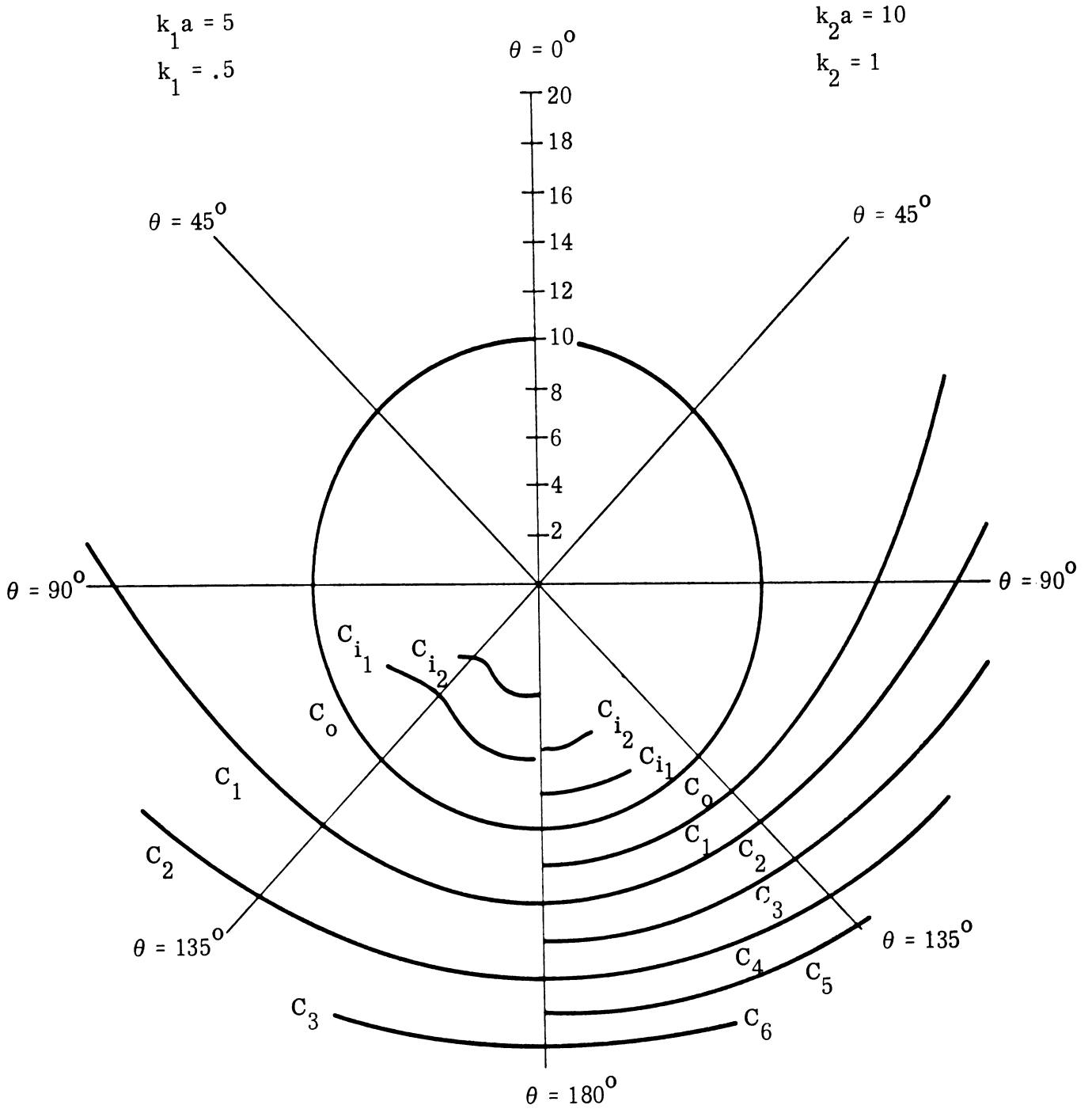
FIG. 4-3: RESULTING SURFACE LOCI FOR A SPHERE OF RADIUS
a , DETERMINED FOR k = .5, k_2 = 1 AND PLOTTED
VERSUS THE RADIANT DEPENDENCE R TO ILLUSTRATE
THE SHIFTING OF ADDITIONAL SURFACE LOCI (C_{i_n} ,
C_1, C_2 ...).

The computational results are presented in Figures 4-4a through 4-7d. Inspecting these figures it can be shown that within a conical section about specular direction of apex angle $\theta_o \simeq 30^o$, rather satisfactory results are obtained. The deviation from the actual (proper) locus in the region exterior to this domain have been expected by theory. Comparing the results of the two boundary conditions it can be said that within a narrow conical section about specular direction the condition $\left\{ \underline{E}_T \times \underline{E}_T^* \right\} = 0$ is superior to $\left\{ \left| \underline{E}_i \right| - \left| E_s^* \right| \right\} = 0$, where it was found that the resulting locus for $\left\{ \left| \underline{E}_i \right| - \left| \underline{E}_s \right| \right\}$ lies interior to both the proper locus and that for $\left\{ \underline{E}_T \times \underline{E}_T^* \right\} = 0$. It was shown that with increasing number of expansion terms, the resulting loci of either condition approach the proper one more closely. The additional concentric hyperbolic surface loci of $\left\{ \underline{E}_T \times \underline{E}_T^* \right\} = 0$ exterior to the proper surface locus are again spaced equidistantly with $k \Delta R = \pi/2$ in the specular direction, and no hyperbolic surfaces were found within the proper one, though for the larger prolate spheroid such surfaces should be expected but the associated minima may be too small to be found with the employed searching increment.

Considering the results exterior to the conical section about specular direction, those deviations have been expected by theory. It was shown (7644-1-F, 8579-1-Q) that the spherical partial wave representation of the near scattered field was convergent down to the minimum sphere enclosing the loci of the prolate spheroid. Hence to determine the flank-parts (equatorial cross-section) of the prolate spheroid, either an alternative representation must be used, or else in the partial wave expansion the origin of the coordinate system must be translated from the center. However in the representation employed, where the origin was at the center, the results of the condition $\left\{ \left| \underline{E}_i \right| - \left| \underline{E}_s \right| \right\}$ for the case $ka = 1$, $a/b = 2$ yield very satisfactory results in this region (see Figs. 4-4f and 4-4g) if the local polarization properties are such the $\underline{E}_i$ is parallel to the scattering surface in the equatorial plane. This behavior, namely
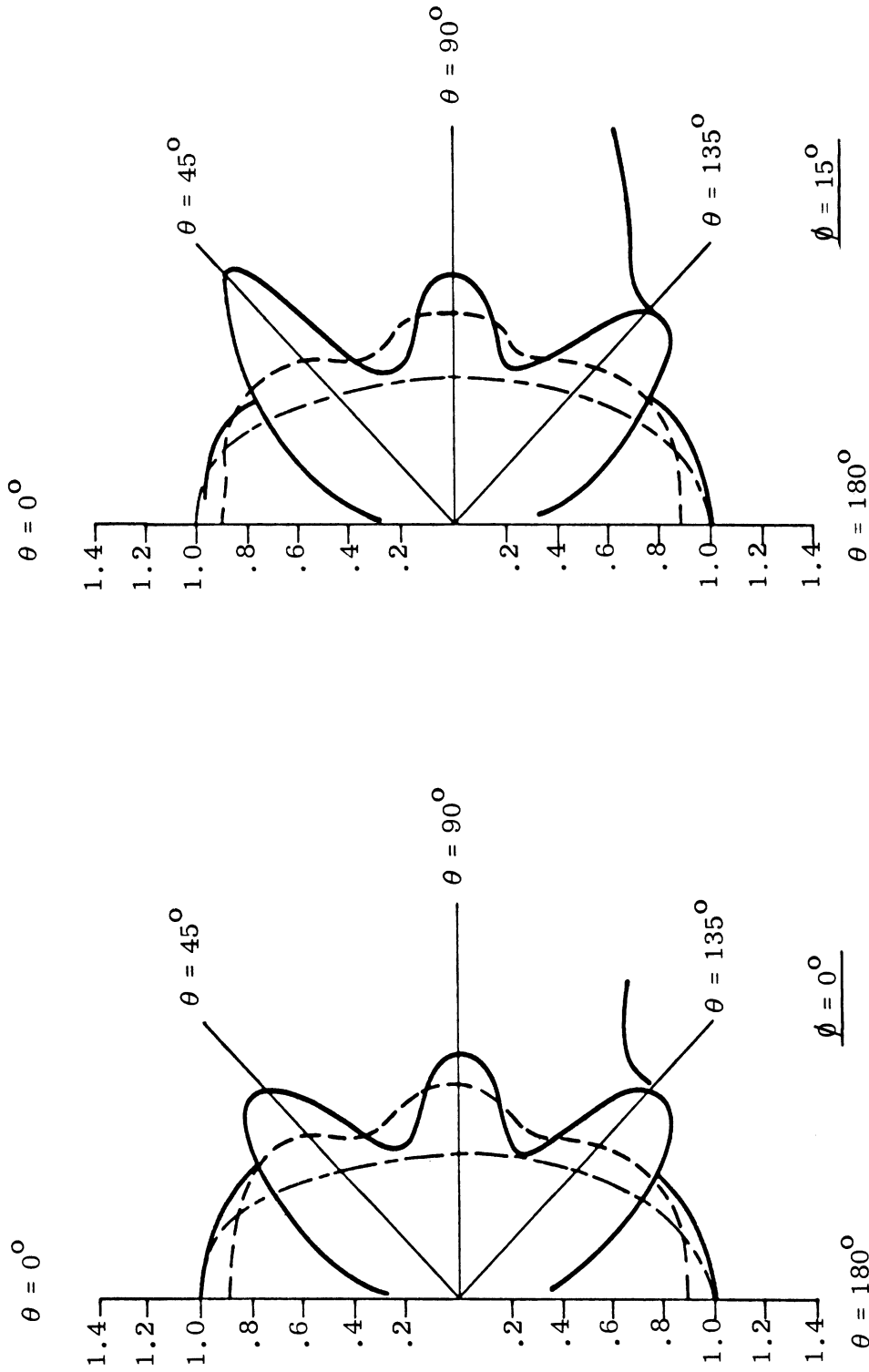
FIG. 4-4a ($\phi = 0^{\circ}$)

FIG. 4-4b ($\phi = 15^{\circ}$)

RESULTING SURFACE LOCI FOR THE PROLATE
SPHEROIDAL TEST CASE ka = 1, N = 6.

$$\left(- - - \left\{ |\underline{E}_i| - |\underline{E}_s| \right\} \quad \underline{\qquad} \quad \left\{ - |\underline{E}_T \times \underline{E}_T^*|^2 \right\} \quad - - - - \quad \{\text{proper locus}\} \right)$$
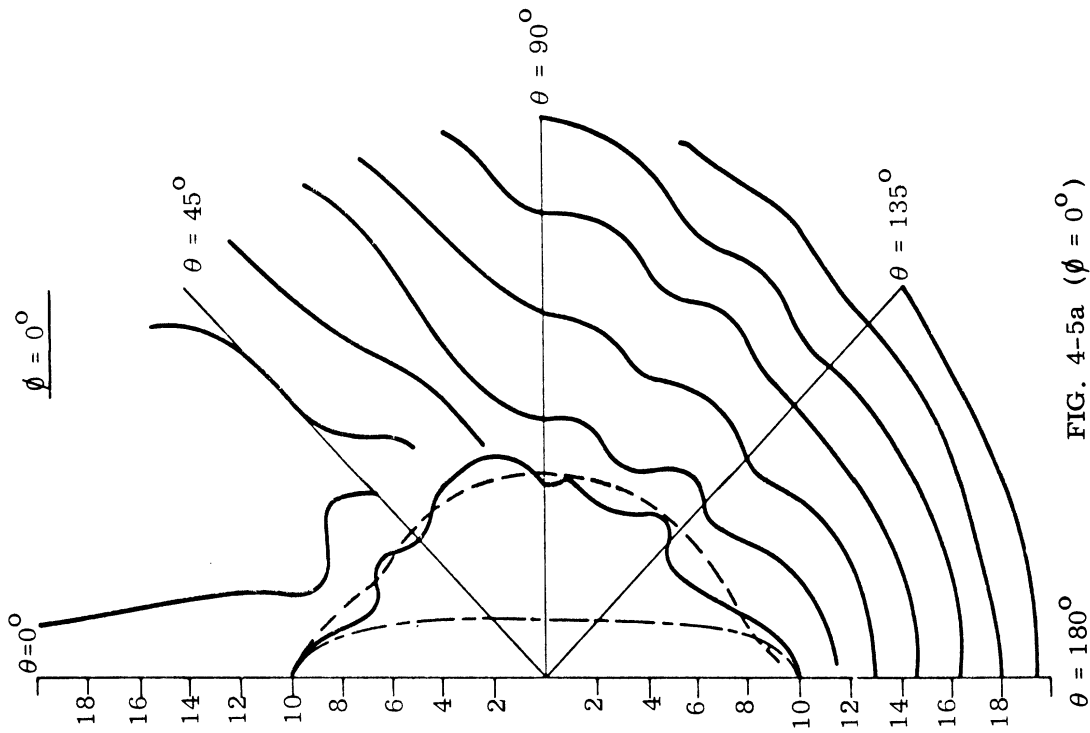
75

FIG. 4-4c ($\phi = 30^\circ$)

FIG. 4-4d ($\phi = 45^\circ$)

RESULTING SURFACE LOCI FOR THE PROLATE
SPHEROIDAL TEST CASE $ka = 1$, $N = 6$.

$$\left(- - - \left\{ |\underline{E}_i| - |\underline{E}_s| \right\} \quad \underline{\quad\quad} \quad \left\{ - |\underline{E}_T \times \underline{E}_T^*|^2 \right\} \quad - - - - \quad \left\{ \text{proper locus} \right\} \right)$$
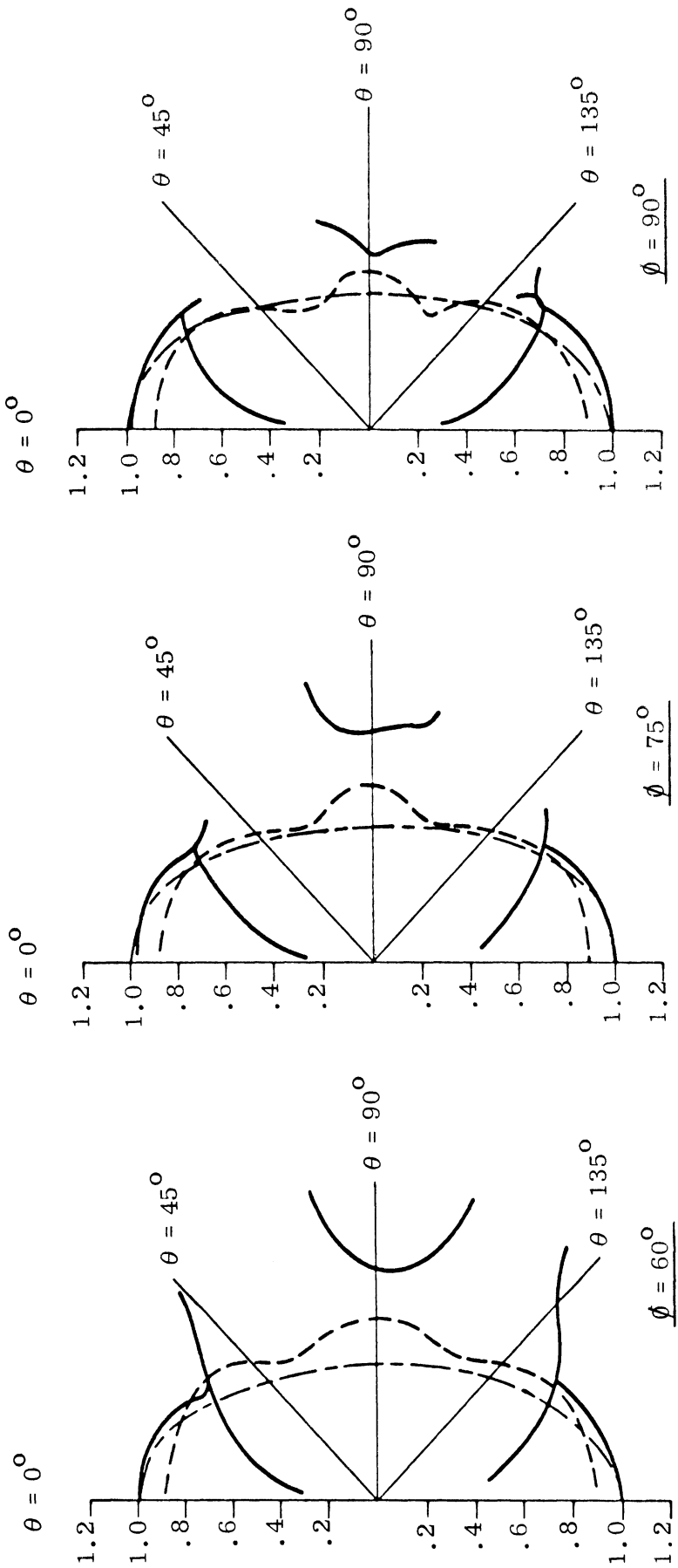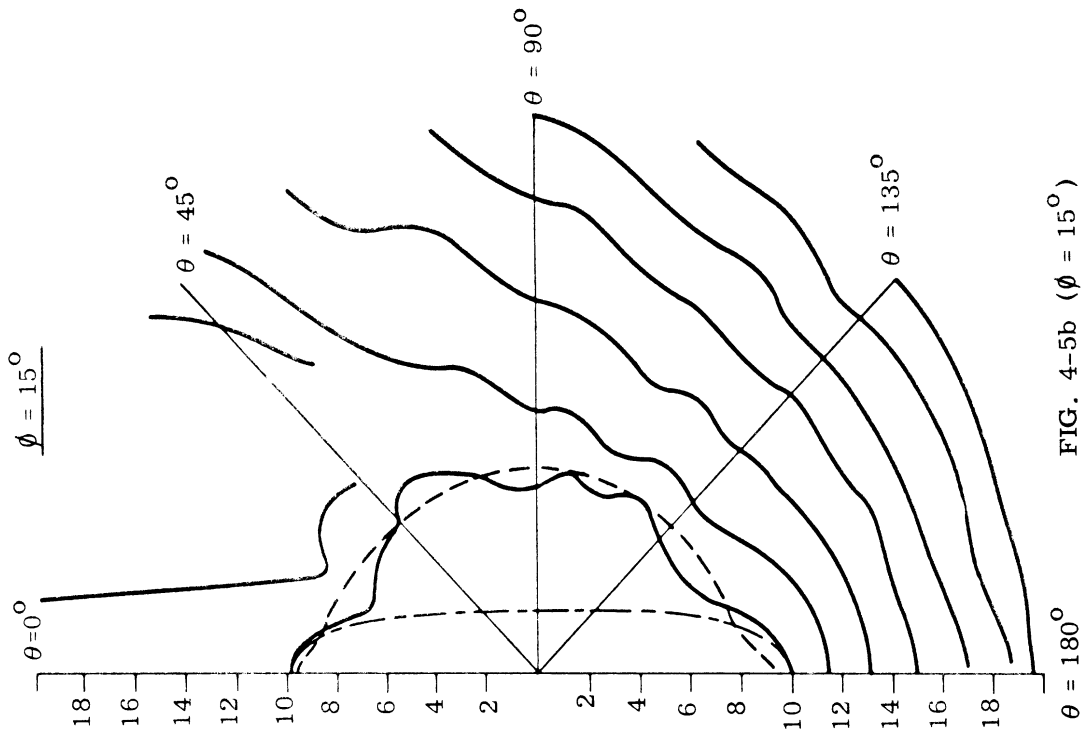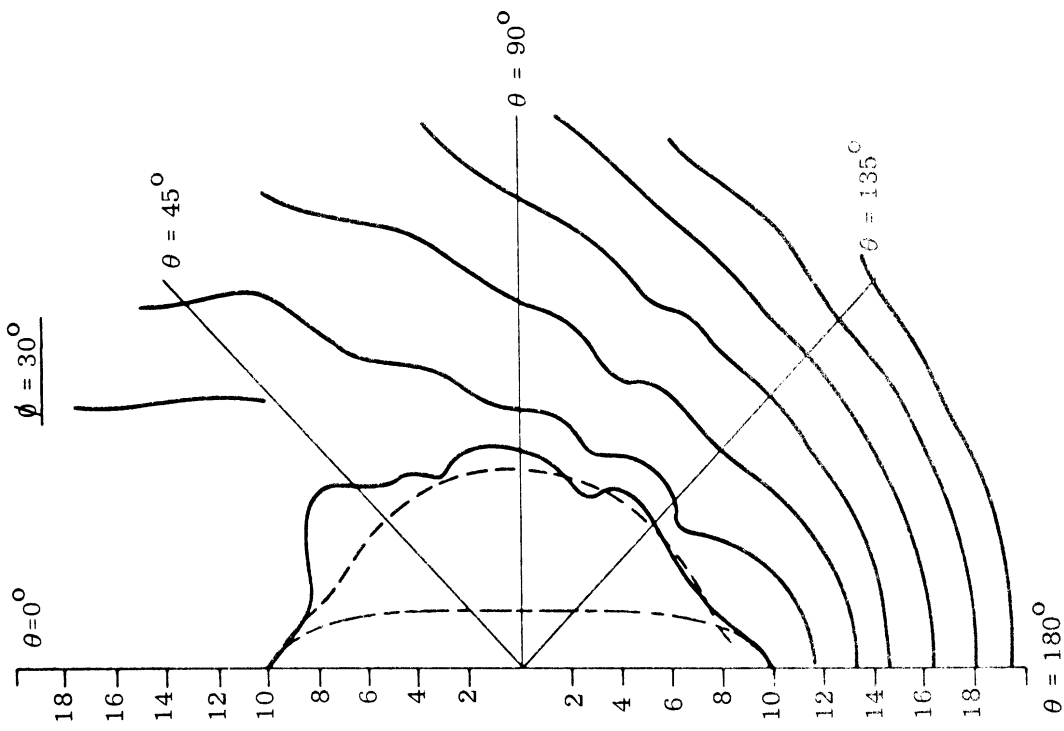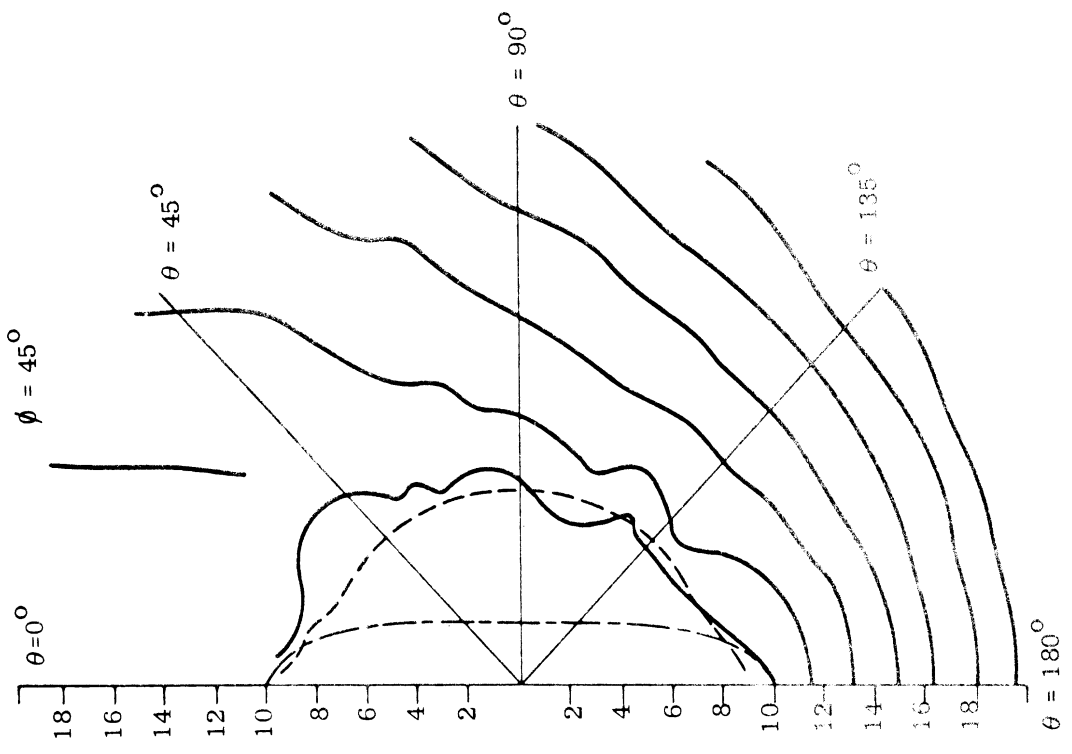
FIG. 4-4e ($\phi = 60^\circ$)

FIG. 4-4f ($\phi = 75^\circ$)

FIG. 4-4g ($\phi = 90^\circ$)

RESULTING SURFACE LOCI FOR THE PROLATE
SPHEROIDAL TEST CASE $ka = 1$, $N = 6$.

$$\left(- - - \left\{ |\underline{E}_i| - |\underline{E}_s| \right\} \quad \underline{\quad\quad} \left\{ - |\underline{E}_T \times \underline{E}_T^*|^2 \right\} \quad - - - - \left\{ \text{proper locus} \right\} \right)$$

77

$$\phi = 15^{\circ}$$

$$\theta = 0^{\circ}$$ $$\theta = 45^{\circ}$$ $$\theta = 90^{\circ}$$ $$\theta = 135^{\circ}$$ $$\theta = 180^{\circ}$$

FIG. 4-5b $(\phi = 15^{\circ})$

$$\phi = 0^{\circ}$$

$$\theta = 0^{\circ}$$ $$\theta = 45^{\circ}$$ $$\theta = 90^{\circ}$$ $$\theta = 135^{\circ}$$ $$\theta = 180^{\circ}$$

FIG. 4-5a $(\phi = 0^{\circ})$

RESULTING SURFACE LOCI FOR THE PROLATE
SPHEROIDAL TEST CASE ka = 10, a/b = 5, N = 16.

$$\left(- - - \left\{ \left| \underline{E}_i \right| - \left| \underline{E}_s \right| \right\} \qquad \longrightarrow \left\{ - \left| \underline{E}_T \times \underline{E}_T^* \right|^2 \right\} \qquad - - - - \left\{ \text{proper locus} \right\} \right)$$
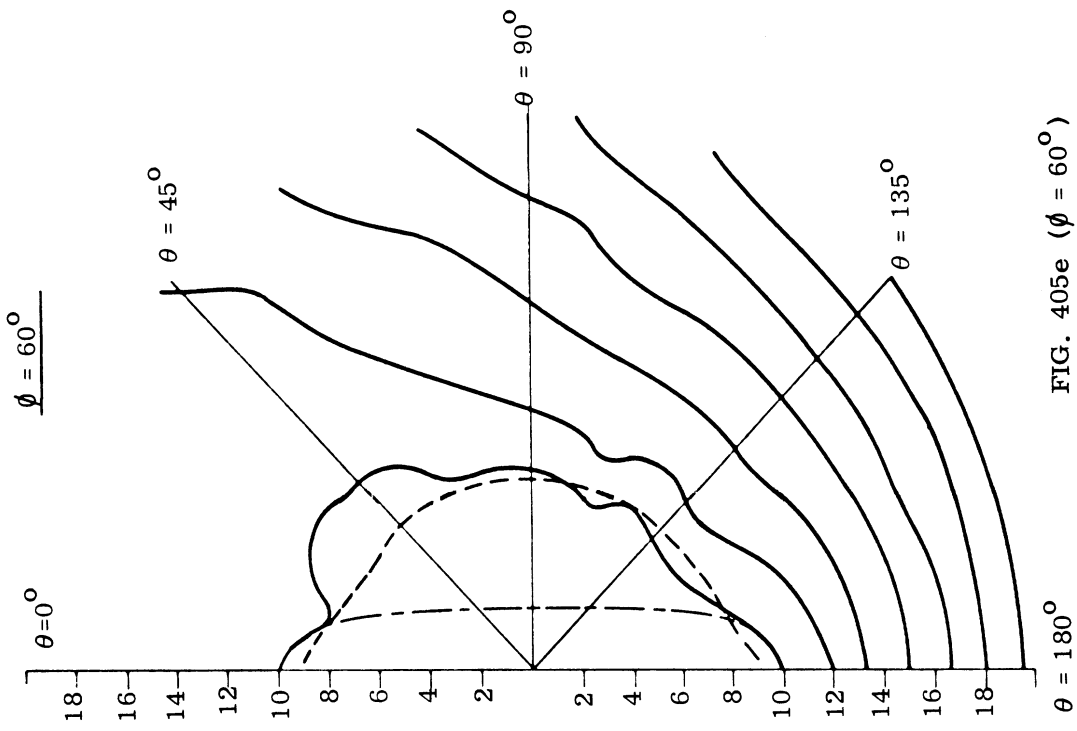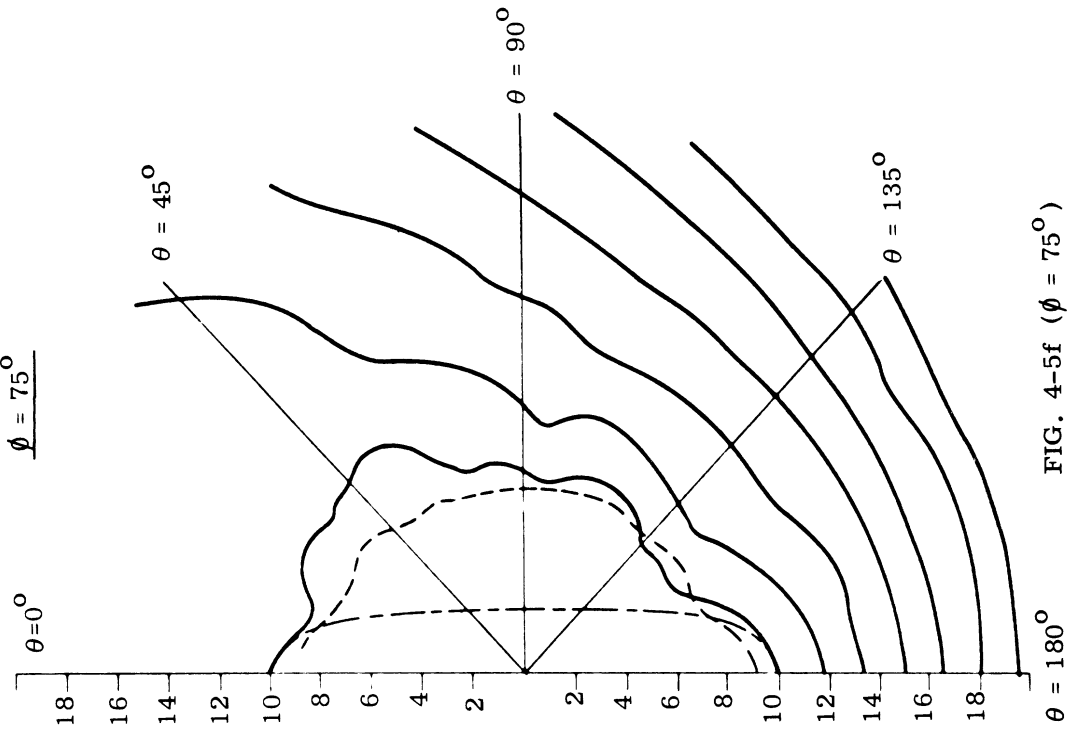
78

FIG. 4-5c ($\phi = 30^\circ$)

FIG. 4-5d ($\phi = 45^\circ$)

RESULTING SURFACE LOCI FOR THE PROLATE
SPHEROIDAL TEST CASE $ka = 10$, $a/b = 5$, $N = 16$.

$$\left(--- \{|\underline{E}_i| - |\underline{E}_s|\} \quad \longrightarrow \quad \{- |\underline{E}_T \times \underline{E}_T^*|^2\} \quad ----- \quad \{\text{proper locus}\} \right)$$

$\phi = 75°$

$\theta = 0°$

$\theta = 45°$

$\theta = 90°$

$\theta = 135°$

$\theta = 180°$

FIG. 4-5f ($\phi = 75°$)

$\phi = 60°$

$\theta = 0°$

$\theta = 45°$

$\theta = 90°$

$\theta = 135°$

$\theta = 180°$

FIG. 405e ($\phi = 60°$)

RESULTING SURFACE LOCI FOR THE PROLATE
SPHEROIDAL TEST CASE ka = 10, a/b = 5, N = 16.

$$- - - \left\{ \left| \underline{E}_i \right| - \left| \underline{E}_s \right| \right\} \qquad \qquad \left\{ - \left| \underline{E}_T \times \underline{E}_T^* \right|^2 \right\} \qquad - - - - \left\{ \text{proper locus} \right\}$$
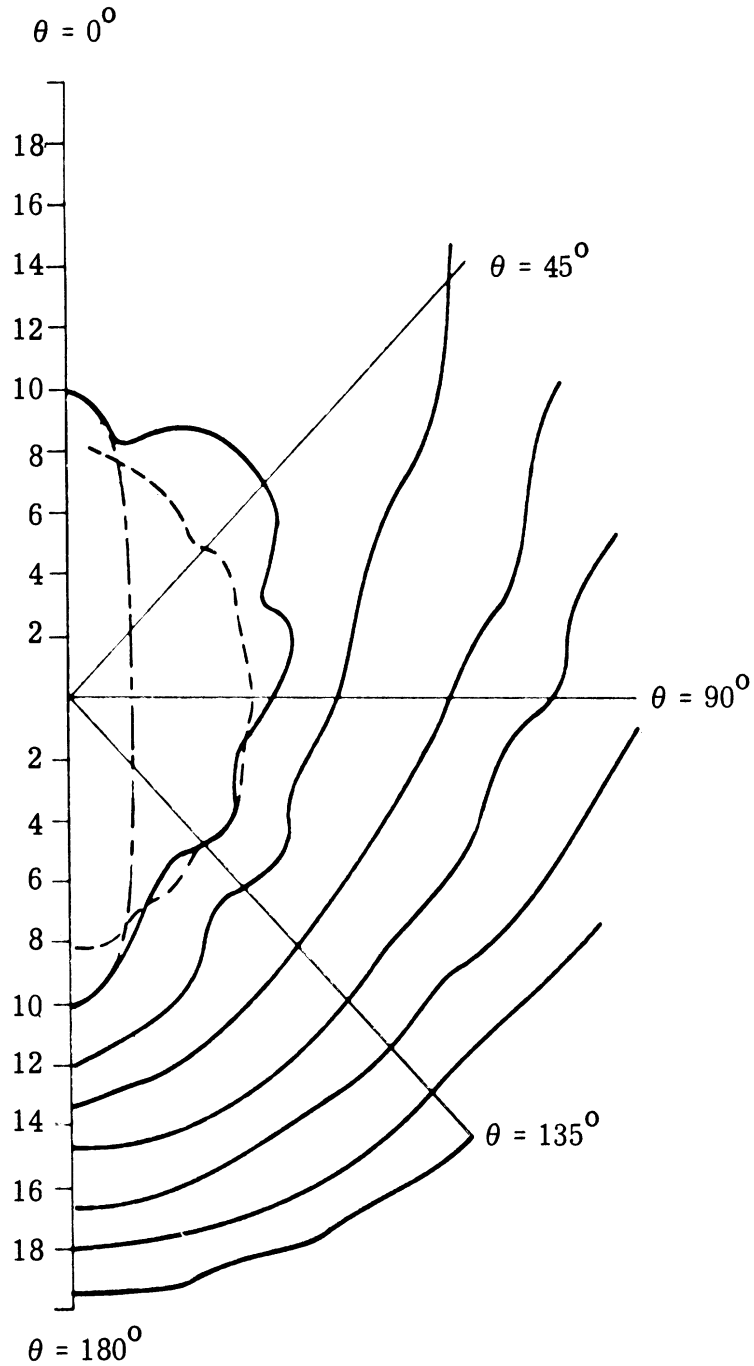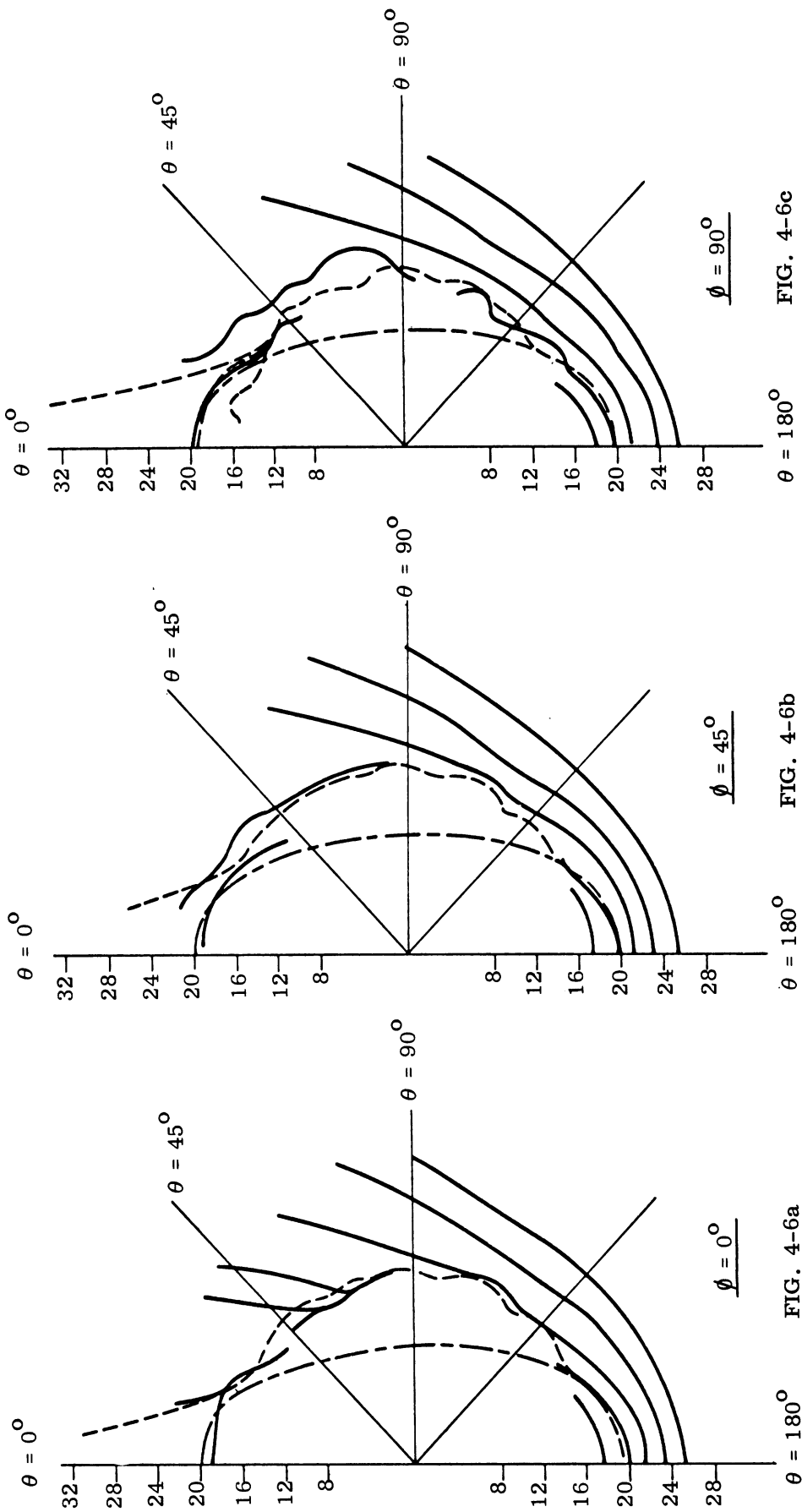
80

FIG. 4-5g: RESULTING SURFACE LOCI FOR THE PROLATE
SPHEROIDAL TEST CASE ka $= 10$, a/b $= 5$, N $= 16$. ($\phi = 90^{\text{o}}$)

$$\left(---\rightarrow\left\{|\underline{E}_i| - |\underline{E}_s|\right\} \quad ----\left\{-|\underline{E}_T \times \underline{E}_T^*|^2\right\} -----\left\{\text{proper locus}\right\}\right)$$

81

RESULTING SURFACE LOCI FOR THE PROLATE
SPHEROIDAL TEST CASE ka = 20, N = 16.

$$\left(\; - - - - \left\{\left|\underline{E}_i\right| - \left|\underline{E}_s\right|\right\} \quad\text{———}\quad \left\{-\left|\underline{E}_T \times \underline{E}_T^*\right|^2\right\} \quad - - - - - \left\{\text{proper locus}\right\}\right)$$

FIG. 4-6a

FIG. 4-6b

FIG. 4-6c

$\phi = 0^\circ$

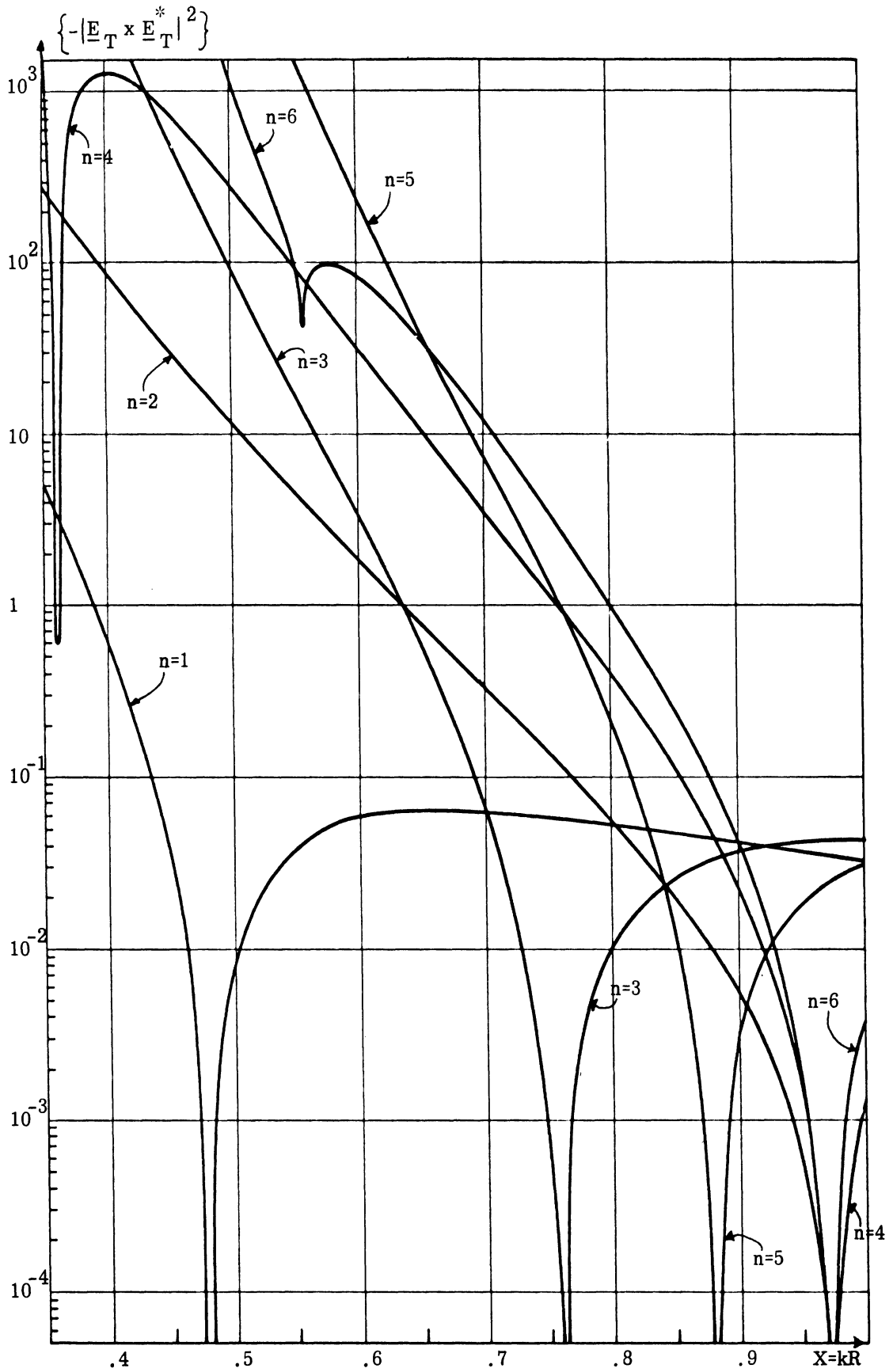$\phi = 45^\circ$

$\phi = 90^\circ$

FIG. 4-7a: PLOT OF $\left\{-|\underline{E}_T \times \underline{E}_T^*|^2\right\}$ VERSUS THE RADIANT VECTOR FOR THE SPHEROIDAL TEST CASE ka=1, a/b = 2 AND FOR A VARYING NUMBER OF EXPANSION TERMS n=1, 2, 3, 4, 5, 6. $\phi = 0^o$, $\theta = 135^o$.

83

FIG. 4-7b: PLOT OF $\left\{ \left| |E_i| - |E_s| \right| \right\}$ VERSUS THE RADIANT VECTOR FOR THE PROLATE SPHEROIDAL TEST CASE ka=1, a/b = 2, FOR A VARYING NUMBER OF EXPANSION TERMS n=1, 2, 3, 4, 5, 6. $\phi = 0^o$, $\theta = 135^o$.
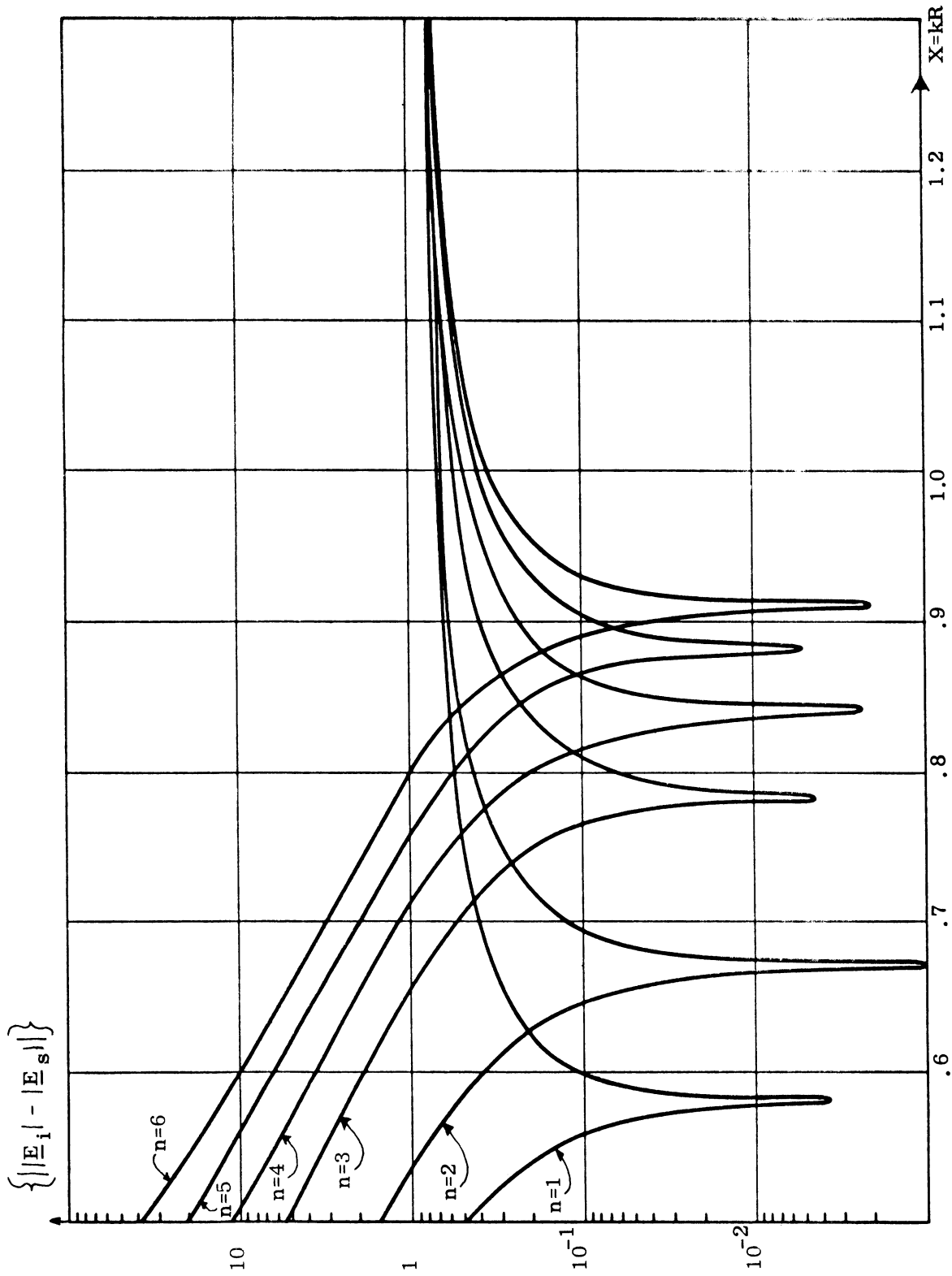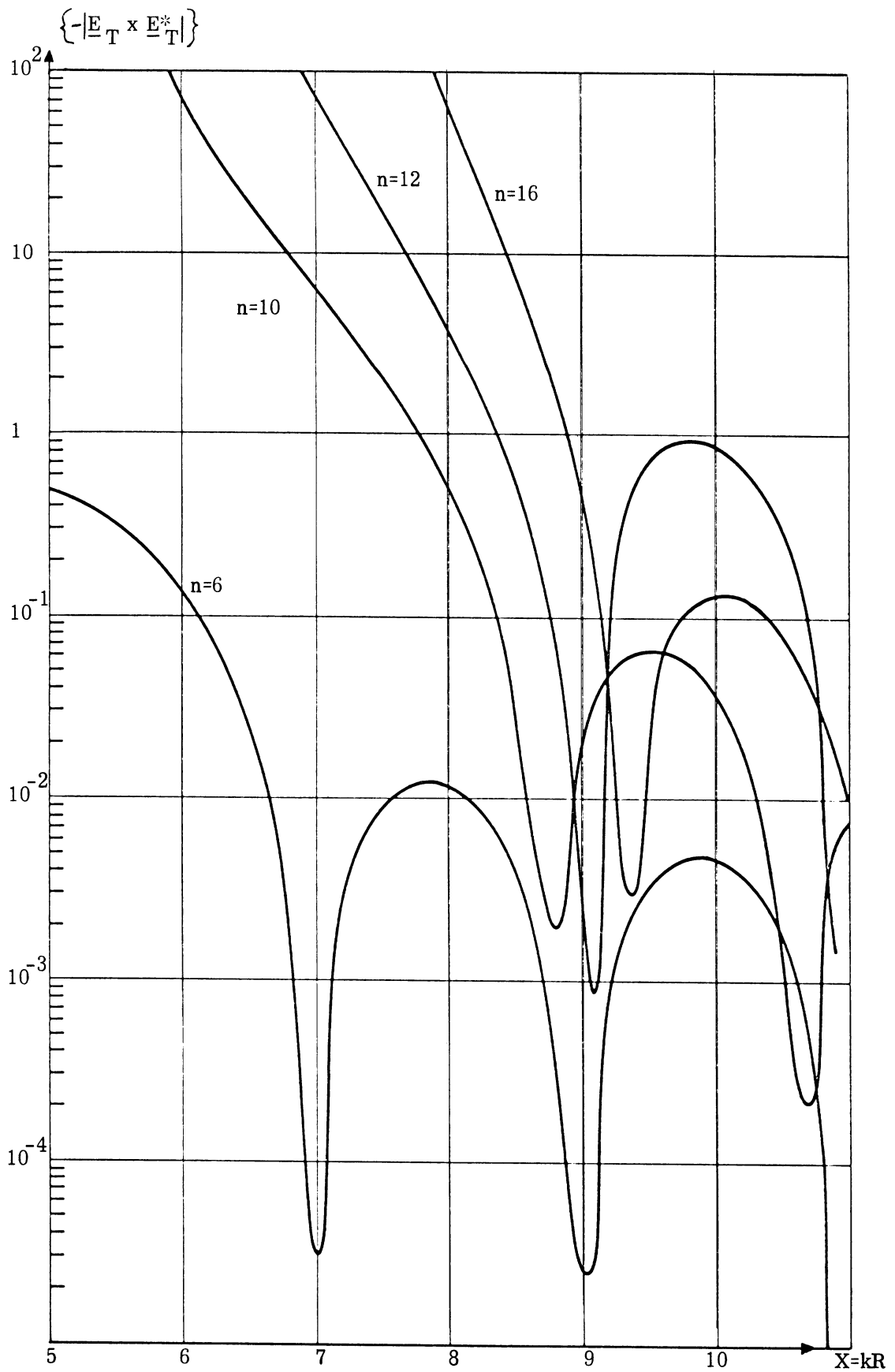
84

FIG. 4-7c: PLOT OF $\left\{- \left| \underline{E}_T \times \underline{E}_T^* \right|^2 \right\}$ VERSUS THE RADIANT VECTOR X = kR
FOR THE PROLATE SPHEROIDAL TEST CASE ka = 10, a/b = 5
FOR A VARYING NUMBER OF EXPANSION TERMS n=6, 10,
12, 16. $\phi = 0°$, $\theta = 135°$.

FIG. 4-7d: PLOT OF $\left\{\left|\underline{E}_i\right| - \left|\underline{E}_s\right|\right\}$ VERSUS RADIANT VECTOR X = kR
FOR THE PROLATE SPHEROIDAL TEST CASE ka = 10,
a/b = 5 FOR A VAYING NUMBER OF EXPANSION TERMS
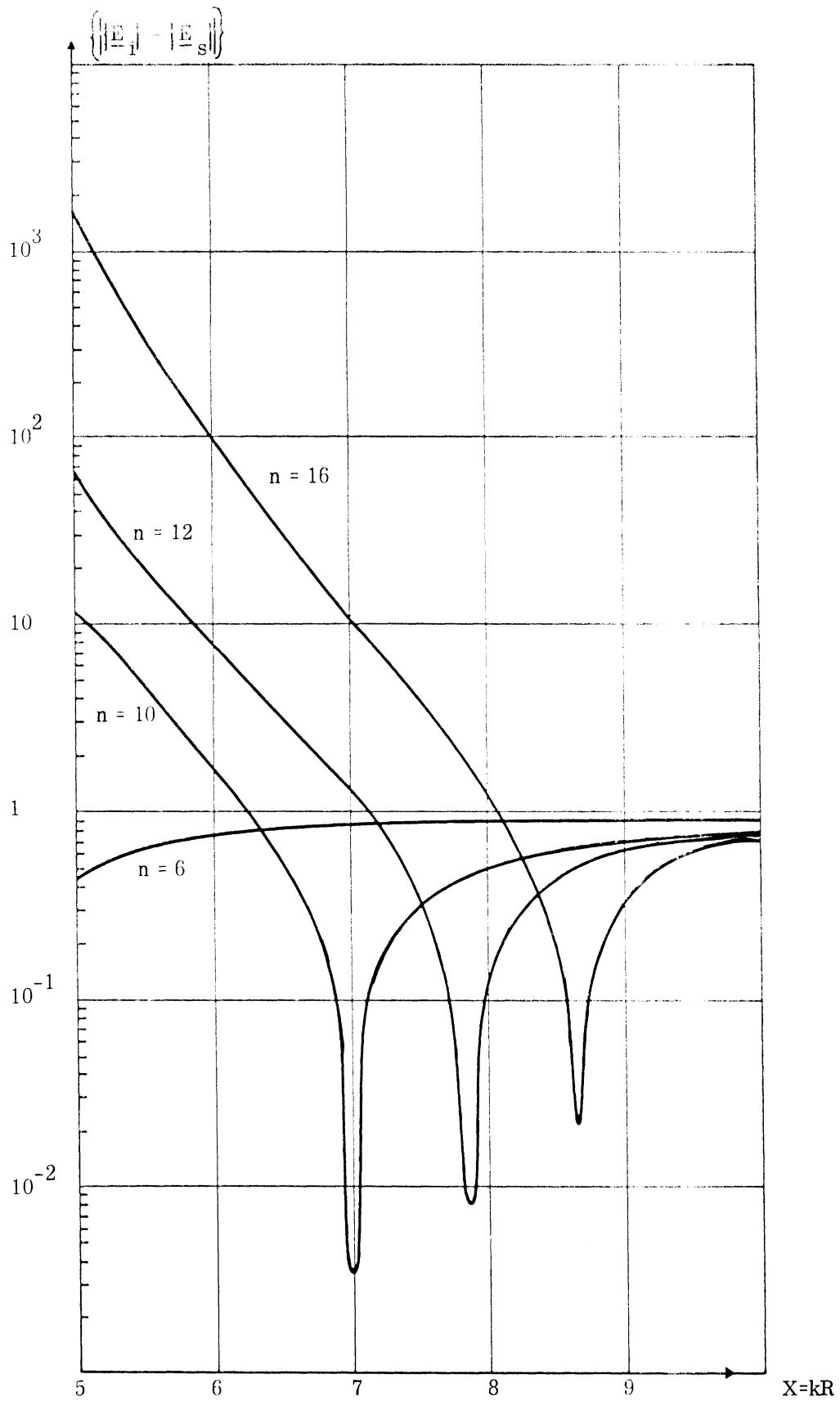n = 6, 10, 12, 16. $\phi = 0^o$, $\theta = 135^o$.

86

that both boundary conditions will yield the best result for these particular polarization properties, was expected (8579-3-Q) and was found for all employed test cases. Thus the simultaneous application of both conditions at low frequencies, such that $ka \simeq 1$, may be sufficient for a perfectly conducting scatterer of prolate spheroidal shape. The additional minima of $\left\{ \underline{E}_T \times \underline{E}_T^* \right\}$ that lie within the proper surface locus are of extremely small amplitude with respect to that about the proper surface locus and show a sharp dip, thus can be determined only if an extremely small searching increment is used, and may therefore be disregarded.

Summarizing the results obtained for the prolate spheroidal test cases, it can be concluded as well that the simultaneous application of the two conditions at two different operational frequencies is the proper method of determining the point which may lie on the surface of the scatterer within that conical section which is exterior to the minimum sphere enclosing the two focal points.

REFERENCES

Barrar, R.B. and C.L. Dolph (1954) "On a Three Dimensional Problem of
Electromagnetic Theory," Journ. Rad. Mech. and Anal., Vol. 3, No. 6,
725-743.

Brown, W.P. (1962), A Theoretical Study of the Scattering of Electro-
magnetic Impulses by Finite Obstacles. CIT Antenna Laboratory Technical
Report No. 28.

Erd'elyi, Magnus, Oberhetteinger, Tricomi (1954), (BATEMAN Manuscript
Project) Tables of Integrals, Vol. 2, McGraw-Hill Book Company, Inc.
New York.

Waterman, P.C. (1965), "Matrix Formulation of Electromagnetic Scattering,"
Proc. IEEE, 53, 805 (and private communications).

Weston, V.H. and J.J. Bowman (1966), "Inverse Scattering Investigation -
Quarterly Report, 1 April - 30 June 1966," The University of Michigan
Radiation Laboratory Report No. 7644-3-T, AF 19(628)-4884.

Weston, V.H., J.J. Bowman, Ergun AR (1966), "Inverse Scattering Investigations,
Final Report, 1 October 1965 - 30 September 1966," The University of
Michigan Radiation Laboratory Report No. 7644-1F, AF 19(628)-4884.

Weston, V.H., (1967), "Inverse Scattering Investigation - Quarterly Report
No. 1, April 1966," The University of Michigan Radiation Laboratory
Report No. 8579-1-Q, ESD-TR-67-517, Vol. I.

Weston, V.H., W.M. Boerner and C.L. Dolph (1967), "Inverse Scattering
Investigations, Quarterly Report No. 3, November 1967," The University
of Michigan Radiation Laboratory Report No. 8579-3-Q, ESD-TR-67-517,
Vol. III.

DISTRIBUTION

Electronic Systems Division
Attn: ESSXS   27 copies
L.G. Hanscom Field
Bedford, Mass. 01730

Electronic Systems Division
ESTI   23 copies
L.G. Hanscom Field
Bedford, Mass. 01730

DOCUMENT CONTROL DATA - R & D

(Security classification of title, body of abstract and indexing annotation must be entered when the overall report is classified)

1. ORIGINATING ACTIVITY *(Corporate author)*	2a. REPORT SECURITY CLASSIFICATION
The University of Michigan Radiation Laboratory, Dept. of Electrical Engineering, 201 Catherine Street, Ann Arbor, Michigan 48108	UNCLASSIFIED
	2b. GROUP N/A

3. REPORT TITLE

INVERSE SCATTERING INVESTIGATION
QUARTERLY REPORT NO. 4

4. DESCRIPTIVE NOTES *(Type of report and inclusive dates)*

Fourth Quarterly Report (3 October 1967 to 3 January 1968)

5. AUTHOR(S) *(First name, middle initial, last name)*

Vaughan H. Weston
Wolfgang M. Boerner
Dallas R. Hodgins

6. REPORT DATE	7a. TOTAL NO. OF PAGES	7b. NO. OF REFS
February 1968	88	8

8a. CONTRACT OR GRANT NO.	9a. ORIGINATOR'S REPORT NUMBER(S)
F19628-67-C-0190	ESD-TR-67-517, Vol. IV
b. PROJECT NO.	
c.	9b. OTHER REPORT NO(S) *(Any other numbers that may be assigned this report)*
d.	8579-4-Q

10. DISTRIBUTION STATEMENT

This document has been approved for public release and sale; its distribution is unlimited.

11. SUPPLEMENTARY NOTES	12. SPONSORING MILITARY ACTIVITY
	Deputy for Surveillance and Control Systems Electronic Systems Division, AFSC, USAF, L G Hanscom Field, Bedford, Mass. 01730

13. ABSTRACT

The plane wave representation is generalized in terms of a three-dimensional Fourier transform, to yield an expression, which when combined with the incident field, gives the total electric field everywhere inside and outside non-magnetic scattering bodies. This representation requires the knowledge of the scattering matrix and its analytic continuation in the frequency domain. The use of short pulse data to determine the properties of uniformly coated bodies is considered, where the main attention is applied to the illuminated portion of smooth convex bodies at high frequencies. Computational results are obtained, establishing the conditions that are required to determine the surface of a conducting body from knowledge of the total near field. It is shown for the cases treated (sphere and prolate spheroid), that two separate conditions are required. One of these conditions yields a single surface which is an approximation to the proper surface, whereas, the other condition yields a set of surfaces, among which is the exact surface.

14. KEY WORDS	LINK A		LINK B		LINK C	
	ROLE	WT	ROLE	WT	ROLE	WT
Inverse Scattering						
Electromagnetic Theory						
	LINK A		LINK B		LINK C	
	ROLE	WT	ROLE	WT	ROLE	WT